High-resolution δ^{18}O and assemblage analysis between 1949- and 2000 AD based on planktonic foraminifera from the Storegga Slide, eastern Norwegian Sea

Rebekka Hlín Rúnarsdóttir

Department of Earth Science
University of Bergen
2016

High-resolution δ^{18}O and assemblage analysis between 1949- and 2000 AD based on planktonic foraminifera from the Storegga Slide, eastern Norwegian Sea

Rebekka Hlín Rúnarsdóttir

60 ECTS thesis submitted in partial fulfillment of a
Magister Scientiarum degree in marine geology

Supervisor
Hans Petter Sejrup

Department of Earth Science
University of Bergen
28.09.16

Abstract

In this study are presented results from a high-resolution $\delta^{18}O$ and assemblage analysis between 1949- and 2000 AD based on planktonic foraminifera from core GS13-182-01. The core was retrieved from the head of the Storegga Slide, eastern Norwegian Sea. From the core top down to 52.2 cm, 90 samples were analyzed, comprising the last 50 years. This level of resolution is unprecedented in the area, with 1-2 samples representing each year. Additionally, 30 samples between 8000- and 400 cal. yr. BP were analyzed. The high-resolution aids in interpreting multi-decadal and higher frequency climate variability such as the North Atlantic Oscillation (NAO) with evidence of annual temperature changes. Based on the known ecological preference of certain species of planktonic foraminifera, changes in their abundance were used to interpret changes in the dominance of local water masses. The results of the assemblage analysis were comparable to previous planktonic foraminifera studies in the area. Atlantic Water and Norwegian Coastal Water are the most influential in the area with clear indications of NAO influence. Instrumental temperature data from Ocean Weather Station Mike (OWSM) and Trondheim (TRON) was compared to the stable oxygen isotope results from both core GS13-182-01 and P1-003. The results confirm the conclusions of previous studies, predominately Sejrup et al. (2011, 2010) where the local near-surface signal is attributed to a basin wide North Atlantic signal rather than the climate of Scandinavia.

Abstrakt

I denne oppgaven blir det lagt fram resultat fra en studie av stabile oksygenisotoper og foraminiferer med høy tidsoppløsning fra perioden 1949–2000. Dataene som brukes i denne oppgaven er hentet fra kjernen GS13-182-01 fra Storeggaskredet øst i Norskehavet. 90 prøver fra kjernetoppen og ned til 52,2 cm ble analysert, noe som utgjør de siste 50 årene. En så høy oppløsningsgrad har en ikke brukt i dette området før, med 1–2 prøver fra hvert år. I tillegg til disse ble det analysert 30 prøver frå perioden 8000–400 cal. yr. BP. Den høye oppløsningen med bevis på årlige temperaturendringer er til god hjelp i tolkningen av multidekadale og høyfrekvente klimavariasjoner, slik som den nordatlantiske oscillasjonen (NAO). Ved å ta utgangspunkt i kjente økologiske preferanser hos visse arter foraminiferer ble endringer i mengden deres brukt til å tolke endringer i dominans i lokale vannmasser. Atlanterhavsvann og Norskestrømmen er de mest betydningsfulle i området, med tydelige tegn på NAO-påvirkning. Temperaturdata fra værstasjonene M (OWSM) og Trondheim (TRON) ble sammenlignet med resultat fra stabile oksygenisotoper fra både kjerne GS13-182-01 og P1-003. Resultatene stadfester konklusjonene fra tidligere studier, særlig Sejrup et al. (2011, 2010), der det lokale signalet nær vannflaten ble tilskrevet et signal som gjelder hele Nord-Atlanteren i stedet for klimaet i Skandinavia.

Preface

The making of this thesis has been an eventful and instructive process to say the least. Looking back now I can list numerous things I should have done differently in the beginning to make it easier, but making mistakes was an important part of the experience. Learning how to find, read and extract information from different sources, setting it up in an organized way and produce and work with my own data is what my studies had been leading up to. I truly enjoy working with foraminifera and the fields of paleoclimatology and marine geology have become even more interesting to me after working on this thesis. I am happy to say that I feel more mature as a student and as a scientist now than before I started writing.

I was not able to do it all by myself so I want to acknowledge those who helped me in some way. First and foremost, I would like to thank Hans Petter Sejrup for his supervision in this project and helpful comments throughout the whole process. Furthermore, Berit Hjelstuen and Lukas Becker for their data and literature resources and input during our meetings. Vigdis Hope and Nil Irvali for their help with the foraminifera identification. Sædís Ólafsdóttir and Hafliði Hafliðason for moral support when I was feeling stressed and homesick. Áslaug Geirsdóttir for encouraging me to do this project and making it possible for me to work on the thesis at the University of Iceland. Lastly, I would like to thank my parents for supporting me during the course of my studies.

Table of Contents

List of Figures

1 Introduction

Earth's climate is a complicated system governed by external solar, orbital and tectonic forcing. It consists of internally interacting spheres where the atmosphere, vegetation, land surface, oceans and ice covers are the most vital components. External forcing together with a dynamic climate system results in climate variations. Humans have been making scientific observations of these variations for several hundred years during a relatively mild and stable climate (Ruddiman, 2013). On a glacial-interglacial time scale the climate has drastically shifted between extremes, both icehouse and greenhouse conditions, as a response to different forcing and feedbacks. The vastness and full range of Earth's climatic history therefore lies far beyond the human perspective. The geological record contains valuable information concerning minor and major changes in these past environmental conditions, broadening our understanding of past climate beyond the instrumental range (Sejrup et al., 2011). Deep Sea sediment archives are one of the more important ones due to a relatively continuous and stable sedimentation, often resulting in high resolution data sets. Fossil-records from these archives, predominately foraminifera, have been used as a proxy for near sea-surface conditions and other ocean-circulation type research (Curry & Ostermann, 1997).

Abrupt climate change has been the focal point of recent climate research. It is known that minor changes in present times could result in devastating effects on habitability in decades or less. The Northern North Atlantic is in numerous ways a case study when it comes to climate research. Due to accessibility, dynamic polar setting and vast hydrocarbon processing the area has been well documented in terms of bathymetry, oceanography, atmospheric processes, thermohaline circulation and other climate mechanisms (Marshall et al., 2001). In June 2013 a research cruise was conducted by the Department of Earth Science at the University of Bergen (UiB) as a part of the GLANAM (Glaciated North Atlantic Margins) project (2013-2017). The research area was at the Møre continental slope, at the head of the Storegga slide where a 19,7 m long calypso core, GS13-182-01 was obtained at 960 m water depth along with a

3 km long TOPAS profile (Hjelstuen et al., 2013). A core, raised at 851 m water depth, 20 km to the NW, P1-003MC/SC was obtained in 1999 and has been the basis for numerous studies (e.g. Sejrup et al., 2011, 2010; Berstad et al., 2003). Two other cores, MD95-2011 and Troll 8903/28-03, taken further north and south respectively are also examples of records representing environmental changes in the area (e.g. Risebrobakken et al., 2003; Klitgaard-Kristensen et al., 2001).

The two dominant water masses in the area are Atlantic Water and Norwegian Coastal Water, with the latter being warmer, fresher and containing less nutrients. The Norwegian Coastal water has a westerly extent and increased influence over the core site corresponding to local wind patterns. The climate variation dominating these patterns is the NAO which is coupled with the AMOC and AO on a global scale (Marshall et al., 2001). The Storegga slide scar is an ideal location for obtaining high resolution cores due to the high sedimentation rates. However, complex bathymetry components and steep escarpments on the Norwegian continental margin with increased turbulence sets up a high-stress environment for marine organisms (Kjennbakken et al., 2013). In the surface layers, coccolithophorids and other photosynthetic organisms multiply according to favorable access to light and nutrients and sustain the planktonic foraminifera living in the near-surface layer. Numerous studies have previously been performed in the area using planktonic foraminifera (e.g. Sejrup et al., 2011, 2010; Anderson et al., 2010; Risebrobakken et al. 2003, Klitgaard-Kristensen et al., 2001).

Other research includes: Studies on the depositional environment on the Norwegian continental margin (Hjelstuen et al., 2004), detailed Storegga slide geometry (Haflidason et al., 2004), variations in the Norwegian Current (Berstad et al., 2003) and carbonate content studies (Kjennbakken et al., 2013). Sejrup et al. (2011, 2010) concluded that the foraminifera isotope signal recorded in P1-003 could be attributed to solar influence and subsequent influence on atmospheric mechanisms and inflow of Atlantic Water. The strongest correlation was found between summer Sea Surface Temperatures (SSTs) with evidence suggesting that the variability reflected broader North Atlantic changes rather than local climate changes (Sejrup et al., 2011, 2010). The basis for this study is a relative abundance study and stable oxygen isotope analysis on planktonic foraminifera in core GS13-182-01, performed at the

University of Bergen in 2016 with additional data on the core obtained and analyzed by Lukas Becker (Becker et al., in prep.).

The primary objective of this study is to interpret the high-resolution stable oxygen isotope and assemblage analysis data between 1949- and 2000 AD and compare the variability with previous studies, predominately with Sejrup et al. (2011, 2010) and with instrumental data gathered from Ocean Weather Station Mike. Furthermore, the recent evolution of dominant water masses in the area will be documented through the interpretation of planktonic foraminifera assemblages. The influence that known modes of climate variability such as the North Atlantic Oscillation have on the assemblages will also be considered. An additional low-resolution assemblage record spanning mid- to late Holocene will be presented and compared to the more recent high-resolution record.

2 Background

2.1 Bathymetry

The study area is located off the western coast of Norway, in the southeastern part of the Norwegian Sea. The bathymetry and oceanography of this region is to a large extend affected by the location of the mid-Atlantic-ridge combined with the vigorous activity of the Iceland plume. A result of this activity is the Greenland-Scotland ridge which separates the Nordic Seas from the rest of the North Atlantic. Four major basins and two major plateaus comprise the bulk bathymetry of the Nordic Seas (fig. 2.1). In the Greenland Sea, west of the mid-Atlantic ridge there are two deep basins, the Greenland and Boreas basins separated by the Greenland fracture zone, with ocean floor depths ranging up to 3600 and 3200 m respectively. South of Jan Mayen and the adjacent fracture zone is the Iceland plateau (e.g. Blindheim & Østerhus, 2005; Drange et al., 2005; Mork & Skagseth; 2005). In the Norwegian Sea, east of the mid-Atlantic ridge there are two major basins, the Lofoten and Norwegian basins, the former one reaching depths of 3200 m while the latter one exceeds 3800 m in some areas. The Norwegian basin is therefore the deepest and most extensive of these basins, extending from the Iceland-Faroe-ridge eastwards towards the Vøring plateau and the continental slopes of Norway where the study area is located at the head of the Storegga slide scar (see fig. 2.2). The Norwegian basin and the Storegga Slide are important features in the local bathymetry along with the inactive Ægir ridge, the Vøring plateau and the North Sea fan (e.g. Blindheim & Østerhus, 2005; Drange et al., 2005; Mork & Skagseth; 2005). Numerous bathymetrical features of the North Sea can be attributed to repeated tectonic events and compressional episodes, later dominated by glacially attributed erosion and sedimentation. The glacial history of the Norwegian margin has been studied in detail with strong emphasis on the stability of the continental margin (Hjelstuen et al., 2004). The steep slopes have given rise to multiple sliding events, resulting in rapid deposition in the Norwegian deep-sea basins (Haflidason et al., 2004).
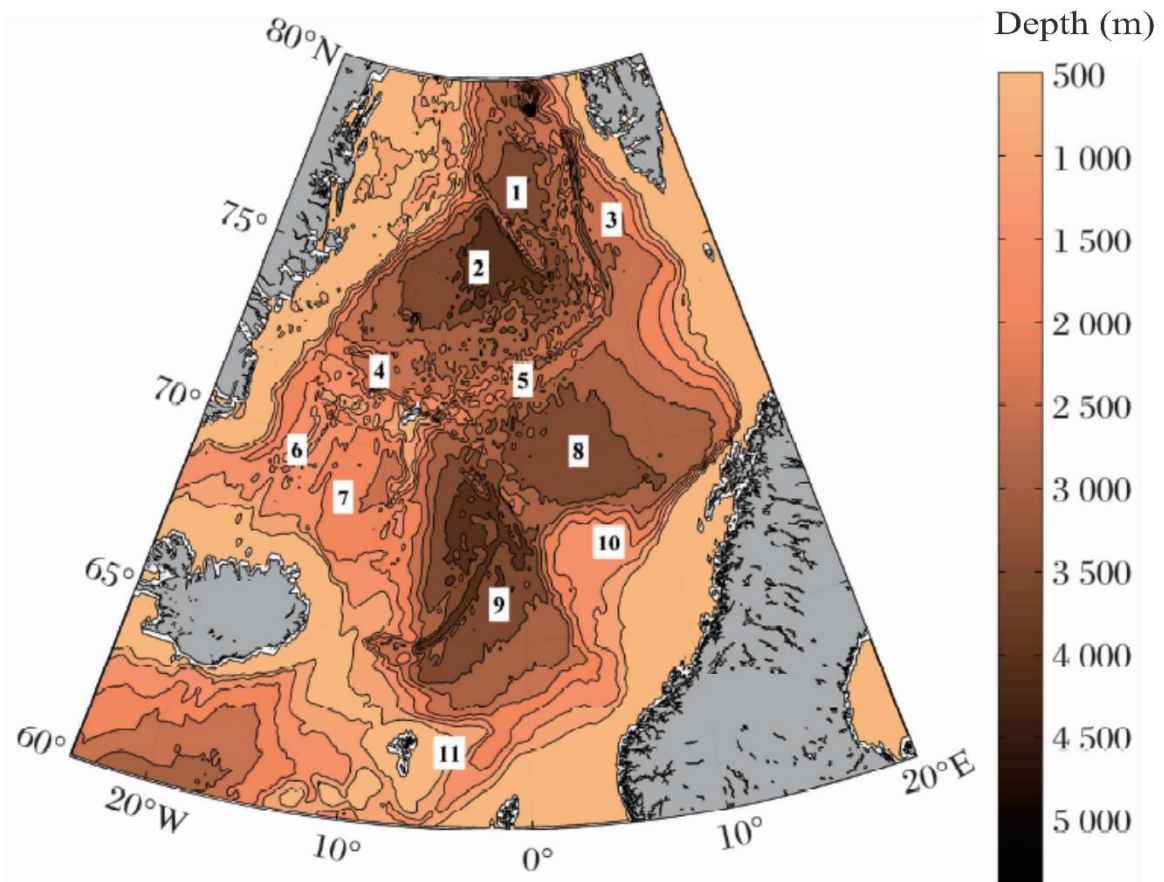
Figure 2.1 Bathymetry map of the Nordic seas i.e. the Norwegian, Greenland and Iceland Seas. (1) Boreas Basin; (2) Greenland Basin; (3) Knipovich Ridge; (4) Jan Mayen Fracture Zone; (5) Mohn Ridge; (6) Kolbeinsey Ridge; (7) Iceland Plateau; (8) Lofoten Basin; (9) Norwegian Basin; (10) Vøring Plateau; (11) Faroe Islands (Shao & Zhao, 2014).

2.2 Regional Geology

In the closest vicinity of the coring location, at the head of the Storegga Slide scar, are several distinct geological and bathymetrical features. To the south of Storegga is the North Sea Fan and the mouth of the Norwegian Channel sub-marine trough. To the North are the Vøring basin, Vøring plateau, Vøring marginal high and the Trøndelag platform (fig. 2.2). To the South-East, towards the coast is the Møre margin that includes major geological formations such as the Naust and Molo formations (fig. 2.3) (Hjelstuen et al., 2013).
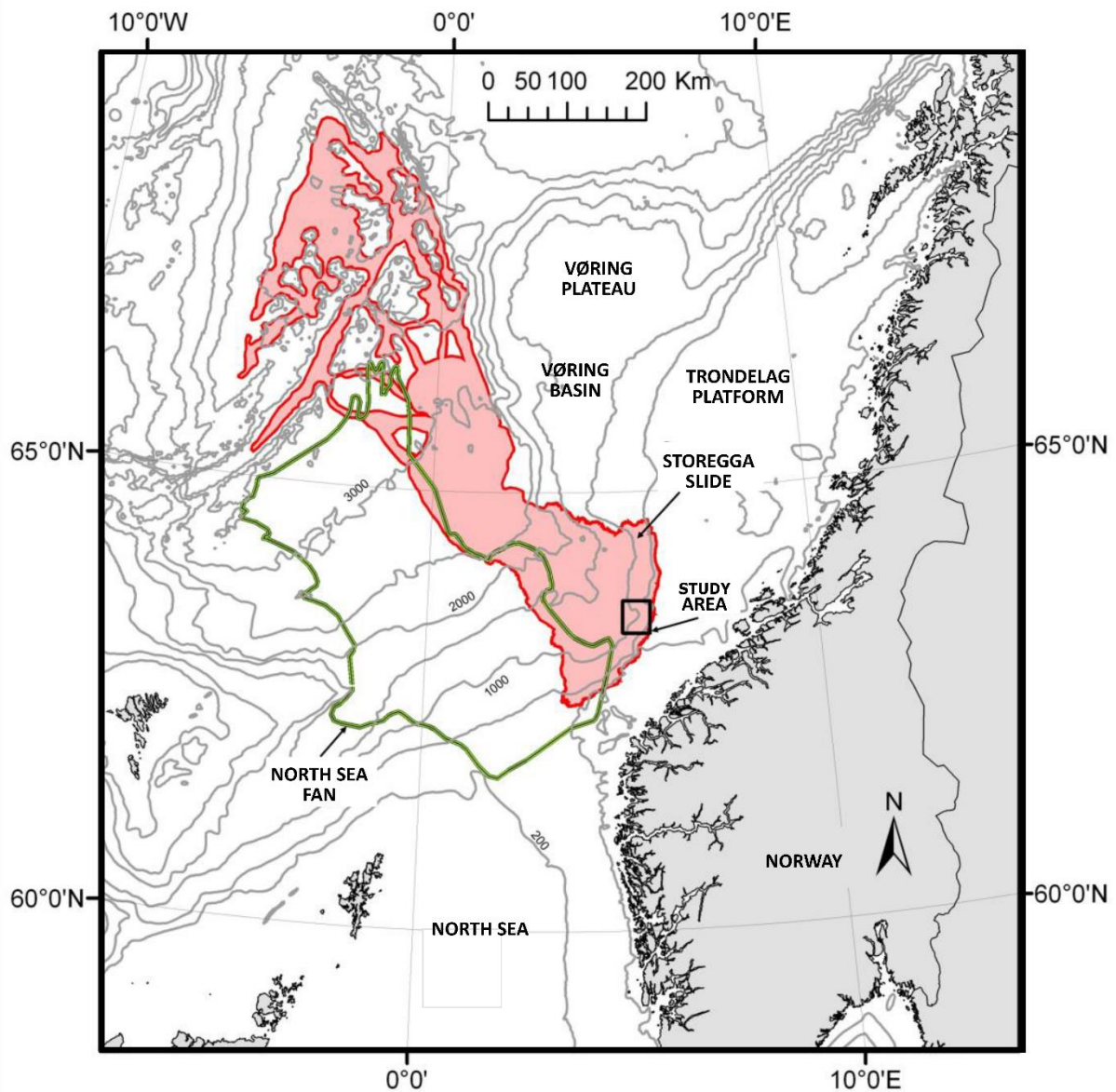
Figure 2.2 Bathymetry map of the Storegga slide and adjacent areas, the North Sea Fan and the Vøring basin, Vøring plateau and Trøndelag platform. The study area is marked with a square (modified from Hjelstuen et al., 2013).

The bulk of the Norwegian landmass can be traced back to two major geological events, the Caledonian orogeny and the opening of the North Atlantic Ocean. The collision of the Greenland and Norwegian landmasses took place roughly 400 million years ago with sediment filling the narrow sea between the plates, the source of Norway's vast hydrocarbon supply. Later formations and present landscape are mostly due to Quaternary glaciations and interglacial processes (Sætre, 2007).

6

The Norwegian fjords were formed and shaped by numerous outlet glaciers coming from the main Scandinavian ice sheet. The ice sheet began to form during the Miocene epoch but during later Plio- and Pleistocene epochs the Northern hemisphere glaciation intensified with subsequent glacial advance into to shelf area. Around 1.1 Ma ago the ice sheet is believed to have reached the shelf edge with confirmed advances on the mid-Norwegian shelf from 0.5 Ma ago (Sejrup et al., 2005; Hjelstuen et al., 2004). During its maximum extent the Norwegian ice sheet therefore completely covered the whole of the land area and continental shelf of Western Norway. The Norwegian Channel offshore deglaciated around 18 ka BP with the Western margin of the ice Sheet being characterized by enormous outlet glaciers (Sejrup et al., 2009). At the beginning of the Preboreal period, very fast melting and calving in the fjords resulted in rapid deglaciation during the early Holocene (Mangerud et al., 2011). This transition from a glacial to interglacial state had profound impact on the subjected land mass due to glacial erosion, glacial sediment depositions and changes in sea-level. The extensive erosion, meltwater and rapidly deposited sediment created formations such as the North Sea fan and furthermore gave way to large-scale land and submarine slides, such as the Storegga slide (Sætre, 2007). 1.1 Ma ago The Norwegian Channel, a vast sub-marine trough adjacent to the Southern coast of Norway became the main transport route of glacially eroded material coming from the Fennoscandian landmasses. At the end of this trough lies the North Sea Fan with a thickness of up to 1500 m and a coverage of 110.000 km^2 between the Storegga slide, the Faroe-Shetland Channel and the Ægir ridge. It is mostly composed of sediments deposited in the last 500.000 years due to vigorous erosion of glaciers occupying the Norwegian Channel (Hjelstuen et al., 2012).

Other glacially attributed features characterize the mid-Norwegian continental shelf, such as smaller cross-shelf troughs and shallow banks separating them. The overall morphology of this area is dominantly due to rapid progradation with the crystalline-sedimentary boundary at around 10-40 km off the coast (Ottesen, et al., 2009). In general, the units that are a part of the shelf area are older closer to the coast. This is mostly due to extensive erosion and uplift of the land mass in combination with basin oriented subsidence. This has also resulted in the eroded sediments being preserved mainly on the middle and outer shelf areas. During past glaciations the changes in ice flow have ultimately altered the sediment distribution with the

location of fast-flowing ice streams being the most important factor. The Møre and Vøring basins have also played a topographical role in shaping the shelf area. To the west of Møre, the deep Møre basin has limited progradation, resulting in a narrow shelf. The shallower Vøring basin has not hindered the process in this way, allowing for a progradation of up to 150 km in the last 3 million years (Ottesen et al., 2009). Examples of near-coast formations are the Molo, Naust and Brygge formations (fig. 2.3). The older deep-marine deposits Brygge and Kai underlay the extensive Naust formation which is dominately glacially derived. The Molo formation has similar origins in progradation and regional uplift (Ottesen et al., 2009).
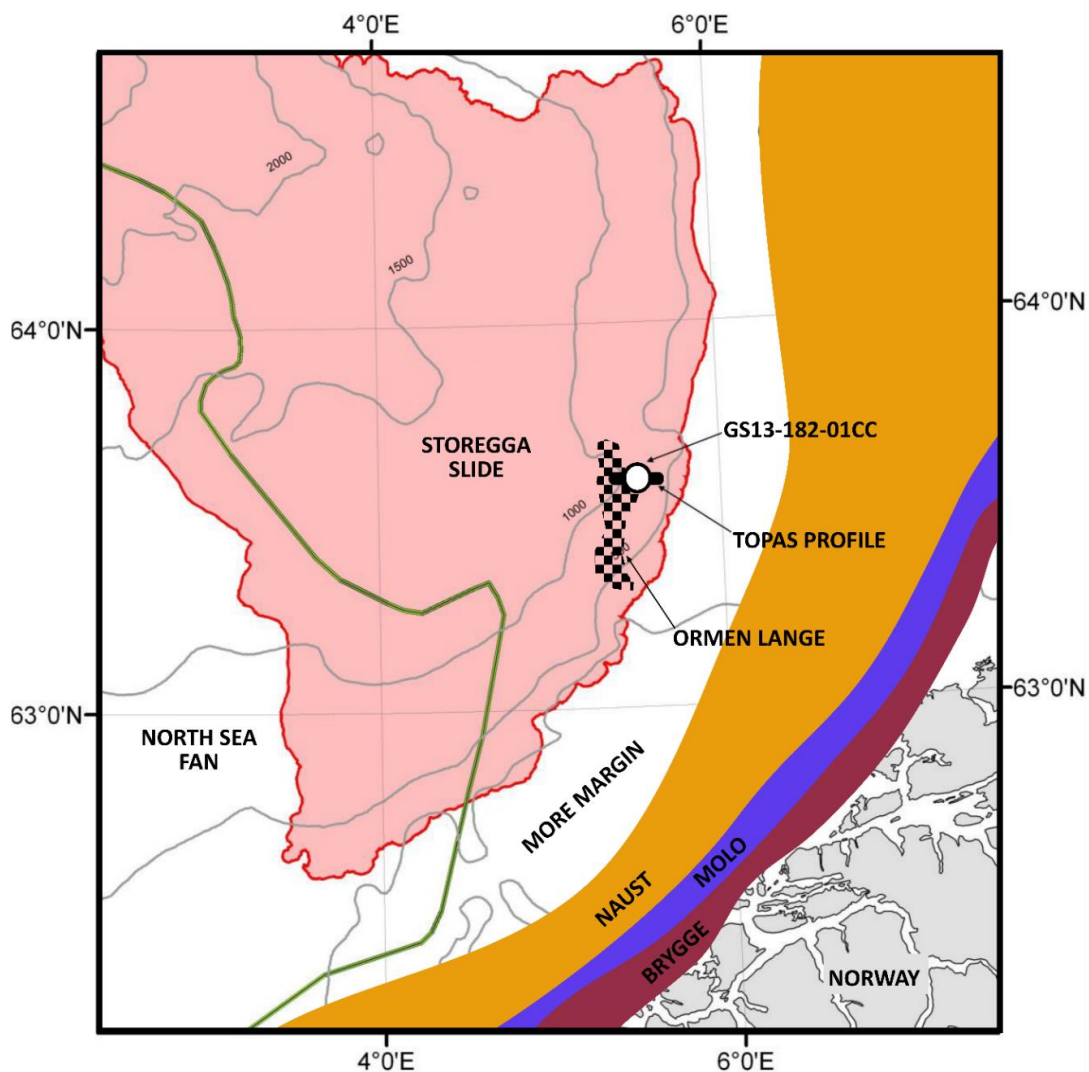
Figure 2.3 Bathymetry map of the head of the Storegga slide and adjacent formations, the North Sea fan, Naust, Molo and Brygge. Ormen lange, the GS13-182-01 coring site and TOPAS profile are also shown (modified from Hjelstuen et al., 2013 and Ottesen et al., 2009).

2.2.1 The Storegga Slide

Recurring glaciations, vigorous erosion and rapid sedimentation have shaped the various landforms in the Norwegian fjords and continental shelf and affected the stability of the coastal areas. The steep continental slopes of Norway have given rise to multiple major and minor submarine landslides with slide activity closely related to glaciations (Haflidason et al., 2004; Hjelstuen et al., 2004). The Storegga slide, dated back to 8000 yr BP, is considered to be one of the greatest submarine slide events to occur on a glacially influenced margin, with an affected area of 95.000 km^2. The Storegga slide depression has seen numerous sliding events in relation to its setting, magnifying the previous depression shape and making it an extensive catchment with high sedimentation rates. The initial slide scar was created in connection with margin build-out to the North and South and is structurally influenced by the Faroe-Shetland and Vøring escarpments along with neighboring structures such as the North Sea fan. The different sediment types and their coverage are shown in figure 2.4. At the head of the Storegga slide there are four main provinces: the exposed failure plane, blocky debris flow, semi-disintegrated slide and compression zone. A small area of in situ sediments, not affected by the sliding can be found North-West of the coring site and is an important reference point in reconstruction the local pre-slide topography. Further down-slope, past the Faroe-Shetland escarpment, there are two large provinces, the debris- and turbitide areas. The turbidite advance was met by the Ægir ridge which subsequently altered the deposition of the turbitide sediments (Haflidason et al., 2004).
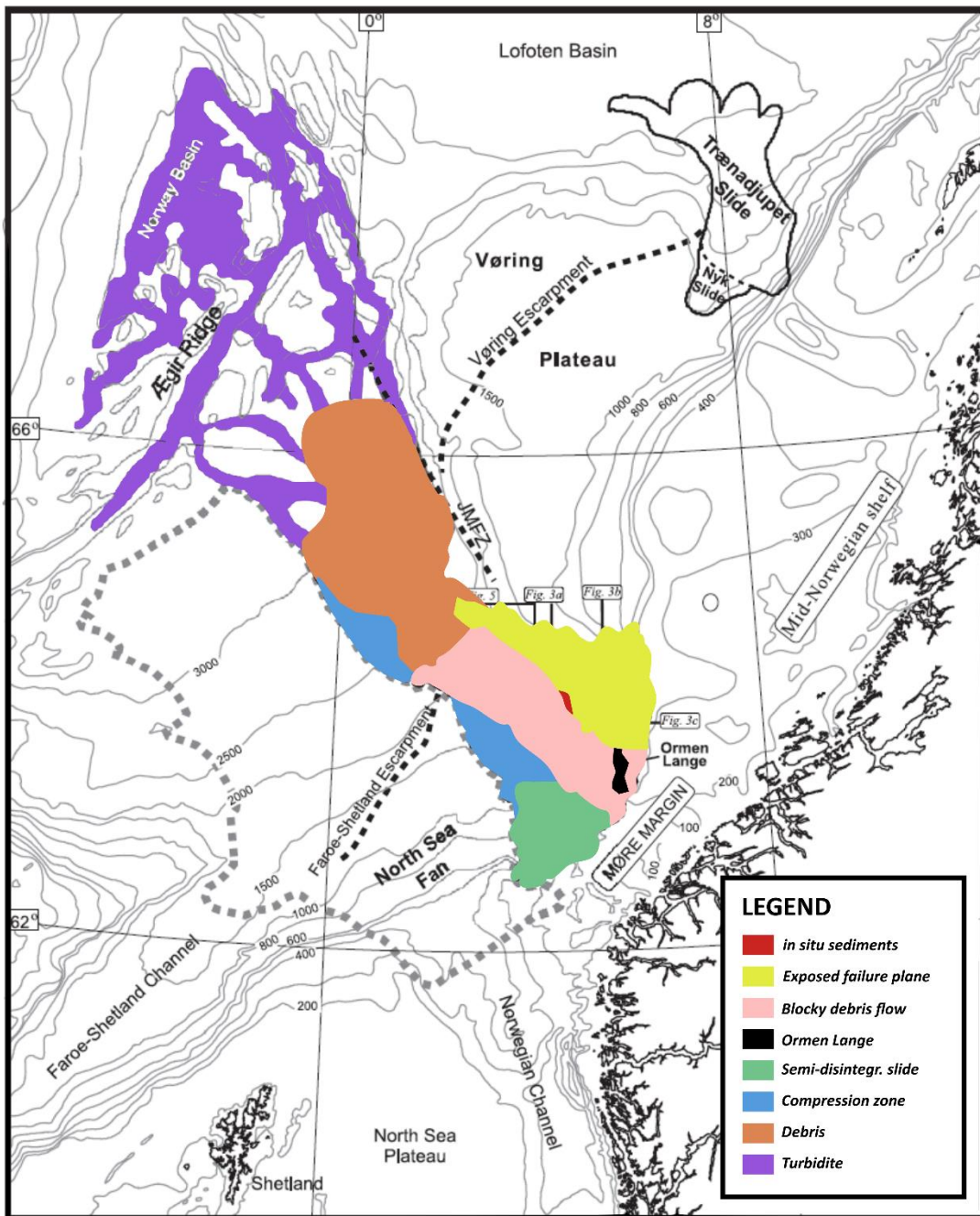
Figure 2.4 Morphology of the Storegga slide along with locations of the Faroe-, Shetland- and Vøring escarpments (modified from Haflidason et al., 2004).

2.3 Oceanography

2.3.1 Thermohaline circulation

What ultimately dominates the global ocean circulation is the Thermohaline circulation (THC). The THC drives the ocean's currents through, as the name suggests, temperature and salinity difference and in the process affects the global climate profoundly. The northern North Atlantic is a site of particular importance in this cycle due to the formation of North Atlantic Deep Water (NADW). These deep waters are formed through the sinking of surface waters through increased density in cooler climates at higher latitudes. This ventilation occurs predominately in the Nordic Seas basin and together with low-latitude mixing creates the density difference that drives the circulation. Recent warming could result in a weaker THC which would in effect influence the climate system, conceivably resulting in cooling of northern Europe (Hansen et al., 2004).
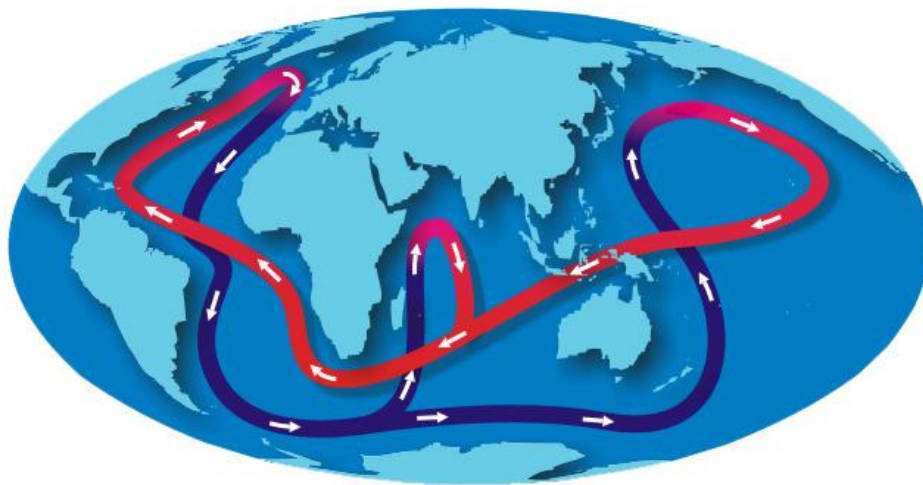
Figure 2.5 The Thermohaline Circulation. A simplified figure of the global conveyor belt that is governed by temperature and salinity difference between water masses (NOAA, 2008).

2.3.2 The Nordic Seas oceanography

The Nordic seas include the Iceland, Greenland and Norwegian Seas and cover the area north of the Greenland-Scotland Ridge and south of the Fram Strait. This area is only 0.75% of the world oceans but is highly dynamic to due to its setting. Water masses with different temperatures, salinities and densities, coming from both higher and lower latitudes meet and interact through frontal mixing, deep convection, subduction and entrainment. Sea ice is formed in the northern part but large areas are ice-free all year, especially in the South-East where warm and nutrient-rich Atlantic Water (AW) comes in from lower latitudes (Drange et al., 2005).

2.3.3 North Atlantic Overflow

As previously mentioned, the North Atlantic basin is divided by the Greenland-Scotland ridge, with most of the deep water formation happening in the northern basin. The deeper currents heading south have to cross the ridge before reaching lower latitudes. This results in approximately 6 Sverdrup (Sv) of overflow water with additional 6 Sv of entrainment water flowing to the depths of the Atlantic as NADW (Hansen et al., 2004). In fig. 2.6 this process is visually outlined.
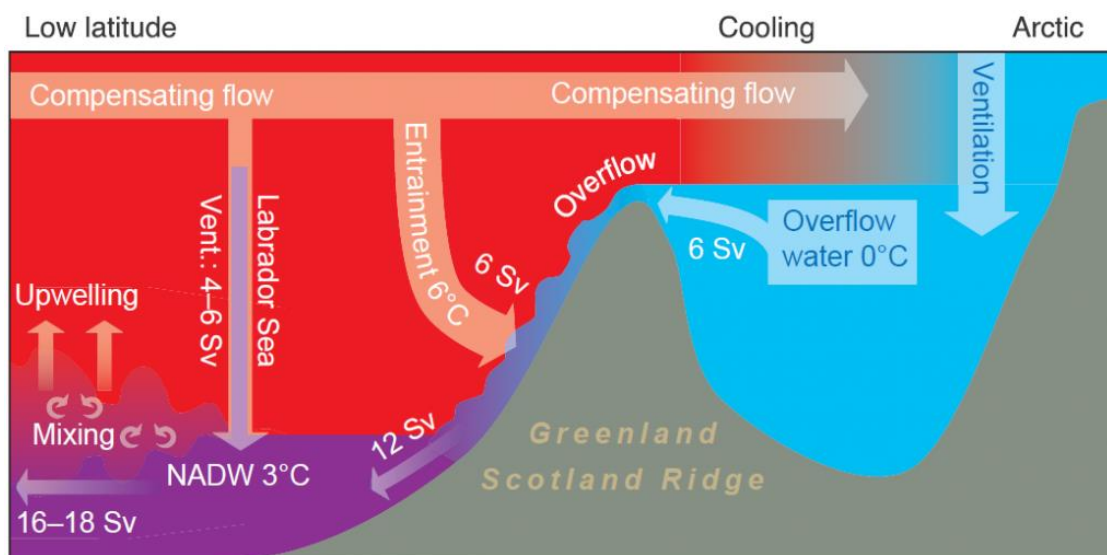
Figure 2.6 The North Atlantic Overflow consists og 6 Sv with an additional 6 Sv from entrainment forming NADW that flows to lower latitudes. The compensation flow consists of warmer Atlantic Water (Hansen et al., 2004).

Ultimately, the overflow process is a vital component of and is density-driven by the THC which is evident by the speed the current reaches before crossing the ridge. The circulation is completed with Atlantic Water flowing to higher latitudes and replacing the sinking water. The overall process is dependent on the density and therefore salinity of the surface waters. Atmospheric changes are expected to increase the freshwater supply in this area and in the process affect the density driven ventilation. Immediate effects could alter the local climate and in the long run effect the deep oceans (Hansen et al., 2004).

2.3.4 North Atlantic Water

The replenishing surface currents from the North Atlantic enter the Nordic Seas, bringing warm (6-13°), saline water (>35.0‰) (see fig. 2.7 and 2.8). The inflow occurs in three places along the Greenland-Scotland ridge. Firstly, in the eastern Denmark Strait the inflow is known as the Irminger current, secondly between Iceland and the Faroe Islands the Faroe current crosses the Iceland-Faroe ridge and thirdly there is Atlantic inflow through the Faroe-Shetland channel (Blindheim & Østerhus, 2005; Drange et al., 2005; Yashayaev et al., 2015). The path these inflow currents take through the Nordic Seas and into the Barents Sea is mostly topographically steered and modified by other currents. In the south-eastern part of the Nordic Seas the Faroe current is forced eastward due to the East-Iceland current which bears Arctic water south-east, forming the Iceland-Faroe front where the currents meet. The Faroe current partly merges with the Faroe-Shetland channel inflow but mostly continues straight into the Norwegian Basin. At the Vøring plateau it turns NW towards Jan Mayen where it partly recirculates to the Norwegian and Iceland Seas. The main branch of the current continues NE towards the Barents Sea and forms the Arctic front on the boundary between Arctic and North Atlantic Water, seemingly fixated at the Mohn ridge north of Jan Mayen (Blindheim & Østerhus, 2005; Yashayaev et al., 2015) (see fig. 2.7 and 2.8).
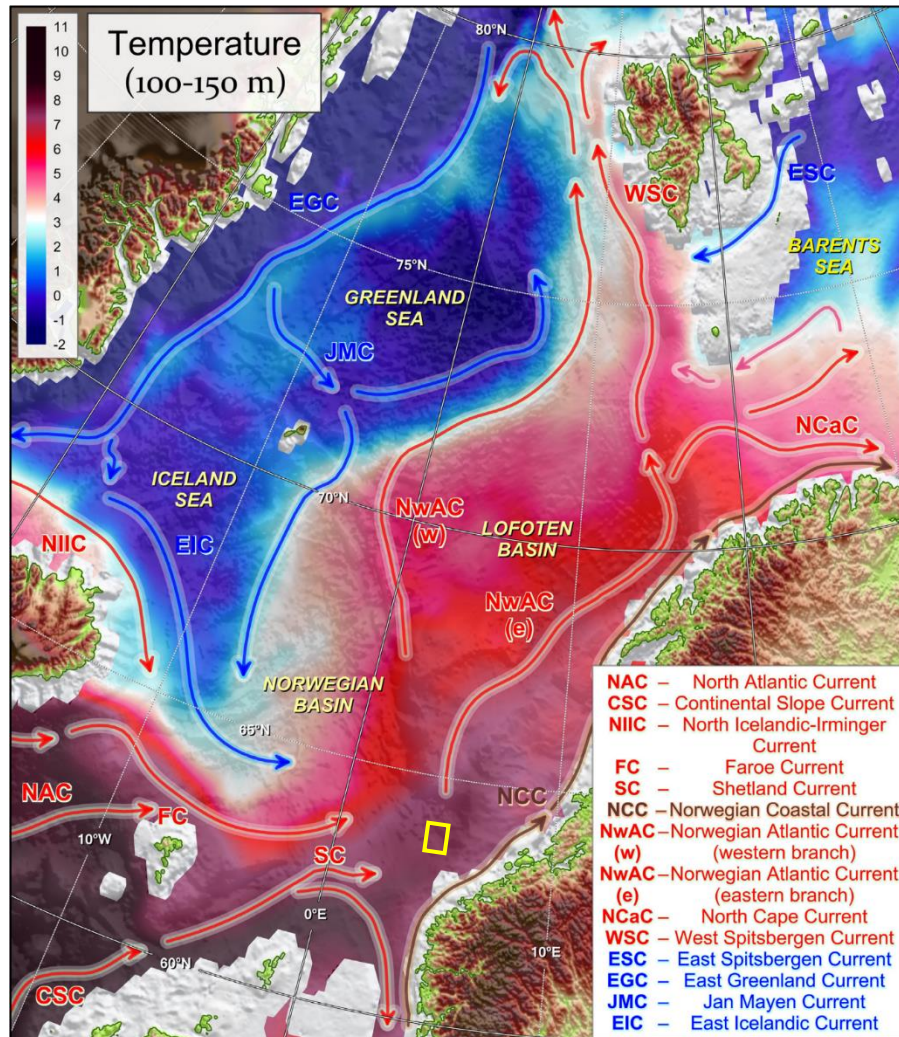
Figure 2.7 Near-surface temperature in the Nordic seas. Major currents and basins are displayed. The study area is marked with a square (Yashayaev et al., 2015).
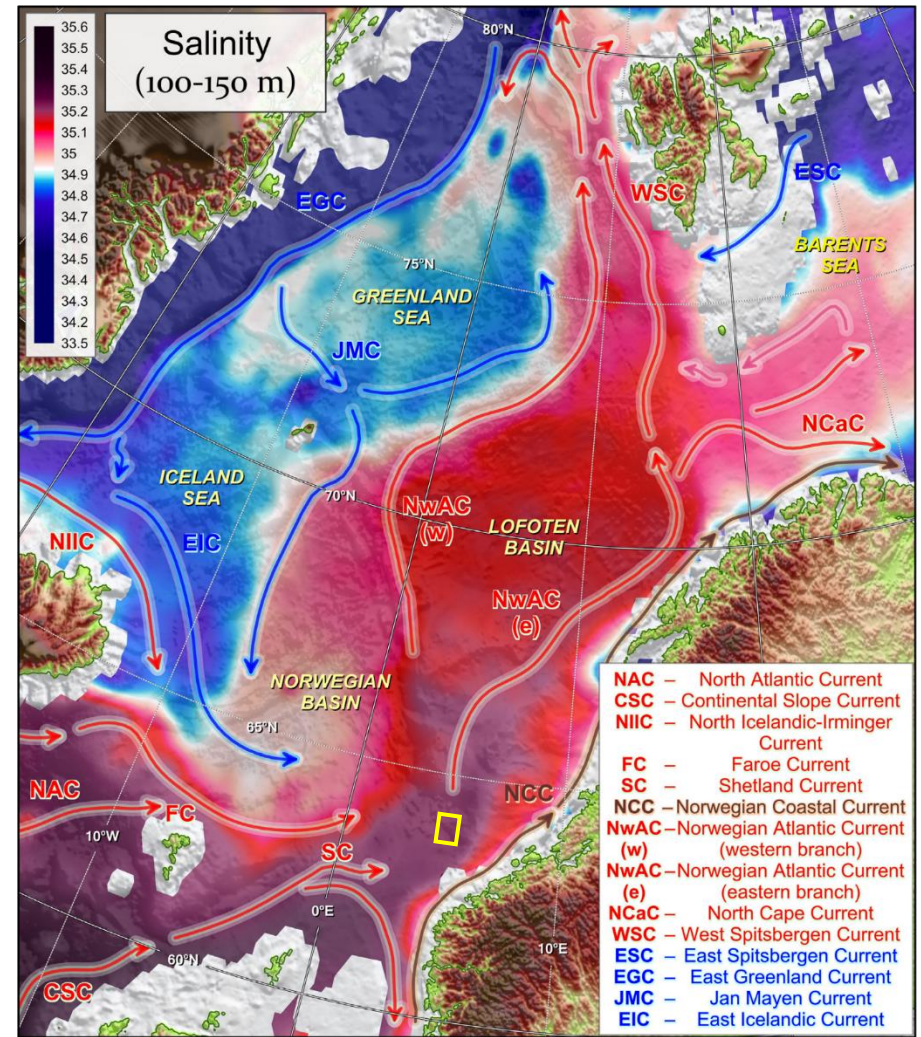
Figure 2.8 Near-surface salinity in the Nordic seas. Major currents and basins are displayed. The study area is marked with a square (Yashayaev et al., 2015).

The most influential current at the coring site is the Norwegian Atlantic Slope Current (NwASC) a branch of the Atlantic Water current with a temperature of 5-10°C and salinity between 35-35.3 psu. The mean annual flow rate of the strongest part of the current is 30 cm s^1. This is observed where the continental slope is steepest. Variations in flow are attributed to internal tides, on a scale of 20 cm s^{-1} and to downslope migration on a scale of 50 cm s^{-1} (Eliassen et al., 2000). The properties of the Atlantic Water current reach down to 400-600 m. Below that, the Norwegian Sea Arctic Intermediate Water (NSAIW) takes over with temperatures between 0.5 to -0.5°C and salinity between 34.87 and 34.9 psu, with maximum influence between 400-800 m and an eastern extent all the way to the Norwegian slope. Deeper in the water column, the Norwegian Sea Deep Water (NSDW) with lower temperature than -0.5 and a salinity of 34.92 psu is dominant (Orvik et al., 2001; Hansen & Østerhus, 2000). The transition between the warmer Atlantic water at the surface and the colder deep waters is abrupt and relocates on a vertical scale (Berstad et al., 2003). From 1958 to 2000 AD the temperature in the deep water increased slightly with both the intermediate and deep waters of the Nordic Seas experiencing freshening over the last four decades (Drange et al., 2005).

The Atlantic Water inflow influences the sedimentation down to 700 m along the southern Norwegian margin, with gravel and sand accumulating from the strong incoming NwASC. Between 700-1200 m the sediments mainly consist of silt and clay, reflecting calmer current setting. Below 1200 m the sediments consist of foraminiferal ooze (Kjennbakken et al., 2013; Berstad et al., 2003; Sejrup et al., 1981). Studies of benthic foraminifera from surface sediments, show a relationship between the main water masses, sediment type and water depth (Sejrup et al., 1981). Kjennbakken (2013) suggested that stronger currents in early-mid Holocene and subsequent increase in vertical turbulence in the area could create poor living conditions for some species. This turbulence can be attributed to the rough bathymetry and steep escarpments in the area and increases stress on the local fauna. Higher diversity towards presents times could therefore be attributed to weaker currents with lower turbulence and therefore more favorable living conditions (Kjennbakken et al., 2013).

Berstad et al. (2003) suggested that within the past 600 years the last 70 years have been the warmest for the Norwegian branch of the Atlantic water current. According to the same study, the transition zone between surface and deeper water masses has become shallower in more

recent years. The vertical shift is believed to be partly influenced by a decrease in the THC. The atmospheric pressure system predominately influences the easterly extent of Atlantic water. This is evident during the positive NAO phase when the arctic front is driven eastward, narrowing the Atlantic water current. As a result of a positive NAO and an eastward forcing wind patterns, inflow of Atlantic water into the Norwegian basin increases (Berstad et al., 2003; Orvik et al., 2001).

2.3.1 The Norwegian Coastal Current

East of the NwASC is the Norwegian Coastal Current (NCC), the other major current in the area. It has water temperatures of 5-10°C and salinity of <34 psu. Being warmer and fresher it is also nutrient depleted when compared to Atlantic Water (Mork & Skagseth, 2010; Sætre, 1988). The NCC originates from fresh water discharge from the Baltic and runoff from Norway and flows northward along the coast. During the winter the general wedge-shape of the NCC is well defined but during summer it tends to extend westward (Klitgaard-Kristensen et al., 2001). The water in the NCC mixes with Atlantic and North Sea Water making the NCC progressively more saline as it draws north. This results in less stratification of the current which is mainly driven by density structure determined by salinity distribution (Sætre, 2007).

As with the extent of the adjacent Atlantic Water current, a range of variables control the pattern and distribution of the NCC. These variables can be short-time meteorological variations, seasonal variations or long-term climate variations (Sætre, 2007). The westerly extent of the NCC predominately depends on the wind pattern associated with seasonality. During the summer, northerly winds cause widening of the NCC, creating a low salinity cap over the core site (Mork & Skagseth; 2010; Sætre, 1988). Between 62- and 65°N, at the head of the Storegga slide, the complex topography affects the NCC by branching it around 63°30'N (fig. 2.9). The bottom topography is narrow at the southern part restricting the more saline Atlantic Water to the slope areas (Section A). To the North, where branching of the NCC occurs, the Atlantic Water covers a broader shelf area below a 100-150 m surface layer of NCC water (Section B) (Sætre, 2007). The Western part of this NCC branch closely follows the headwall of the Storegga slide depression with the GS13-182-01 core site being further east at the Ormen Lange at a depth of 960 m.
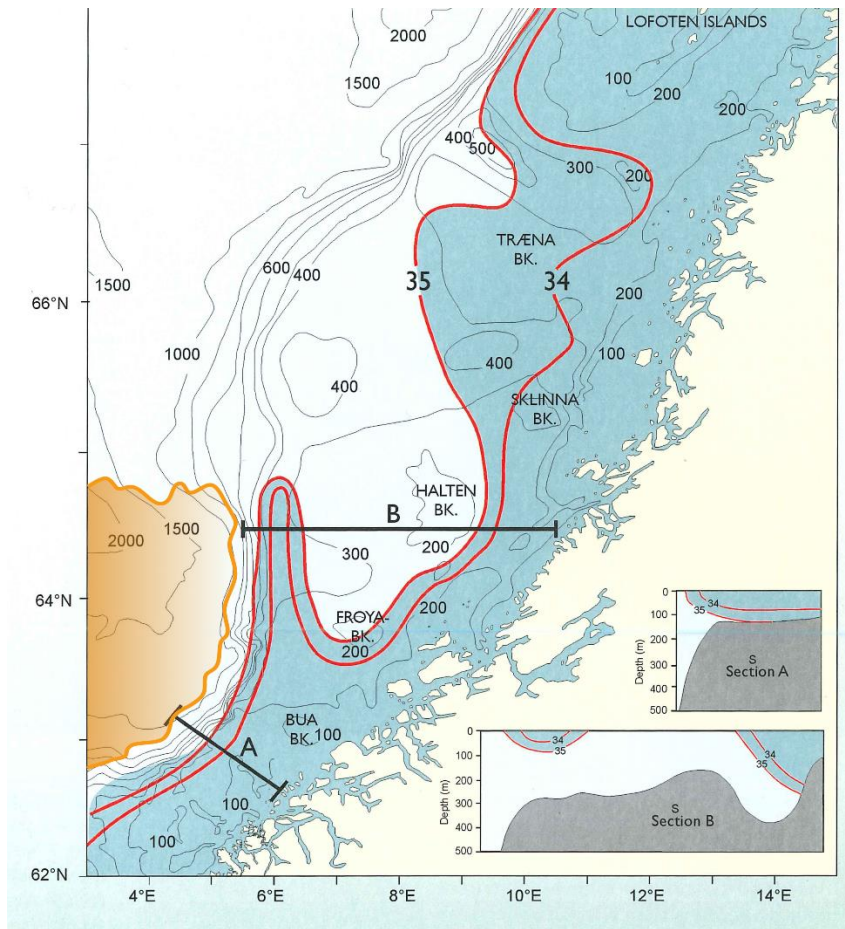
Figure 2.9 The branching of the Norwegian Coastal Current appears around 63°30′N, following the head of the Storegga Slide. Sections A and B show the transition between coastal and Atlantic water. Blue shows the extent of the NCC and orange indicates the head of the Storegga Slide (modified from Sætre, 2007).

2.4 Climate variability

The climate system is characterized by variability that can be expressed on varied time scales. Partly, the climate variability is natural i.e. variability we would expect from a climate system free of exogenous forcing such as volcanic- or human activities. To understand the anthropogenic influence on climate and aid in climate forecasting, the natural variability has been widely studied (Delworth & Mann, 2000). The most important types of variability in the North Atlantic recorded in instrumental data are the North Atlantic Oscillation (NAO) and the Atlantic Multi-decadal Oscillation (AMO) with NAO and the Atlantic Oscillation (AO) dominating the higher latitudes (Sejrup et al., 2010). The NAO has a stronger East-West gradient in the North Atlantic while the AMO is expressed in a more North-South direction. This can be seen in figure 2.10 (Sejrup et al., 2011).
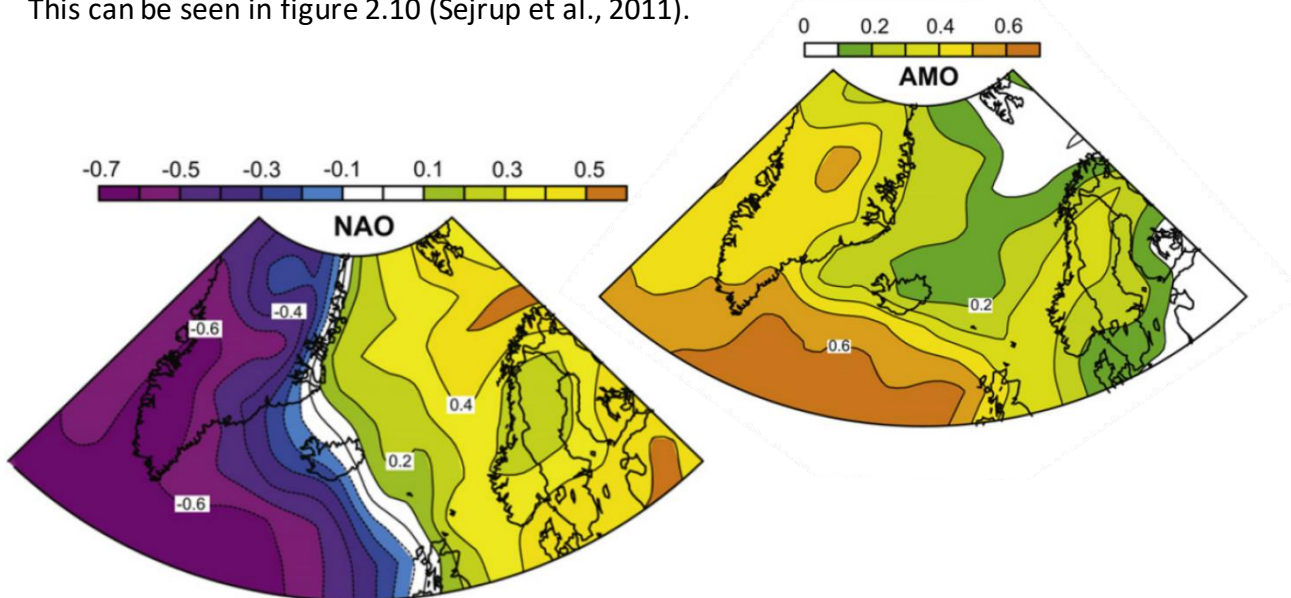
Figure 2.10 The spacial expression of the NAO (East-West gradient) and the AMO (North-South gradient) (Sejrup et al., 2011).

These variabilities influence and are influenced by other climatic features such as the Atlantic Meridional Overturning Circulation (AMOC). In brief the NAO refers to variability in sea level pressure difference between the Icelandic Low and the Azores High, resulting in a shift in the position of the jet stream and subsequently major changes in weather patterns in Europe. The NAO variability has a frequency of 7-10 years and is expressed as atmospheric and subsequent oceanographic changes (Marshall et al., 2001). However, the oceans influence back to the

atmosphere is weak on time scales shorter than a decade (Visbeck et al., 2003). The AMO reflects changes in the SSTs of the North Atlantic Ocean on a multi-decadal timescale and has a frequency of 60-100 years (Marshall et al., 2001). The AMOC accounts for most of the oceanic heat transport poleward and is featured in various global warming scenarios in global climate models. These mechanisms affect different components of the climate system but are correlated with each other and other climate mechanisms on a global scale (Marshall et al., 2001; Sutton & Hodson, 2005). Other types of variability can be isolated, abrupt events such as the great salinity anomaly in the late 1960's which is evident in both temperature and salinity data from the region (Marshall et al., 2001).

2.4.1 NAO

Just as the El Niño–Southern Oscillation (ENSO) dominates the Pacific climate patterns, the NAO is the dominant mode of atmospheric variability in the North Atlantic region (Marshall et al., 2001; Visbeck et al., 2003). Bjerknes (1964) presented pioneer work in observations on the atmosphere-ocean interaction related to NAO variability. A seemingly stochastic, atmospheric process, the NAO is termed negative or positive with each mode influencing temperatures, precipitation and atmospheric patterns in different ways. A basin-wide atmospheric forcing such as the NAO results in altered ocean properties and circulation with local changes including surface temperatures, mixed layer depth, heat content, Ekman transport and sea ice cover (Visbeck at al., 2003). The NAO index scales the atmospheric effects which are predominately expressed as a change in mean wind speed and direction of heat and moisture transport. During a positive index phase, the pressure difference between the Iceland low and the Azores high is abnormally great, resulting in stronger westerly winds. During a negative index phase, both the Iceland low and Azores high are anomalously weak, resulting in weaker westerly winds and storms surging over southern Europe. In a positive mode, these storms would be more frequent and they would be concentrated in Scandinavia (fig 2.11). Therefore, the NAO affects both the strength and the position of the maximum westerlies and storm frequency and intensity with winter season averaged wind stress having the highest correlation at 60°N and 30°N (Visbeck et al., 2003).

By affecting the wind patterns, the NAO alters the extent of various surface water masses in the Nordic Seas, evidentially affecting the inflow of Atlantic Water into the Norwegian Sea.

During a positive phase, southerly airflow west of Norway greatly strengthens and affects the width of the Norwegian branch of the Atlantic current, making it narrower than usual (Blindheim et al., 2000; Visbeck et al., 2003). NAO forcing is most influential between November and April and can result in surface temperature changes on a scale of 0.5° with local changes in the air-sea heat fluxes being the most likely cause. Some regions have shown differences of up to 2°C for strong NAO events (Visbeck et al., 2003).
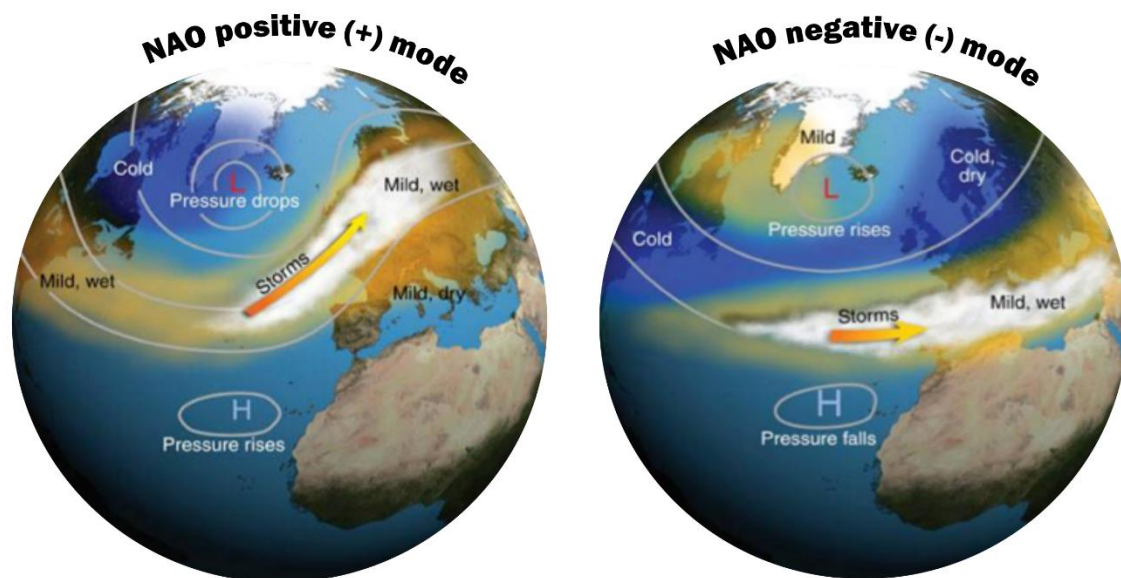
Figure 2.11 Different modes of the NAO. Positive NAO reflects a pressure drop of the Icelandic Low and storm patterns moving over Scandinavia, resulting in mild and wet conditions. Negative NAO reflects a pressure rise of the Icelandic Low and storm patterns moving over the southern part of Europe, resulting in cold and dry conditions in Scandinavia (modified from Climatesnack, 2013).

Between 1970- and mid-1990s there is a documented increasingly positive trend in the NAO index. The 1960s are characterized by large amplitude negative anomalies which change into large amplitude positive anomalies in the 1980s (fig. 2.12). The period of anomalously positive NAO, in addition to influencing the extent of Atlantic Water with strong westerlies, has resulted in notable, local freshening of the upper layers. This can be attributed to an efflux of sea-ice and increased precipitation along the Norwegian Atlantic current (Visbeck et al., 2003). Mork & Skagseth (2012) conclude that changes in circulation and a persistent state of the NAO have contributed to the recent warming trend in the Norwegian Sea (Skagseth & Mork, 2012).

The observed relationship between the NAO and SSTs supports a strong and immediate response of the surface ocean (Kushnir et al. 2002).
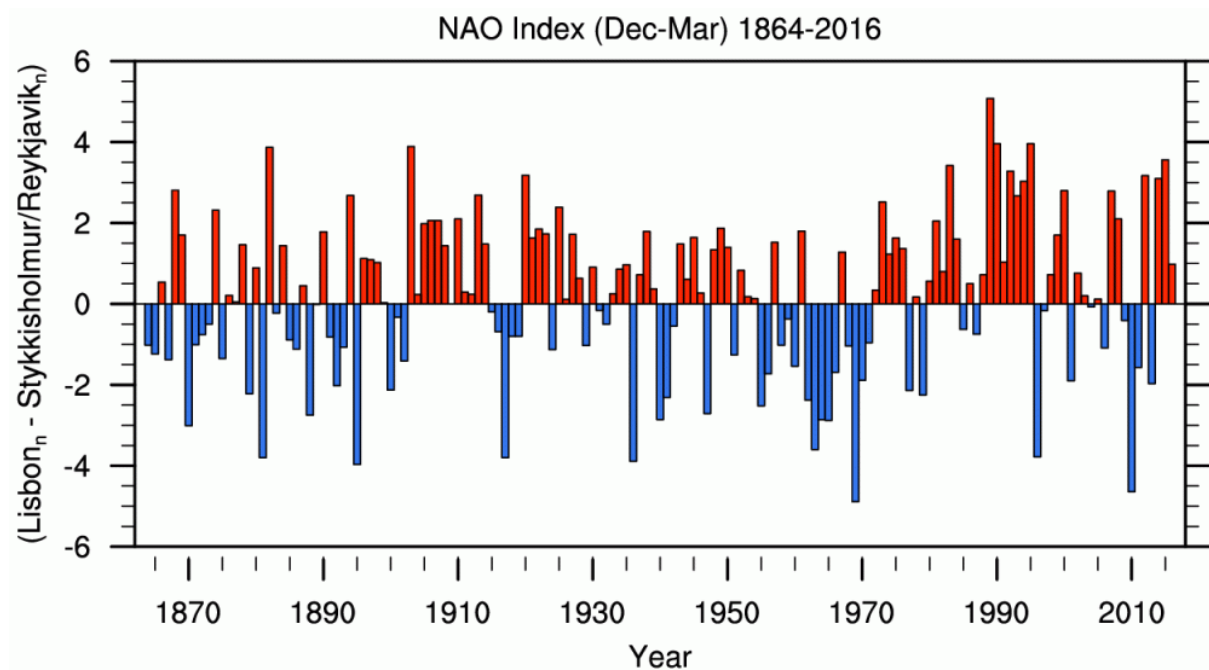
Figure 2.12 The NAO index from 1860 until present. The increasing positive NAO from 1970 to 1990 AD is clear (Hurell, 2016).

A range of mechanisms is believed to influence the NAO variability. Links have been found between changes in SSTs and certain NAO intervals, with the oceanic changes preceding the atmospheric changes by nine months. Stratospheric changes have also been speculated to influence the NAO pattern, preceding anomalous behavior by 1-2 weeks (Hurrell et al., 2003; Marshall et al., 2001). Inter-decadal variations of the NADW formation have been proven to synchronize with fluctuations in the NAO, underlining the dynamic relationship between the THC and the NAO (Hurrell et al., 2003; Marshall et al., 2001).

2.4.2 AMO

The Atlantic Multi-decadal Oscillation has been studied with a particular interest when linked with the THC. As demonstrated in fig. 2.13 the AMO is expressed with an index correlated with SSTs. AMO warm phases are dominant between 1930- and 1960 AD with cold phases occurring from around 1900- to 1925 AD and from 1965- to 1990 AD. These results are based on SSTs,

atmospheric temperatures and precipitation. According to the index we should be entering a warm phase of the AMO with increased summer temperatures and precipitation in western Europe. However, it is not known how the AMO effects will appear in conjunction with anthropogenic forcing (Sutton & Hodson, 2005).
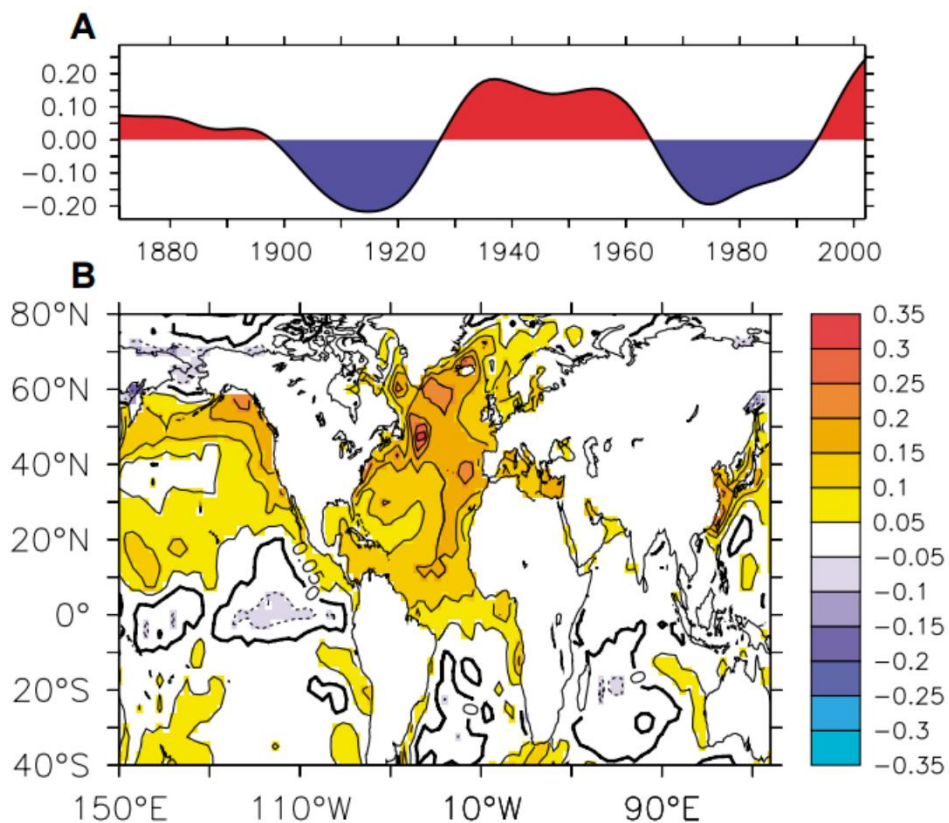
Figure 2.13 The AMO index. (A) shows the AMO index, scaled with °C between 1871- and 2003, based on SSTs observations. (B) shows the spatial variations of the SSTs associated with the AMO variability, clearly concetrated in the North Atlantic (Sutton & Hodson, 2005).

2.4.3 Holocene climate in the Nordic Seas

During the Holocene there have been significant changes in the Nordic Seas climate. From 9000-5000 cal. yr. BP there was a climatic optimum due to increased solar insolation of about 8-10% compared to the present value at 60°N. During this optimum, temperatures were 1.8-2.0°C higher than the average temperature for the last century (Marshall et al., 2001). Multiple recent studies have confirmed that this optimum can be attributed to induced

insolation and alteration by early-Holocene ice sheets and heat transport (Hald et al., 2007; Andersen et al., 2004; Kaufman et al., 2004; Kim et al., 2004). The significance of solar insolation as a direct influence on climate variability has often been overlooked but a direct link between the climate variation trend and solar irradiance has not been established. Result have shown that internal feedbacks predominately drive the variations. Higher frequency climatic variability such as the Medieval Climate Anomaly and the Little Ice Age have been thought to arise from forcing such as freshwater fluxes, volcanism and solar variability (Sejrup et al., 2011; Wanner et al., 2008; Bond et al., 2001). In the Nordic Seas, this variability has been attributed to changes in the inflow of Atlantic Water (Thornalley et al., 2013; Risebrobakken et al., 2011, 2010;). The lack of correlation between solar irradiation and climate is most evident during episodes of cooler climates, with no changes in solar irradiance happening simultaneously. An example of this is the 8.2 ka BP cold event which has been attributed to meltwater drainage of glacial lakes (Muscheler, 2003). However, the coldest period during the Holocene is thought to have been the LIA spanning the years between 1550- and 1925 AD with temperatures 1°C lower than the 20th century average (Marshall et al., 2001).

2.5 Planktonic foraminifera

2.5.1 Structure and ecology of planktonic foraminifera

Foraminifera are marine, free-living, single-celled eukaryotes. They are enclosed by tests that come in a wide range of shapes and sizes. The tests are divided into chambers that increase in number during their lifetime. Secreted tests are predominately composed of calcite and aragonite. There are two types of foraminifera depending on what kind of environment they occupy: benthic and planktonic, the latter being the basis for this study. Planktonic foraminifera have relatively globular chambers for increased buoyancy, allowing them to float in the uppermost layers of the world's oceans (BouDagher-Fadel, 2013).

The two major environmental factors controlling the distribution of planktonic foraminifera are temperature and salinity, with temperature dominating the latitudinal distribution. Certain species govern bipolar provinces, mirrored around the equator, where diversity is the highest (fig. 2.12).
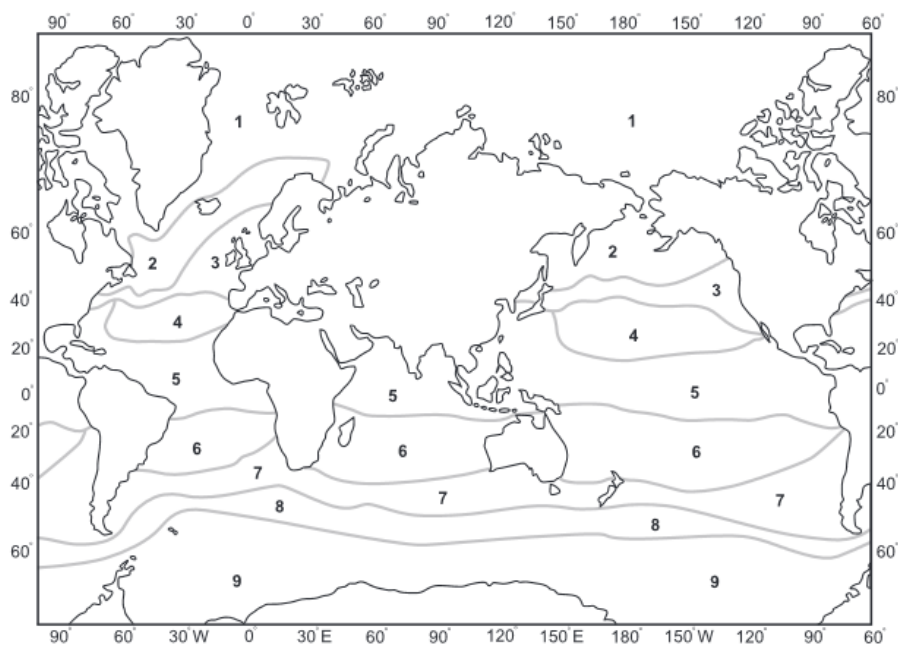
Figure 2.12 Modern planktic foraminiferal provinces. (1) arctic, (2) subarctic, (3) transitional, (4) subtropical, (5) tropical, (6) subtropical, (7) transitional, (8) subantarctic and (9) antarctic (Armstrong & Brasier, 2005).

An example of a high-latitude species is *Neogloboquadrina pachyderma* which is the dominant species in the polar waters of the Northern North Atlantic (Husum & Hald, 2013). A more southerly species is *Globigerina bulloides,* which is more abundant in warmer waters south of Iceland (Fig 2.13). There are around 100 species of living planktonic foraminifera and their importance as biostratigraphical markers lies in their global abundance and rapid evolution (Armstorong & Brasier, 2005). The underlying assumption, that each species of planktonic foraminifera represents a
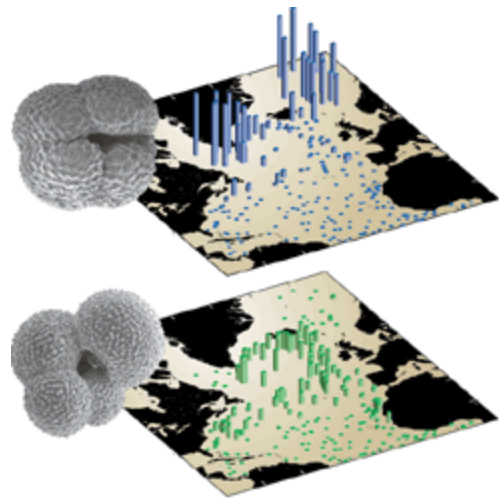
Figure 2.13 N. pachyderma is a polar species while G. bulloides thrives in warmer waters (Curry & Ostermann, 1997).

genetically conservative organsim that prefers a unique habitat is the basis for their use as paleoclimatic proxies. However, identified planktonic foraminifera species traditionally consist of complexes of genetically diverse types. Identification of these morphotypes could increase the accuracy of proxies based on foraminifera but the exact significance of the observed differences has not been fully understood (Kucera & Darling, 2002). The name *N. pachyderma* has long been used for two groups of foraminifera with different temperature preferences, visually distinguishable by coiling-direction. The right-coiling one, which prefers warmer waters, has now been suggested to be recognized as a separate species by Darling et al. (2006) and will henceforth be referred to as *Neogloboquadrina incompta.* However, if the abundance of *N. incompta* is under 3% they should be counted as *N. pachyderma* (Darling et al., 2006).

With temperature as their main restriction, planktonic foraminifera have been widely used for estimating Quaternary sea-surface temperature from the deep-sea fossil records (Armstrong & Brasier, 2005). One branch of these studies focuses on relative abundance studies which incorporates the relative abundance of different species or assemblages with known temperature tolerance parameters. Another method, transfer functions, can reconstruct past marine environments with empirical equations and the comparison to present local fauna assembly (Bradley, 1999). The planktonic foraminifera live in the near-surface layers of the

ocean, predominately at 50-100 m but are known to migrate through the water colum (Husum & Hald, 2013; Armstrong & Brasier, 2005). Since the abundance of foraminifera is highest at a depth of 50-100 m, the foraminifera better represent the near-surface conditions with other organisms such as coccolithophorids and diatoms representing the true surface-conditions (Andersson et al., 2010).

2.5.2 Oxygen isotope signature of planktonic foraminifera

Many important environmental parameters e.g. primary productivity, temperature and atmospheric CO_2 concentration are linked to the chemical composition of calcite in foraminiferal shells (Kucera & Darling, 2002). The analyses of oxygen isotopes can be performed on the calcium carbonate constituting the tests of both foraminifera and coccolithophorids. When the carbonate crystallizes it incorporates the oxygen signal of the surrounding marine environment and preserves it as the organism accumulates at the bottom. The process is temperature dependent locally, with the final isotope signal representing the local temperature and salinity conditions along with the global ice volume (Sejrup et al., 2011, 2010; Bradley, 1999). According to Spero and Lea (1996) the stable isotope signal is affected by the age of the foraminferal test. According to their results *G. bulloides* shows a steady $\delta^{18}O$ increase of up to 0.8 ‰ with shell development from juvenile chambers to the final chamber. Relative to the equilibrium the oldest chambers had depletion of around 1.15 ‰ with the youngest devieting only around 0.30 ‰ (Spero & Lea, 1996).

2.6 Previous research

The cores previously recovered in a close vicinity of the research area are firstly cores P1-003MC/ P1-003SC taken in 1998 at 63°45'44''N; 05°15'19''E and 875 m water depth (Sejrup et al., 2011, 2010), secondly cores MD95-2011/ JM97-948/2A recovered in 1995 at 66°58.19N, 07°38.36E and 1048 m water depth (Andersson et al., 2010; Nyland et al., 2006; Risebrobakken et al., 2003) and core Troll 8903/28-03 collected at 60°52'N, 03°44'E and 345 m water depth along with numerous other adjacent cores (Klitgaard-Kristensen et al., 2001; Haflidason et al., 1998, Sejrup et al., 1994, 1995). The location of these cores can be seen in fig. 2.15. Cores P1-003MC and P1-003SC are located in close proximity of GS13-182-01 at the head of the Storegga slide, with the cores taken at similar depths with comparable oceanographic and atmospheric mechanisms governing the area.

The chronology of cores P1-003MC and P1-003SC is based on ^{210}Pb dates, identification of Icelandic tephra of known age, and wiggle matching of ^{14}C radiocarbon dates. The precise age model, combined with high-resolution sampling of about 12.5 years per sample the cores are well-suited for documenting small-scale changes in the area (Sejrup et al., 2011; Sejrup et al.,
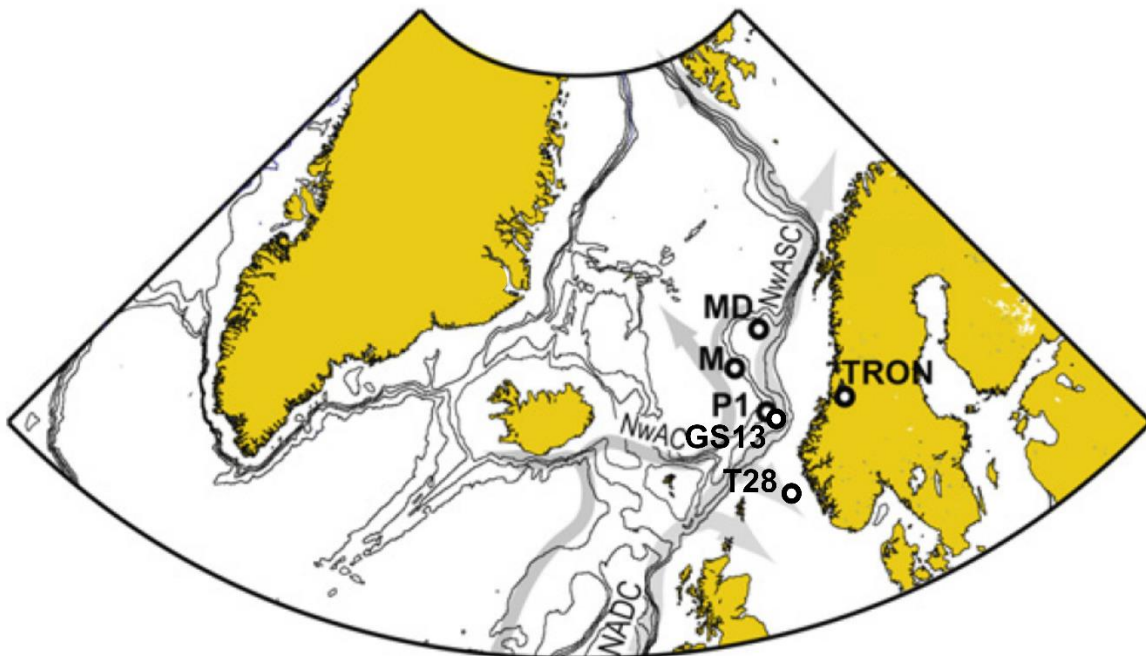
Figure 2.15 Locations of a few paleoclimatic archives. The cores that will be discussed here are P1, GS13, T28 and MD. Also presented are OWSM (M) and Trondheim (TRON). Temperature data will be used from both these localities (modified from Sejrup et al., 2011).

27

2010; Berstad et al., 2003). The age model of core MD95-2011 is based on twelve ^{14}C AMS dates and the presence of the Vedde ash layer. MD95-2011 is situated to the North of our study area (Andersson et al., 2010; Nyland et al., 2006; Risebrobakken et al., 2003). The chronology of Troll 8903/28-03 is based on 22 AMS dates and the identification of the Vedde and Saksunarvatn ash layers and is situated to the south of our study area (Haflidason et al., 1998; Klitgaard-Kristensen et al., 2001). All cores offer good insight into recorded large- and small scale Holocene climate variabilities with stable isotope analysis performed using *N. incompta*. Smaller-scale variability documented during the Holocene are e.g. a ~81-year cycle (Risebrobakken et al., 2003) and decadal to millennial variability recorded in other natural and historical archives (Sejrup et al., 2011). Climatic shifts with longer periodicity on a scale of 1500 years are recorded by both Klitgaard-Kristensen et al. (2001) and Bond et al. (1997).

Klitgaard-Kristensen et al. (2001) focus on the bottom and surface water masses changes since the early deglaciation based on foraminifera assemblages. According to their findings, the magnitude of North Atlantic Water inflow is recorded by the abundance of certain planktonic foraminifera species. Short-lived small amplitude oscillations with an unknown driving force are recorded in the ocean circulation. Risebrobakken et al. (2003) and Andersson et al. (2010) focus on planktonic foraminifera in core MD95-2011. Andersson et al. (2010) conclude that an early-Holocene climate optimum is evident between 11-5 ka BP at the middle to high latitudes of the North Atlantic with a clear maximum at 6 ka BP. However, the optimum is predominately recorded in organism living at the surface e.g. alkenons and diatoms (Andersson et al., 2010). Risebrobakken et al. (2003) conclude that during the early and mid-Holocene there were abnormally cold subsurface conditions at the MD95-2011 coring site as a result of stronger westerlies and eastward migration of subsurface Arctic water. With less atmospheric forcing during late-Holocene, Atlantic water influence increased at the site (Risebrobakken et al., 2003). Sejrup et al. (2010), based on oxygen isotope record from core P1-003 conclude that surface temperatures are being recorded in planktonic foraminifera and that the record has a good correlation with solar variability proxies for the last 1000 years. The decadal to century scale variation is on a scale of 1 to 2°C. Sejrup et al. (2011) furthermore show that the solar variability correlation to the SSTs is less during the whole of the Holocene. Both Sejrup et al. (2011) and (2010) conclude that the proxies are recording North-Atlantic

conditions on a broader-scale as opposed to the local climate of Scandinavia (Sejrup et al., 2010; 2011). In figure 2.16 a comparison of stable oxygen isotopes from P1-003 with both SSTs at OWSM and temperature at Trondheim is presented. In the discussion, the stable oxygen isotope data from GS13-182-01 will be compared to these results. As with previous studies of climate variations in historical times, instrumental data will be used as reference, in this case data from Weather

Figure 2.16 Results from Sejrup et al. (2011) where stable oxygen isotopes are compared to JAS temperature at OWSM and Trondheim (Sejrup et al., 2011).

Station Mike (OWSM) (figure 2.15). OWSM has documented changes in the hydrography of the area since 1948 and produced data important for climate observation and reconstruction during this time period (Drange et al., 2005).

3 Materials and methods

This study presents new high-resolution planktonic foraminifera assemblage analyses and stable isotope data from core GS13-182-01. In addition, some sedimentological and chronostratigraphic analyses largely performed by Lukas Becker at the University of Bergen are included (Becker et al., in prep). The core was obtained during Institute for Marine Research (IMR) cruise no. 2013108 and University of Bergen cruise no GS-13-182 spanning the time period of 25th -26th of June 2013 (Hjelstuen, 2013).

3.1 Field methods

3.1.1 Research vessel

Coring took place on the research vessel G.O.SARS which is owned by the University of Bergen and the Norwegian Institute of Marine Research, with a length of 77.4 m and top speed reaching 17.5 knots. It has noise reduced engines, two sheltered hangers and heavy duty cranes to maneuver various equipment for environmental and geological research (Hjelstuen, 2013).

3.1.2 TOPAS profile

To determine the optimal location for the calypso coring, one roughly 3 km long, E-W trending, seismic profile was assembled in the Storegga Slide. To obtain the profile a TOPAS PS18 system was used. It is a single, narrow beam sub-bottom profiler system with various different pulses available. The system is set according to depth and locality, with higher frequencies yielding higher resolution but penetrating shallower. In this case the Chirp (LFM) pulse was applied during the whole cruise. Chirp waveforms are a burst of two high frequency waves used to increase the total transmitted energy which results in increased signal-to-noise ratio and subsequently expanded penetration.

The profile and coring location can be seen in figure 3.1. The thickness of the Holocene package can be seen above the sediments from the Storegga slide (Hjelstuen, 2013).
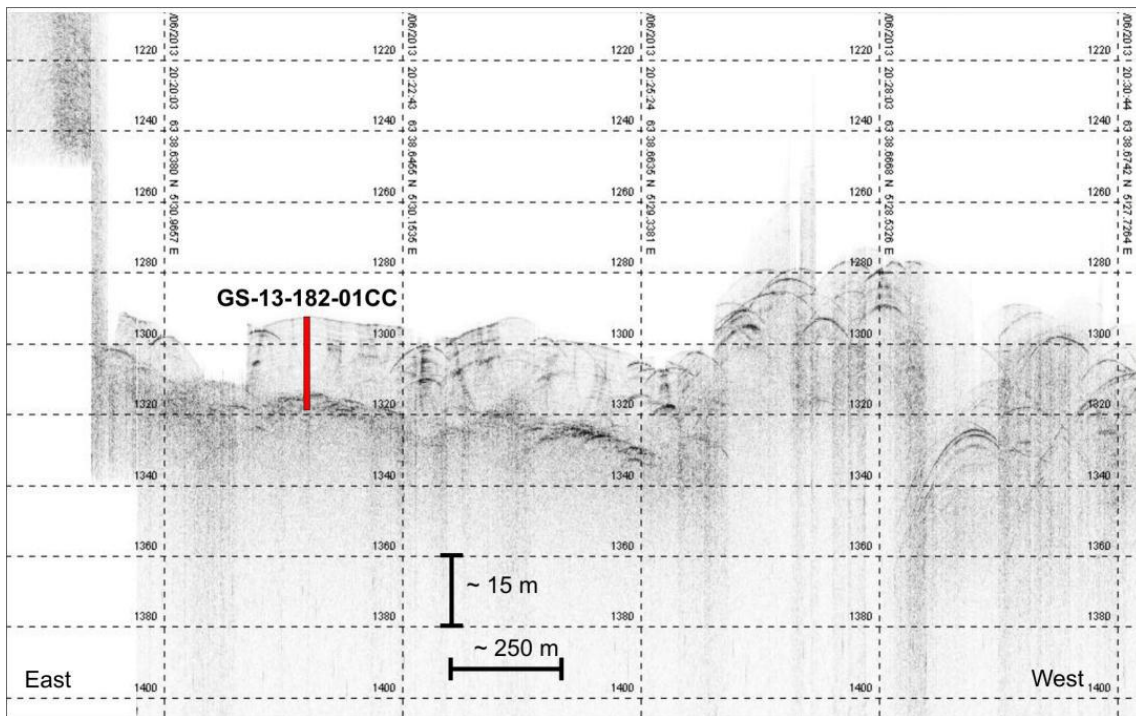
Figure 3.1 The ~3 km long Topas profile taken as a part of coring GS13-182-01, at the head of the Storegga slide (Hjelstuen, 2013).

3.1.3 Coring

Weather conditions were optimal while coring took place, with a calm sea and wind speed of 5 kt. A calypso corer with an added weight of 500 kg was used to obtain the 19.7 m long core at 63° 38.643 N, 5° 30.480 E, Ormen Lange and water depth of 960 m. Total number of sections was fourteen, from A1/A2 to M (Hjelstuen, 2013). Marine sediment archives can be affected due to the coring process with core top sediments being most prone to disturbance.

3.2 Lab methods

3.2.1 Sample preparation

The core was sampled every 0.5 cm starting from the top of the core, leaving at least 0.5 cm between the plastic liner and the sample material. Each sample was marked with an index number and sample depth and weighed before and after drying for at least 24 hours at 50°C. The samples were prepared in a flask with distilled water and H_2O_2 and put on a shaking table for at least 48 hours, letting gas escape through the unsealed lid. The samples were wet sieved with the sieve sizes 63, 125, 150 and 1000 µm, dried and brushed into a brass tray and weighed. Finally, the samples were put in glass within their grain size fraction.

3.3 Chronology

The age model was largely based on the same methods used for the accurately dated P1-003 core which was retrieved 18 km NW of GS13-182-01 (Sejrup et al., 2010). In the case of P1-003, the age model is based on ^{210}Pb and ^{137}Cs dating (Berstad et al., 2003) and identification of historic tephra from eruptions in 1947 AD (Hekla), 1918 AD (Katla) and 1875 AD (Askja) with the largest deviation being 1-12 years for Askja (Haflidason, 2000). For older parts of the historical record, a "wiggle-match" method (Pearson,1986) is used for the ^{14}C age of planktonic foraminifera (Sejrup et al., 2010).

The age model for GS13-182-01 is constructed by Bayesian age modelling through the R-based script BACON (v.2.2) (Blaauw et al., 2011). Within BACON all ages are calibrated with the Marine13 calibration curve which includes a global reservoir effect correction of 405 years (Reimer, 2013). Furthermore, the local reservoir correction (delta R) of Sejrup et al. (2010), 160 years after 1000 years BP and 175 years before 1000 years BP is applied to the age model. The GS13-182-01 age model consists 4 Accelerator Mass Spectrometry (AMS) ^{14}C dates on planktonic foraminifera. The top 50 cm of the core are dated using ^{210}Pb dating. In the top part, ^{137}Cs is measured as well. Since Caesium does not occur naturally, higher concentration indicate when atomic bombs are tested or used. The curve first shows an increase from zero in 1945 with the bombing of Hiroshima and Nagasaki, then a maximum of bomb tests in 1963 and lastly a large peak during 1986 due to the exploding reactor in Chernobyl (Becker et al., in

prep.) If the sedimentation rate between 1945 and 1963 is calculated and applied to the decades until present times the result is that 0 cm (core top) is from the year 2010.

Additionally to the ^{14}C and ^{210}Pb dating, a "peak-to-peak" correlation with the Ca/Fe curve of core GS13-182-01 and Ca/Fe curve of core P1-003 are applied, resulting in 29 tie points (Becker et al., in prep). The result of the age model run in BACON can be seen in figure 3.2. The grey zone behind the black line indicates the 95% significance envelope (2σ). The completed age model is presented in figure 3.3. (Becker et al., in prep).
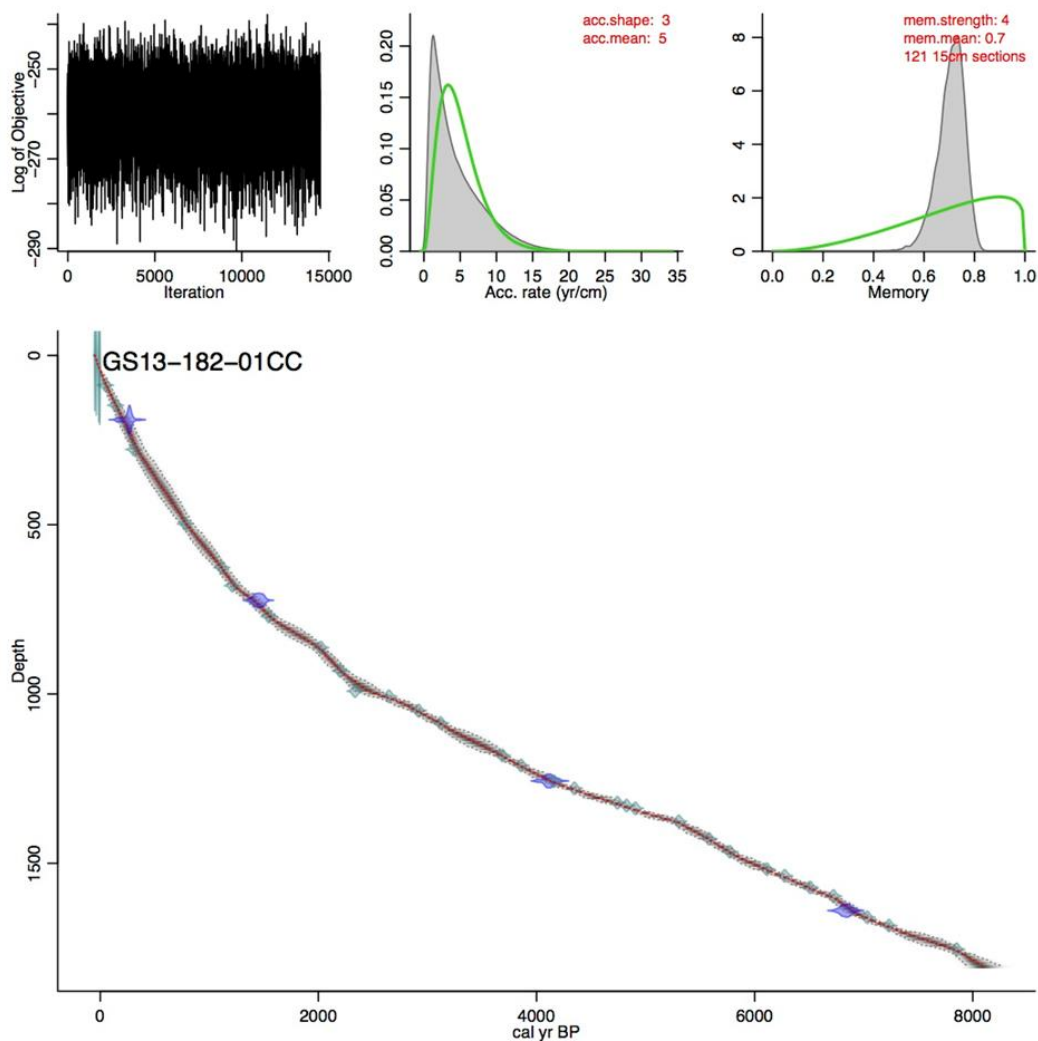
Figure 3.2 Results from the BACON run for the GS13-182-01 age model (Becker et al., in prep).
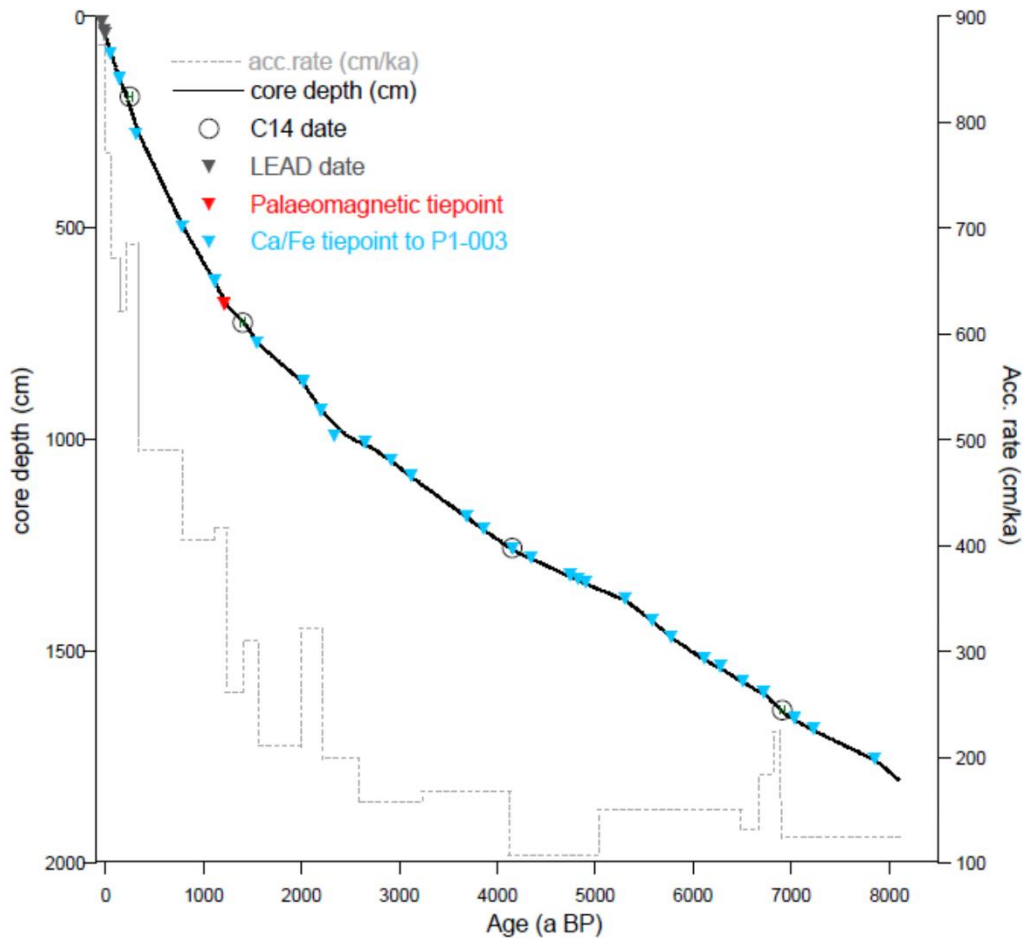
Figure 3.3 The age model used for GS13-182-01, with dated levels and Ca/Fe tiepoints indicated. The black line marks the weighted mean age-depth relationship. The accumulation rate is given in the stippled line (Becker et al., in prep).

Sedimentation within the Storegga slide area is believed to be several millimeters per year. For core P1-003 the sedimentation rate results in a resolution of 2.5–10 years in single 0.5 cm to 1.0 cm thick sample (Sejrup et al., 2010). In core GS13-182-01 the top 90 samples cover the last 50 years, meaning that each year is represented by 5.8 mm accumulation of hemi-pelagic sediment. Therefore each year is covered by 1-2 samples within this interval. The high-resolution is beneficial if the established age model is reliable. When concluding about high-frequency events in these types of marine archives the age model can be an important source of error. According to calculations from Becker et al. (in prep.) the ± 2 sigma error of the age model indicates that the uncertainty at the very top of the core is ±6 years and thereafter more or less constant at ±4 years. For core P1-003 the uncertainty is less than 10 years for the period between 1850 and 1998 AD (Sejrup et al., 2011).

3.4 Foraminifera analysis

The foraminifera analysis of core GS13-182-01 was performed in two steps. Firstly, 30 samples were chosen with a spacing averaging 250 years throughout the whole core. These samples constitute for an overview of the whole core which spans the time from 8000 year BP. Secondly, a high-resolution study consisting of 90 samples analyzed from the top of the core (2000 AD) to a depth of approximately 52.2 cm, covering the last 50 years was conducted. All samples were counted in the size fraction >150 µm. The samples needed no splitting and in all cases all planktonic foraminifera in the samples were picked and counted. Due to the high sedimentation rate in the area the samples generally contained around 200 foraminifera. Ideally >300 foraminifera should be counted in each sample (Klitgaard-Kristensen et al., 2001). The abundance of foraminifera generally but not regularly increased with depth. The samples could have been merged to fulfill the >300 requirement but a decision was made to analyze the data as it appears throughout the core segment. The assemblage analysis was conducted using the LEICA M125 optical microscope at the University of Bergen. After counting, 25+ individuals of the species *N. incompta* were gathered on a separate slide for oxygen and carbon isotope analyses.

To visually document the planktonic foraminiferal taxa identification, Scanning Electron Microscopy (SEM) was used. SEM can be used for a wide range of analyses and imaging of various surfaces. When examining samples, conductivity throughout the sample and the base is of vital importance. In this case, the foraminifera were picked, put on a carbon tape covering the top of an aluminum stub and coated with gold-palladium to ensure this conductivity. The coating was performed in a sputter coater in a ratio of 40/60 respectively. In a sputter coater the coating is applied in a vertical direction in vacuum (Irene Heggstad, personal communication, June 13, 2016). After preparation of the samples they were examined and photographed in the Zeiss Supra 55 VP microscope at University of Bergen. Minor issues came up because of charging foraminifera, most likely due to small contact area with the carbon tape, which can be attributed to their round shape. Apart from that, the process was greatly successful and yielded numerous detailed images of the foraminifera.

The identification of the different foraminifera was based on information from the 'Marine Species Identification Portal' (MSIP, 2016) and 'World register of Marine Species' (WORMS, 2016) with helpful tips from Sædís Ólafsdóttir, Nil Irvali and Vigdis Hope. V. Hope furthermore recounted a control sample with minimal deviation in results. In figure 3.3 the most abundant species of planktonic foraminifera found in core GS13-182-01 can be seen.

Table 3.1 The most abundant species of planktonic foraminifera in core GS13-182-01

Species in order of discovery
Globigerina bulloides (d'Orbigny, 1826)
Turborotalita quinqueloba (Natland, 1838)
Globorotalia inflata (d'Orbigny, 1839)
Orbulina universa (d'Orbigny, 1839)
Neogloboquadrina pachyderma (Ehrenberg, 1861)
Globigerinita uvula (Ehrenberg, 1861)
Globigerinita glutinata (Egger, 1893)
Neogloboquadrina incompta (Cifelli, 1961)
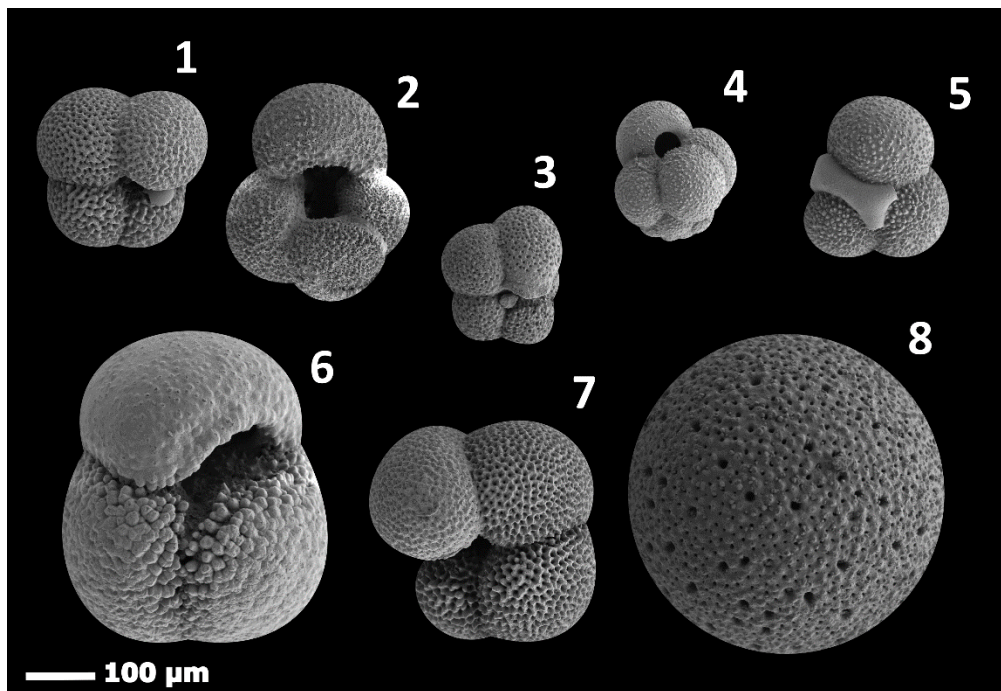
Figure 3.3 The most abundant planktic foraminifera species found in core GS13-182-01. (1) *N. pachyderma*, (2) *G. bulloides*, (3) *T. quinqueloba*, (4) *G. uvula*, (5) *G. glutinata* (6) *G. inflata*, (7) *N. incompta* and (8) *O. universa*.

Both *T. quinqueloba* and *G. uvula* are easily recognizable due to their relatively small size and *O. universa* and *G. inflata* due to their relatively large size and distinct shape. Looking at the foraminifer from all angles can aid in identification. An example of this is *G. bulloides* shown in fig 3.4.
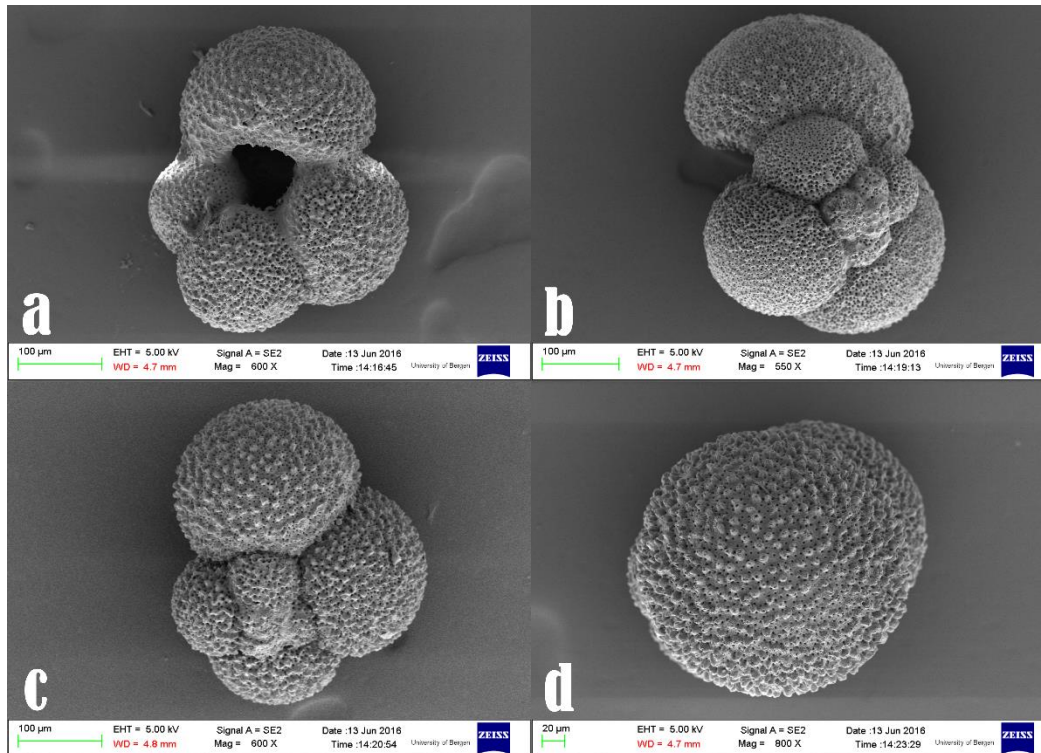
Figure 3.4 *G. bulloides*. (a) umbilical side, (b) spiral side, (c) back view, (d) top view.

In figure 3.5 (a) few examples of the species *N. incompta* are presented. Picture (a) shows an individual who is not fully grown. The last chamber has evidently not reached its full size when compared to picture (b). Pictures (c) and (d) show two more individuals of *N. incompta* where the last chamber is considerably larger. Figure 3.5 shows the species *G. inflata.* Pictures (a) and (b) show two different individuals while (c) and (d) show back and top view. Lastly, broken and unknown foraminifera were counted separately with those counts predominately consisting of broken, unrecognizable foraminifera.
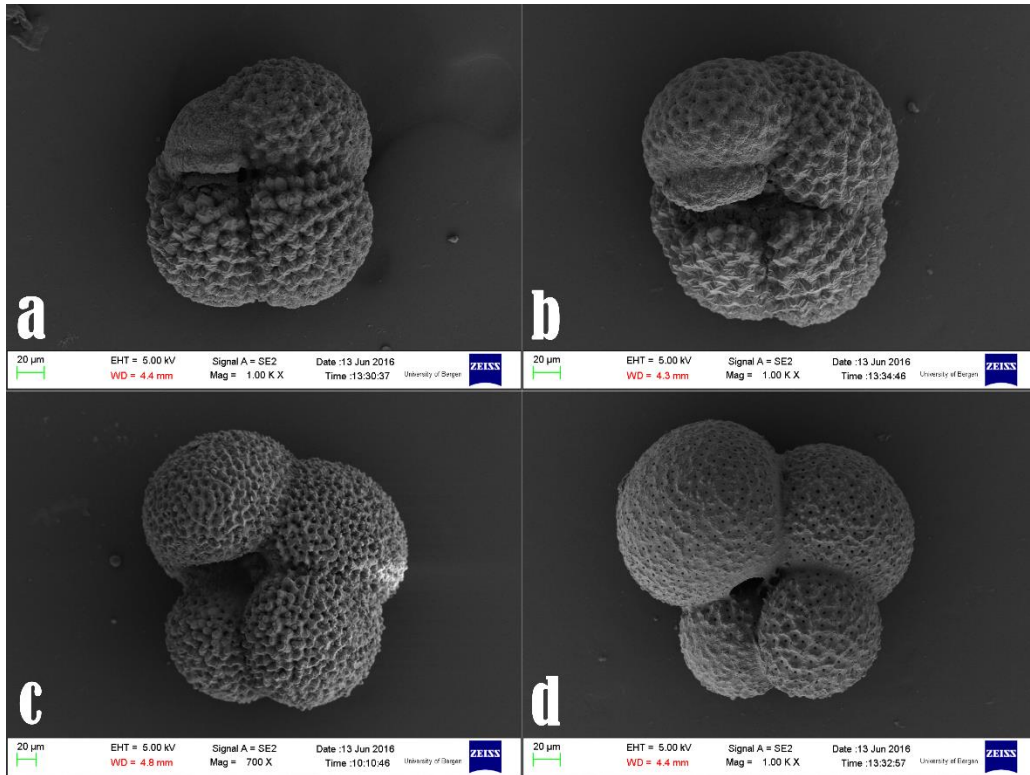
Figure 3.4 *N. incompta* showing different morphologies.
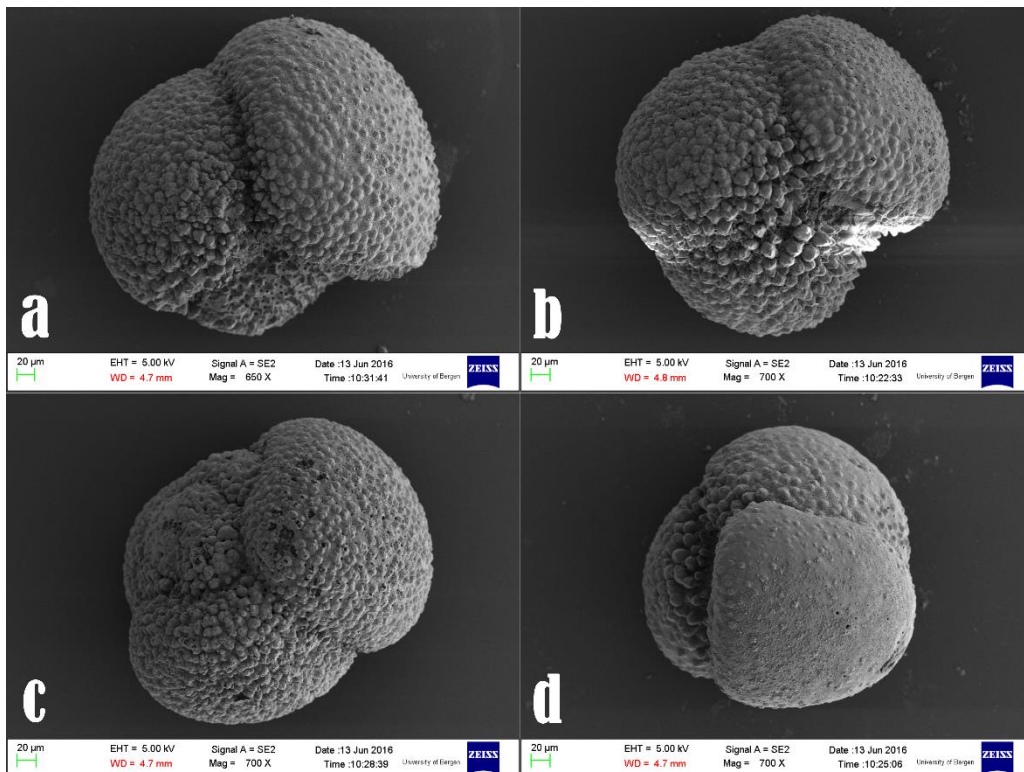
Figure 3.5 *G. inflata*. (a) and (b) different morphologies umbilical side (c) back view, (d) top view

3.5 Isotope analyses

Isotope analyses was performed by Rune Egil Søraas at the University of Bergen. The method involves cleaning the carbonate before analysis, extraction of carbon dioxide for mass spectrometric analysis and comparison of the isotopic signal of the gas and a laboratory standard (Shackleton, 1974).

3.5.1 Stable Isotope analysis

Study of stable oxygen isotopes in ice- and marine sediment cores has greatly aided paleoclimate research. The method is based on analyzing fossil water in terms of isotope distribution either as ice or, as in this case, through material deposited from solution. The underlying assumption is that the foraminifer, in this case *N. incompta* calcifies in equilibrium with seawater (Poole, 1994). When calcium carbonate, which forms the bulk of the foraminifera test, crystallizes in water ^{18}O is concentrated in the test relative to the water. Subsequently, the water will have a higher concentration of the lighter isotope ^{16}O. This deviation is compared to the standard isotopic composition of water which is referred to as SMOW (standard mean ocean water). The result is expressed as $\delta^{18}O$ as can be seen in the equation below (Shackleton, 1974; Bradley, 1999).

$$\delta^{18}O = \frac{\left(\frac{^{18}O}{^{16}O}\right)_{sample} - \left(\frac{^{18}O}{^{16}O}\right)_{SMOW}}{\left(\frac{^{18}O}{^{16}O}\right)_{SMOW}} \times 10^3\ ‰$$

The $\delta^{18}O$ of planktonic foraminifera is controlled by the temperature and salinity of the ocean water they live in, which in turn is affected by the global ice volume. The fractionation process of the isotopes is highly dependent on temperature and isotopic analysis can therefore shed a light on palaeotemperatures. The rule of thumb states that each isotopic change of 0,23‰ redirects to a change of 1°C, if temperature is the only variability, with higher values indicating a colder setting (Shackleton, 1974). If the temperature is fixed it has been suggested that a change of 0,6‰ in $\delta^{18}O$ corresponds to a 1‰ change in salinity (Craig & Gordon, 1965) This is evident for the North Atlantic, with the relationship in the Nordic Seas being closer to 0,2-

0,3‰ $\delta^{18}O$ for every 1 ‰ PSU (Israelson & Buchardt, 1991). According to data from Weather Station M, salinity changes in the area at 50 m depth are on a scale of 0,15 ‰ on an inter-annual bases. The monthly variation has been recorded to reach slightly higher values. Sejrup et al. (2010) calculated that the salinity contributed insignificantly to the $\delta^{18}O$ in core P1-003 when compared to temperature. It is to be expected that the same will apply for the signal in core GS13-182-01 and that the oxygen isotope changes in *N. incompta* predominately reflect temperature changes (Sejrup et al., 2010).

3.5.2 Previous stable isotope studies

The accurate chronology of core P1-003, supported by wiggle matching and tephrochronology, yielded an extremely detailed age model. Precise dating is important when comparing stable oxygen isotope records to instrumentally gathered data. In the case of core P1-003, the isotope record was compared to air temperature records from Trondheim, provided by the Norwegian Meteorological Institute and SSTs from OWSM (Sejrup et al., 2011). Sejrup et al. (2011) suggest that the 2.5 and 7-year average summer temperature variability in Trondheim is captured in the isotope data. However, both the P1-003 isotope record and near-surface temperature data from OWSM do not show a clear decreasing trend in temperatures indicated in Trondheim for the past 60 years. Thus, the signal is thought to be more related to a North Atlantic oceanic signal, rather than climate variability in western Norway (Sejrup et al., 2011).

3.5.3 Complications with isotope analyses

The results from the isotope analysis of core GS13-182-01 were in part unexpected when compared to the results from core P1-003. The uppermost part of the core was characterized by short bursts to heavier isotopes, well out of the range of natural temperature changes. According to lab technicians at the University of Bergen this could be related to complications with lab equipment. Five samples in total were rerun, returning similarly heavy values. The period where these bursts are not seen is considered to be more reliable when interpreting the results.

3.6 Parallel research

Lukas Becker analyzed considerable amounts of data from core GS13-182-01. The ones relative to this study will be presented here and used for later discussion. This includes grain size (3.6), concentrations of foraminifera per gram dried sediment, water content (fig 3.7) and carbonate content (fig 3.8).

3.6.1 Grain size

The grain size analysis was done with the standard sizes of sieves: 1000 μm, 150 μm, 100 μm and 63 μm. Most variability can be seen in size fractions >150 μm and >63 μm, with both fractions showing slight increase towards present times. The only event that can be seen in all fractions is a peak in 1991. Several peaks can be seen in individual fraction sizes.
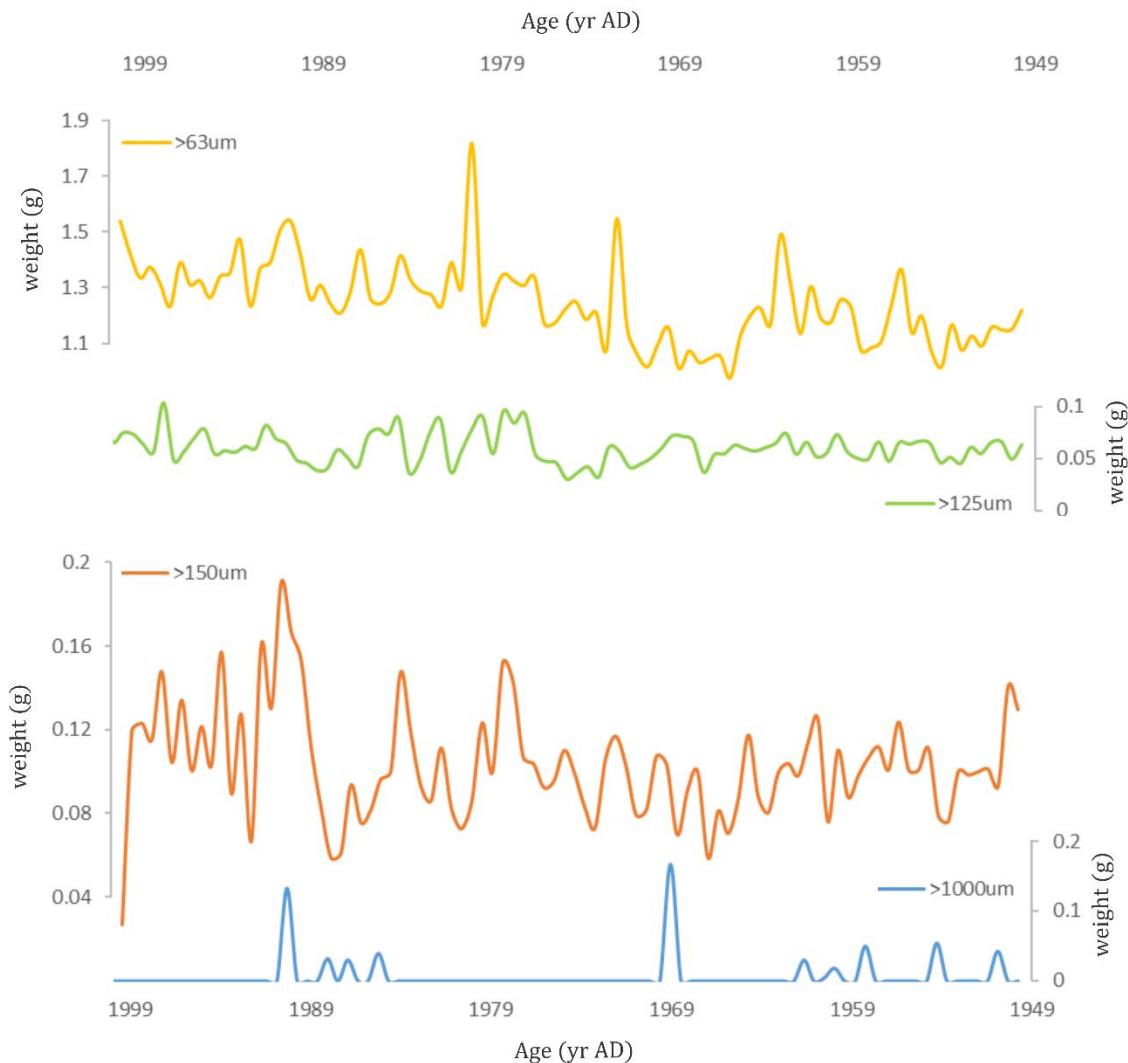
Figure 3.6 Grain size results from core GS13-182-01 (Becker et al., in prep).

3.6.2 Water content and concentration of foraminifera

Since the samples are taken from the top of the core, some variability, especially in the uppermost part can be attributed to the calypso coring effects. It is common knowledge that the top of a core is more prone to watering effects and disruption then deeper parts. In figure 3.7 (a) the concentration of foraminifera per gram dried sediment results are presented. According to the marker placement, the shifts to higher and lower contents of foraminifera are marked by more than just single samples, which strengthens the argument that the variability is real. The clearest observation made from the graph is that the foraminifera content increases with depth, which was to be expected from a core segment with watered down core top. However, the lowest foraminifera count, with a low variability, are in a period from approximately 1975-1990. Towards the very top of the core the concentration increases again.

The water content curve shown in figure 3.7 (b) suggests that the core segment was not as watered down as expected, since it shows low variability. The scale of this small variability is only between 58-61% with two distinct drops in 1971 and 1993. This is known to be the result of the lab work process, where a batch of samples was left out to dry while other samples were being prepared. In later discussion, the water content will therefore not be considered a major factor in interpreting the results of the analysis. The concentration of foraminifera should be considered more important in interpretation of the results.
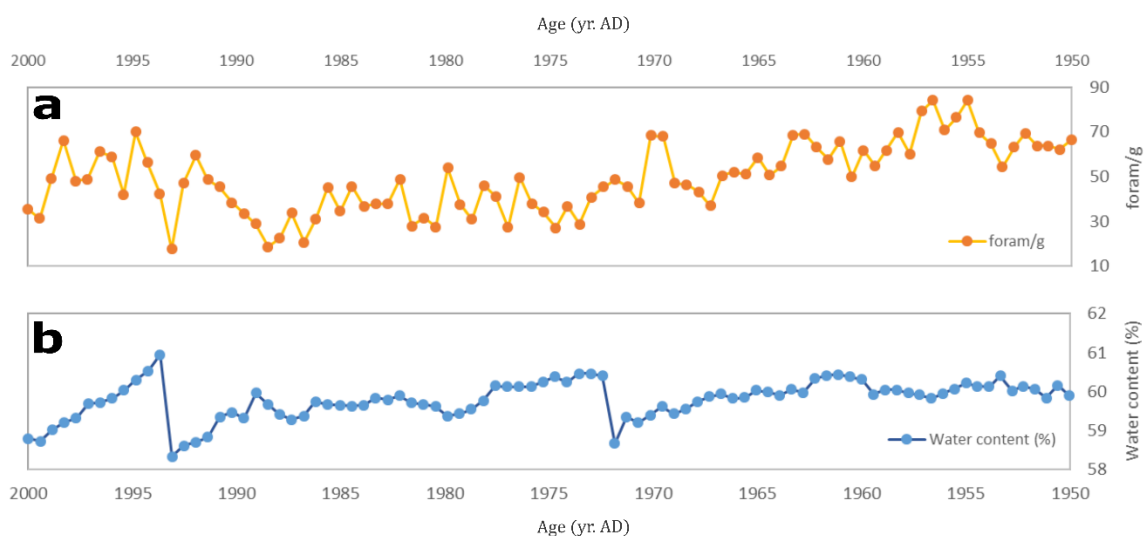
Figure 3.7 Water content and the concentration of foraminifera results from core GS13-182-01 (Becker et al., in prep).

3.6.3 Ca/Fe

An ITRAX scanner is used for high-resolution XRF analysis of sediment cores and measures 24 relative element concentrations for every measured point. The Ca/Fe curve was obtained using the results from this analysis, by deviding the relative concentration of Calcium with the relative concentration of Iron to normalise the Calcium values (Becker et al., in prep). Kjennbakken et al. (2013) studied the Ca/Fe signal from core P1-003 and those results will be discussed in relation to the GS13-182-01 curve in later chapters.
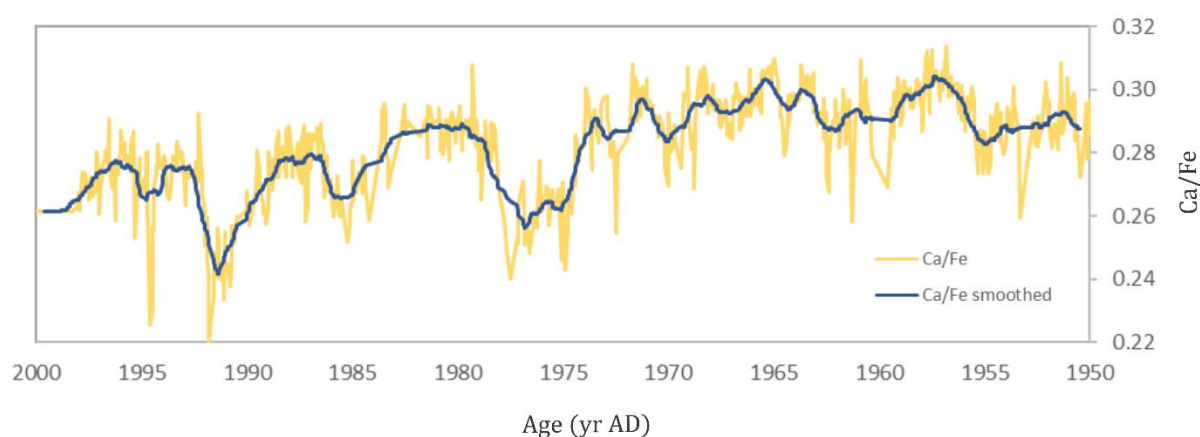
Figure 3.8 Ca/Fe results from core GS13-182-01 (Becker et al., in prep).

4 Results

4.1 Foraminifera analysis

The results of the foraminifera analysis will be twofold, first the 30 samples constituting the planktonic foraminifera overview of GS13-182-01 covering the time period from 7927- to 437 cal. yr. BP, according to the age model by Becker et al., (in prep.), will be presented in chapter 4.1.1. Secondly, the 90 samples between 1949-2000 that are predominately the focus point of this study will be presented in chapter 4.1.2. In brief, the results largely agree with previous studies in the area. According to previous studies the most abundant species in the area are *N. incompta, T. quinqueloba, G. bulloides* and *N. pachyderma* (Husum & Hald, 2013; Andersson et al., 2010; Risebrobakken et al., 2003; Klitgaard-Kristensen et al., 2001; Johannessen et al., 1994;). The results here show *N. incompta, T. quinqueloba* and *G. bulloides* as the three most abundant species.

4.1.1 Overview sampling analysis

The results from the overview sampling analysis can be seen in figure 4.1. The most prominent changes are the shift of the species *N. incompta* towards higher abundances during late-Holocene with the species *N. pachyderma* simultaneously shifting towards lower abundances, when compared to the late-Holocene period. During the mid-Holocene, between 8000-7000 cal yr. BP there is a distinct maximum of the species *O. universa, G. glutinata, G. inflata* and *N. pachyderma*. During the same period, *N. incompta* and *G. uvula* are in record lows. Between 6000-2500 cal. yr. BP *N. incompta* keeps a steady value between 40-70%, *G. quinqueloba* between 5-15% and *N. pachyderma* below 10%. *G. uvula* shows a distinct peak at 3500 cal. yr. BP. From 2500 cal. yr. BP until present *N. incompta* drops from a high of 70% to a minimum of 40%. Simultaneously, *G. bulloides* reaches a maximum of almost 30%. Other species, apart from *G. glutinata* seem to show a slight increase in abundance during this period.
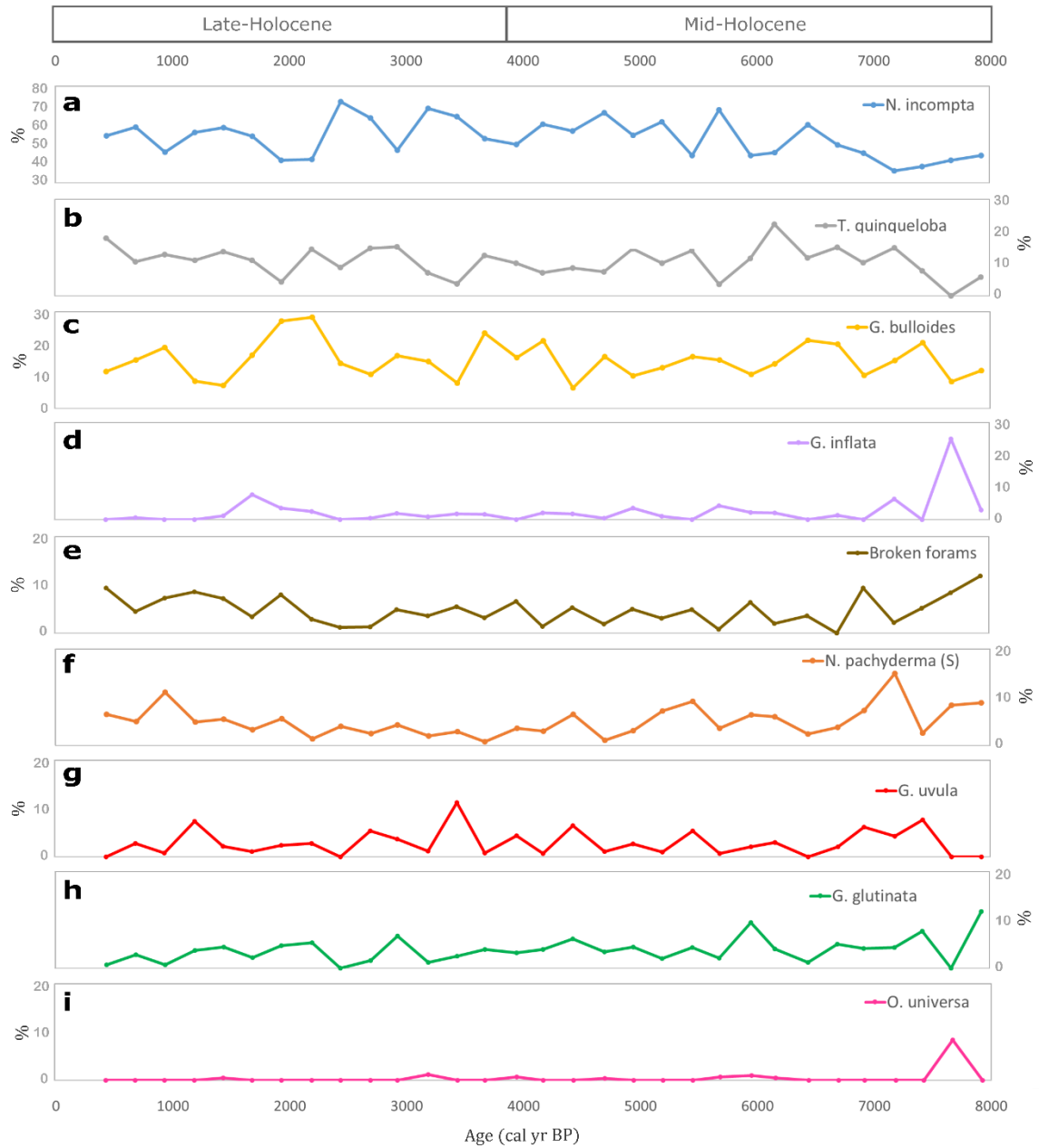
Figure 4.1 Results from the foraminifera analysis of 30 samples between 8000-400 cal. yr. BP from core GS13-182-01, (a) *N. incompta*, (b) *T. quinqueloba*, (c) *G. bulloides*, (d) *G. inflata*, (e) broken forams, (f) *N. pachyderma*, (g) *G.uvula*, (h) *G. glutinata*, (i) *O. universa*.

45

4.1.2 Analysis between 1949-2000

Results from the foraminifera analysis between 1949-2000 AD can be seen in figure 4.2 and figure 4.3. In this segment the results will be presented systematically according to decade. Distinctly dominating the fauna assembly is *N. incompta*, with variability between a little less than 50% up to almost 80%. Following are *G. bulloides* and *G. quinqueloba* with predominate abundances of 5-15% and 5-20% respectively.

Between **1950-1960** AD *N. incompta* increases in abundance from 65% to 80%, which is the maximum abundance it reaches throughout the whole studied period. *N. pachyderma* and *T. quinqueloba* both have low values, the latter one abnormally when compared to other periods. This is accompanied by low variability for this species. The *T. quinqueloba* abundance progressively increases in variability from 1949 to the present day. During this decade, other species generally have median values when compared to later times.

Between **1960-1970** AD there are subtle changes in the abundance of certain species. *N. incompta* decreases in abundance to around 65%. *G. bulloides*, *G. glutinata* and *G. uvula* increase their values slightly. *N. pachyderma* reaches higher values, varying slightly below 10%, previously below 5%. *T. quinqueloba* increases its value rapidly from 5% to 15%.

Between **1970-1980** AD *N. incompta*, *G. bulloides* and *G. uvula* start to decrease in abundance. Throughout the whole period *G. bulloides* has small variability in abundance with values mostly fluctuating just below 10%. Just before 1970 the abundance decreases until it reaches a minimum around 1980. *G. glutinata* and *G. inflata* both start to rapidly increase in abundance with *G. glutinata* reaching its maximum of 18% in 1980 and *G. inflata* having a burst of 9% in 1975. *N. pachyderma* reaches mininum values again after having relatively high values for two decades. *G. quinqueloba* shows a great range of variability in this decade, going from <1% to reaching a maximum of 22% in 1975.
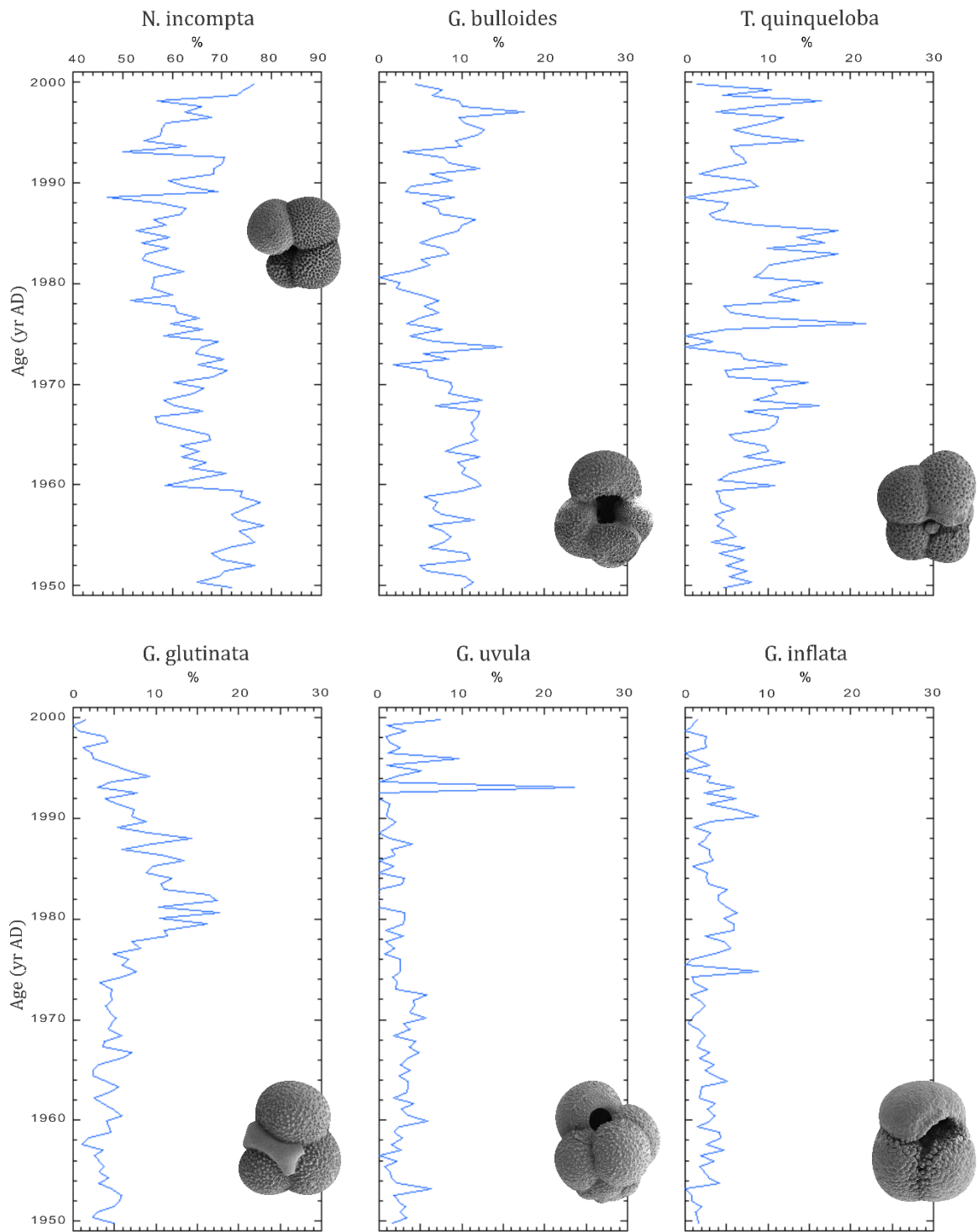
Figure 4.2 Results from the foraminifera analysis of 90 samples between 1949-200 AD from core GS13-182-01.
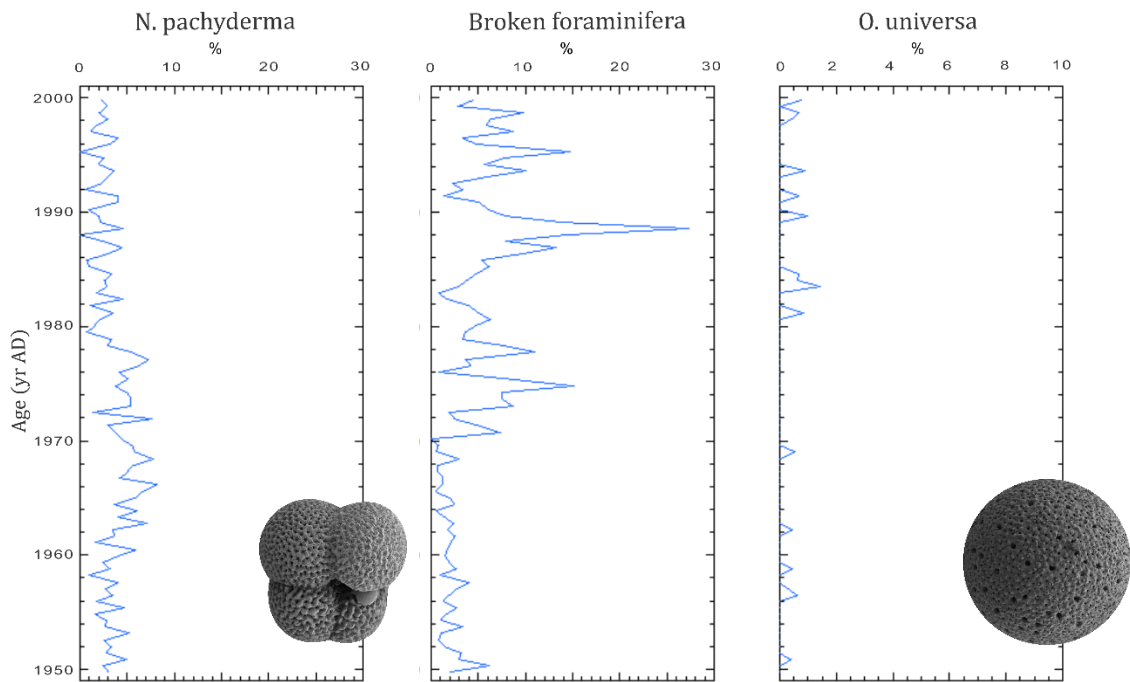
Figure 4.3 Results from the foraminifera analysis of 90 samples between 1949-200 AD from core GS13-182-01.

Between **1980-1990** AD *G. glutinata* and *G inflata* decrease in abundance, *N. pachyderma* and *G. uvula* still has low values. *N. incompta* reaches its lowest values, *G. quinqueloba* has values of 20% until the period of steady increase terminates abruptly in 1985, reaching a low of <1% before continuing to increase in abundance towards the present day. During this decade, *G. bulloides* slightly increases in abundance and broken foraminifera reach their maximum of >25%.

Between **1990-2000** AD *G. inflata* and *G. glutinata* continue to decrease in values. *G. uvula* has a sudden burst that reaches 23% in 1993 and continues to stay relatively high towards the year 2000 AD. *T. quinqueloba* and *G. bulloides* show significant variability with the latter showing values similar to 1950-1960. *N. incompta* increases in abundance, reaching similar values as the maximum between 1950-1960. *O universa* shows more peaks between 1980-2000 when compared to previous decades, staying under 2% at all times.

When looking at these results there are a few comments to be made. *N. pachyderma* was not as abundant as expected with the species varying below 5% at most times. For the Holocene period the species is more abundant, varying around 10% and reaching 20% during mid-Holocene. Between 1960-1980 the abundance slightly increases and reaches up to 8% several times in that period. This species is more abundant in the results from Risebrobakken et al. (2003) with values predominately fluctuating around 20-40%.

Broken foraminifera were the ones unidentifiable because of partial breakage of the tests. Conclusions based on these results should be kept to a minimum since the breaking of the foraminifera tests can be the result of lab preparation, such as sieving. However, the numbers of broken foraminifera increases significantly after 1970 with a distinct top of 27% in 1988 AD. Broken foraminifera during the Holocene period stay below 10% at all times. That indicates abnormality in the samples showing higher values during the period between 1970-1990 AD. Lastly, the least abundant species, but the most distinct one, *O. universa* has only a few individuals in some samples. Though not really discernable, the abundance seems to be higher after 1980 AD.

The results from the foraminifera analysis can be summarized as indicating a distinct change in environment mode happening around 1970, with that period of distinct change often lasting until mid-1990s, depending on the species. *T. quinqueloba* seems to follow a different pattern when compared to the other species. *N. incompta* clearly dominates the assembly and can therefore make a strong argument in later concluding discussions. Each species has a preference when it comes to their environment and their abundances can therefore shed a light on which water masses where dominating in which periods. This will be discussed in more detail in the following chapters.

4.2 Stable isotopes

The results from the stable isotope analyses can be seen in figure 4.4. The carbon record has limited informative value for this study but the graph shows a clear trend towards lower values with time. The oxygen shows a very different trend. This oxygen isotope analysis is first of its kind in this region, with previous work not focusing on the high-resolution aspect. The results should be concluded on with caution since they clearly have a different trend within the same core section.
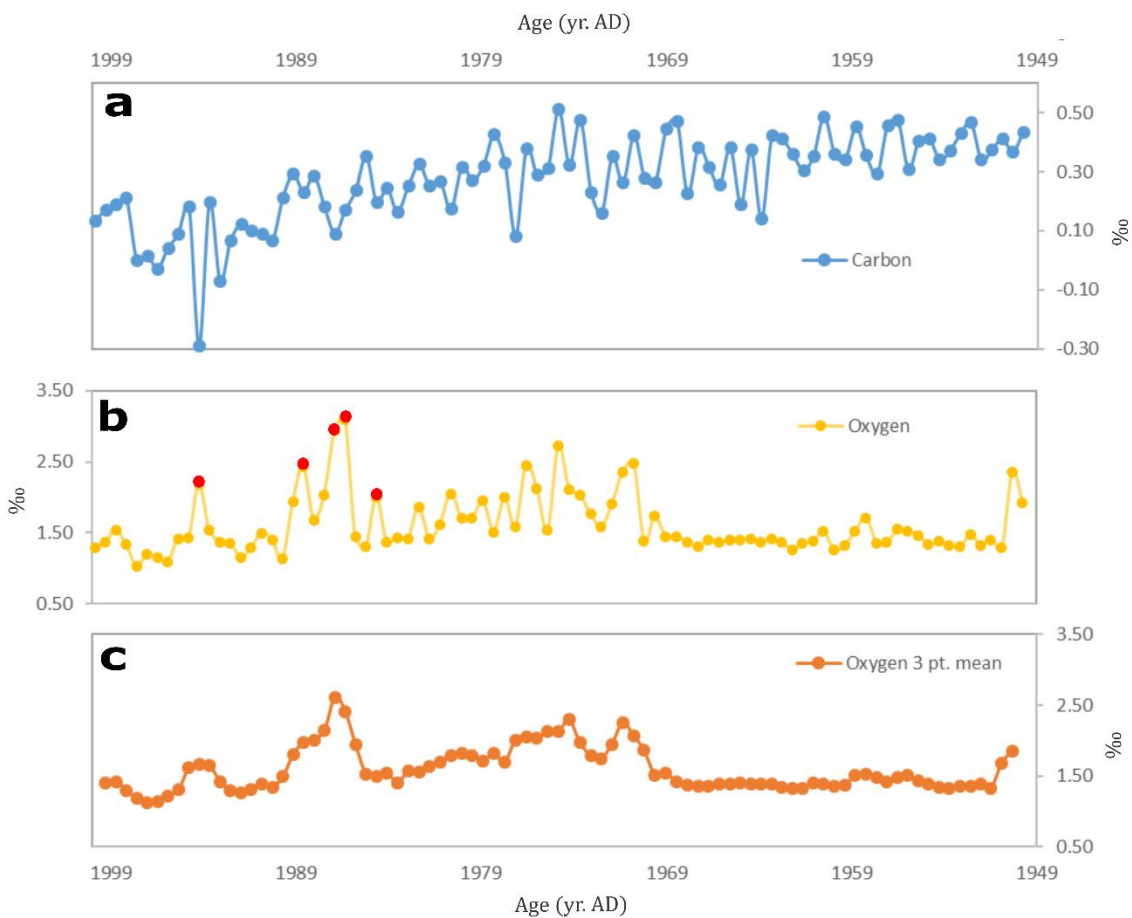
Figure 4.4 Results from the stable isotope analysis from core GS13-182-01, (a) Carbon, (b) oxygen with rerun samples marked in red, (c) oxygen as a 3 point mean.

What is evident is that after 1970 AD bursts to heavier isotopes, meaning colder or more saline, start appearing until around 1990 AD. We would expect a smoother curve from a correct chronology, such as the curve shows before 1970 AD. Coring, lab calibration, lab equipment or other unknown factors could explain the offset of the curve. On the other hand,

we can see that the spikes are coming from a flat area with some of them accounting for more than one data point, which strengthens the argument that they represent real changes. These bursts are nonetheless too big to be directly related to temperature or salinity changes. In the case of these results a few samples were rerun. In figure 4.4 (b) these samples are marked with red. However, they returned with only slightly lower values. For these samples, the latter run is shown in the graph. Due to the uncertainty of the validity for these abnormally high values the discussion will focus on the two decades between 1950- and 1970 AD that are believed to display natural variability.

5 Discussion

5.1 Sedimentological characteristics

5.1.1 Grain size

Fluctuations in the depth of the lower boundary of the Norwegian branch of the Atlantic current have been investigated by examining grain size data in core P1-003 (Berstad et al., 2003). The surface sediment distribution along the Norwegian continental margin is closely linked with the oceanographic setting. As previously established, the sediment below 700 m at the coring site is fine-grained, consisting mainly of silt and clay, indicating calm current setting. According to the chronology of core P1-003 there was a change in sedimentation rate around 4000 yr. BP. The chronology of GS13-182-01 indicates a change around 2000 yr. BP. The area therefore shows some difference in this aspect. However, according to the grainsize data presented in chapter 3 there are no major changes in the sedimentation pattern during the last 50 years.

5.1.2 Carbonate content

Kjennbakken et al. (2013) researched the concentration of carbonate in core P1-003. To reconstruct the carbonate content of the sediment, Fe-normalized Ca counts were used, previously verified by SEM to accurately reflect the carbonate content. As previously established, the same method was used for core GS13-182-01. Though foraminifera contribute to the carbonate content, photosynthesizing coccolithophorids are the dominate influence, especially the large-sized *Coccolithus pelagicus.* Carbonate secreting organism productivity depends predominantly on nutrient availability, temperature and salinity. In the North Atlantic, these factors are influenced by the inflow of Atlantic Water. Therefore, we would expect the carbonate trend to correlate with instrumental SST, as recent studies have shown (Kjennbakken et al., 2013). This positive correlation is evident after the present oceanic setting was established 2000-3000 yr. BP. Before that the correlation varied considerably, which suggests a different factor influencing the carbonate content in early-mid Holocene

(Kjennbakken et al., 2013). When looking at the data from core GS13-182-01 since 1949 AD (figure 5.1) it is evident that before 1975 AD the average Ca/Fe was considerably higher than in more recent times. If we compare this to the temperature trend, we however see no clear correlation. The average temperature difference between the periods of 1950-1970 AD and 1975-1995 AD is only 0.1°C. With the higher temperature during 1975-1995 AD correlating with lower Ca/Fe values. When comparing the Ca/Fe to the abundance of *N. incompta* and concentration of foraminifera we see clear positive correlation. The Ca/Fe values do not reach a considerable low during the 1975-1995 AD but a change in the trend is definitely visible.
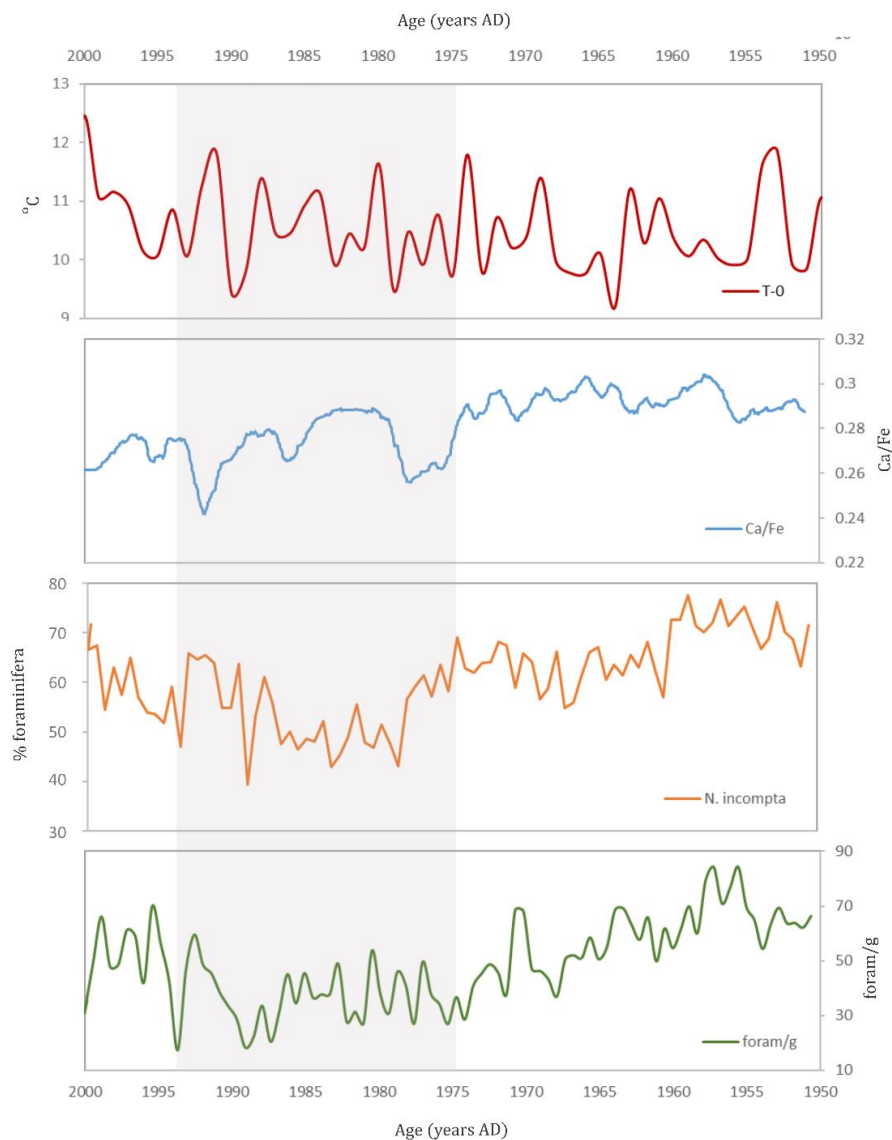
Figure 5.1 Comparison of temperature at 0 m depth at OWSM, Ca/Fe content of core GS13-182-01 provided by Lukas Becker (Becker et al., in prep.), abundance of *N. incompta* and foraminifera concentration.

53

Other factors to consider include solar insolation, carbonate dissolution, winnowing and atmospheric patterns. Kjennbakken et al. (2013) suggested that the centennial scale Ca/Fe ratio over the past 500 years was in anti-phase with the solar insolation, with the strength of the relationship varying and with known solar cycles not clearly visible in the dataset. Carbonate dissolution, related to more test fragments and lower shell weight in foraminifera, should not be an influential factor. Broken foraminifera abundance increases after 1970 AD but it has been established that foraminifera only account for a part of the carbonate content. Kjennbakken et al. (2013) argued that winnowing i.e. weaker current systems was a major factor in changing the carbonate content in late Holocene. On a more recent time scale, increased southerly winds introducing more nutrients at the core site, would factor in the productivity of the local organism in a positive way. These changes in atmospheric patterns are connected to the NAO (Kjennbakken et al., 2013).

5.2 Physical parameters

5.2.1 Temperature

In Andersson et al. (2010) the difference between the surface and near-surface signal is evidentially represented by different groups of organisms. The surface by photosynthesizers and near-surface by zooplankton such as foraminifera. Furthermore, the individual foraminifera species have preferable habitat depths and are also known to migrate through the water column (Husum & Hald, 2013). The assemblages therefore consist of proxies representing different environments since the sea surface and near-surface do not always experience temperature changes simultaneously. Furthermore, seasonal changes happen in the mixed layer above the thermocline (Andersson et al., 2010). The calcification of foraminifera, the process of secreting calcium carbonate ($CaCO_3$) to form their tests is preferable at a certain depth and at a certain time. According to Berstad et al. (2003) and Fraile et al. (2009) the calcification period for *N. incompta* is summer (JAS). In the case of GS13-182-01 we will be using the spring-summer time of JJA. An apparent offset between the stable oxygen isotope signal of *N. incompta* and *N. pachyderma* indicates that *N. incompta* calcifies at shallower depths than *N. pachyderma* (Risebrobakken et al., 2003). This has been contradicted by other studies (Ottens, 1992; Ostermann et al., 1999) and these studies put the calcification depth of *N. incompta* anywhere between 30 m (Ostermann et al., 1999) and 75 m (Ottens et al., 1992) depending on location. Following the example of Sejrup et al. (2010) the presumed depth of calcification for *N. incmopta* is 50 m and therefore compared with instrumental temperature and salinity data from this depth (Nyland et al., 2006; Sejrup et al., 2010).

Jansen et al. (2008) suggests that deeper dwelling species are more likely reflecting winter-ventilation signals as a response to the proximity of the thermocline. During winter the seasonal stratification of the surface oceans breaks down resulting in a mixing at a depth of 100 m. Species living at that depth would therefore record a signal related to the mixing and not to surface temperature changes during summer (Jansen et al., 2008). *N. incompta* and *G. bulloides* are near-surface dwelling species and should therefore record changes within the mixed layer with deeper-dwelling species such as *G. inflata* reflecting the discussed winter-ventilation (Jansen et al., 2008; Andersson et al., 2010). However, the evidence for this

indifference is unclear in the results presented by Andersson et al. (2010). Polar foraminifera are also known to have rather deep habitats (Husum & Hald, 2013).

The temperature record from OWSM shows a similar warming trend towards the present day both at 0 m and 50 m depth (figure 5.2). The only major deviation between the records is an apparent warm burst after 1970 AD at 50 m depth. According to Sejrup et al. (2011) the stable oxygen isotope signal of *N. incompta* is most likely compatible with the summer temperatures at 50 m depth (Sejrup et al., 2011) with the correlation with SSTs expanding throughout the last 1000 years (Sejrup et al., 2010). According to Husum & Hald (2013) the most precise reconstructions of subsurface temperatures were found by using summer temperatures at 100 m depth.
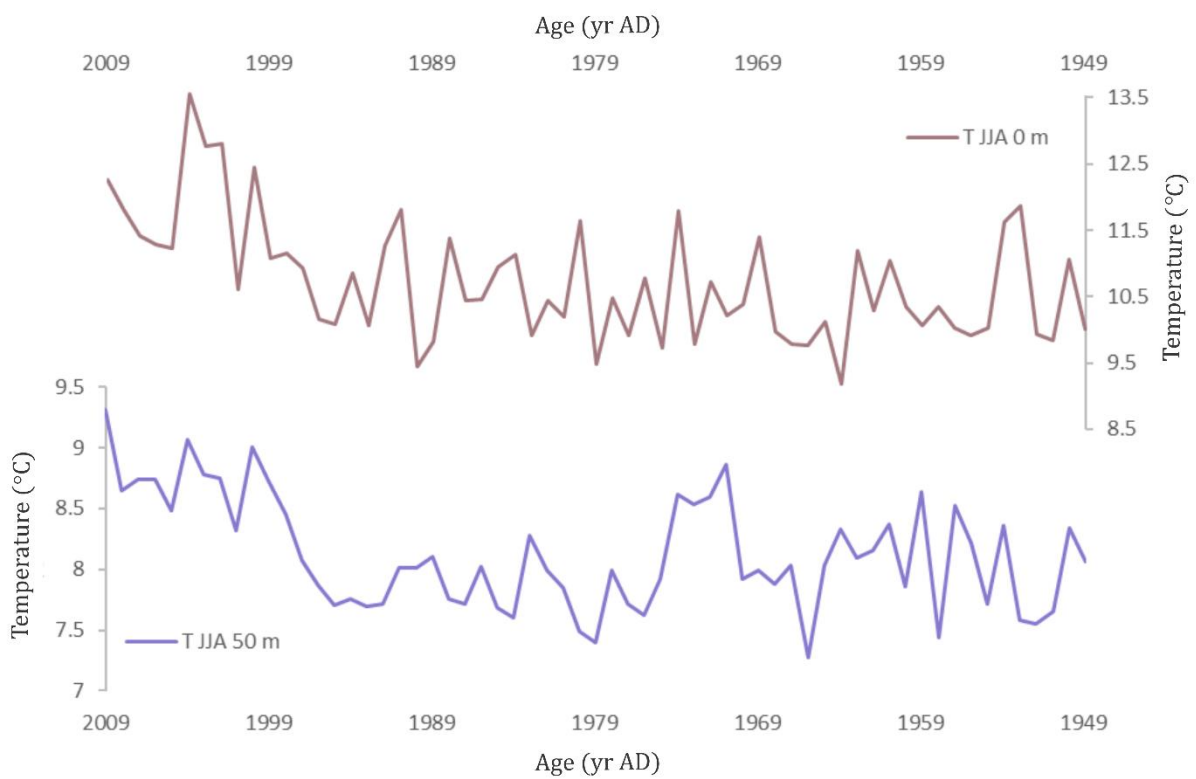
Figure 5.2 Temperature data from OWSM at 0 m and 50 m depth. Notice that the time scale is extending to 2009, capturing the current warming trend.

5.2.2 Salinity

The last decade has been characterized by warming and increased salinity according to records from OWSM. We saw before that the temperature increase has been drastic. However, in the salinity records depicted in figure 5.3 this increase in salinity is not evident in the decades leading up to that. A drop in salinity is evident at 50 m after 1970 AD until 1980 AD. At 0 m the salinity does not show any significant changes apart from relatively small spikes to lower salinity until 1999 AD where a larger drop is recorded. In Sejrup et al. (2011) it is speculated that the influence of the lower salinity NCC could have been stronger in the past even though it has not been recorded in neither core P1-003 nor MD95-2011 (Sejrup et al., 2011; Risebrobakken et a., 2003). Therefore, following the example of Sejrup et al., 2010, the salinity will not be considered to be an important influence on the isotopic signal in core GS13-182-01 (Sejrup et al., 2010).
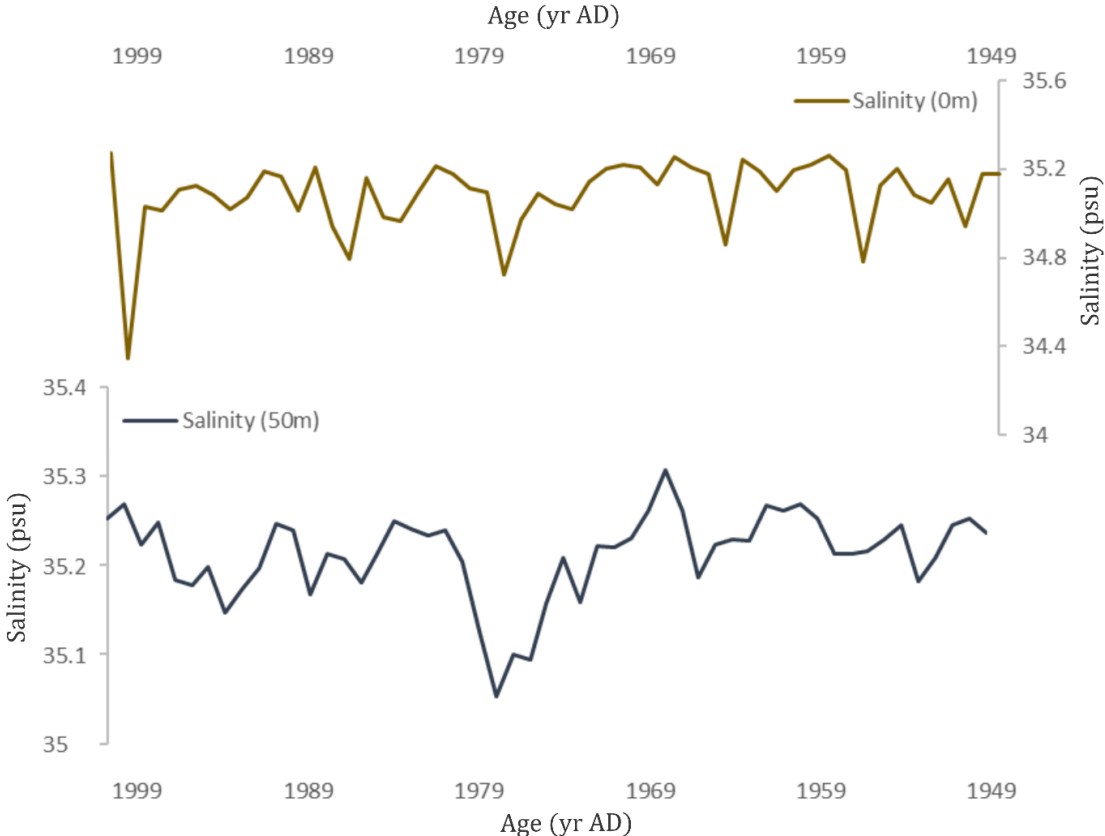
Figure 5.3 Salinity data from OWSM at 0 m and 50 m depth.

5.3 Assemblages analysis

When the results of the foraminifera faunal records from GS13-182-01 are compared to previous studies such as Risebrobakken et al. (2003), Anderson et al. (2010) and Klitgaard-Kristensen et al. (2001) the results are analogous. According to Klitgaard-Kristensen et al. (2001) The Holocene is dominated by *N. incompta* with *G. bulloides* and *G. quinqueloba* as important secondary species. *N. incompta* abundances change from 50% to around 70% from early to late Holocene. *G. bulloides* abundances change from a maximum of 50% to <10% during the same period (Klitgaard-Kristensen et al., 2001). As previously mentioned our results show that from mid to late Holocene *N. incompta* increases in abundance from 30-50% to around 60-70% which is in accordance with the present values. Risebrobakken et al. (2003) generally show higher abundances of *N. pachyderma* in core MD95-2011, as expected from a core situated further north. Both Risebrobakken et al. (2003) and Klitgaard-Kristensen et al. (2001) report *N. pachyderma* being dominant during the deglaciation, with values around 95%. Later interglacial values are around 23% which is significantly higher than is recorded in GS13-182-01 (Risebrobakken et al., 2003).

As previously mentioned, planktonic foraminifera display distinct ecological preferences when it comes to their environment. The assumption that these habitat preferences stay the same through time is the basis for their usage as proxies for paleoclimate research (Morard et al., 2016; Kucera & Darling, 2002; Curry & Ostermann, 1997). The boundaries of water masses are characterized by diverse foraminiferal assemblages and oceanic fronts are often dominated by certain species. Mixing in these localities increases primary productivity and subsequently increases diversity. The previously established faunal provinces do not always reflect the actual assemblage distribution in the surface layers with seasonal variability and current systems being a highly influential factor (Ottens, 1991). One aspect of assemblage analysis that has not been fully exploited in research is the study of morphology diversity. It has been shown for some foraminifera species that their morphotypes prefer specific environments. Morphological modelling could therefore increase the precision of transfer functions and aid in palaeoclimate research and paleoceanography (Morard et al., 2016, Kucera & Darling, 2002).

Previously considered as a morphotype for *N. pachyderma*, based on coiling direction, *N. incompta* is now known as a separate species with distinctly different ecology. It has been proven that the coiling preference is a genetic trade and not environmentally controlled, as previously thought and that could affect the usage of these species as signal carriers (e.g. Norris & Nishi, 2001; Darling et al., 2006). However, it has been established that the two different coiling forms of *N. pachyderma* thrive in different temperatures with the habitat preference being close to a 100%. *N. pachyderma* is a sub-polar species known to constitute around 50-70% of the assemblage at 67°N (Runarsdottir, 2014) and is therefore considered as an indicator of arctic water influence. In high-arctic waters the species constitutes 96-99% of the foraminifera faunal assembly with the percentage dropping down to 50% in areas with Atlantic Water influence (Husum & Hald, 2012). The right-coiling form prefers more tempered waters, including the North Atlantic current (Darling et al., 2006) even though the species has been found in the sedimentary records of higher latitudes (e.g. Runarsdottir, 2014; Bauch et al., 2003).

In studies of core tops it has been shown that the living assemblage of planktonic foraminifera sets the transition between the *N. pachyderma* and *N. incompta* in the range between 4-10°C and in the North Atlantic, *N. pachyderma* does not live in waters with higher temperatures than 10°C (Darling et al., 2006). As previously stated, the results presented for core GS13-182-01 show that *N. pachyderma* has a lower abundance then 10%, most often under 5% with the exception of a period between 1960 and 1980 AD where it reached its maximum abundance. The trend of *N. incompta* does not directly support the assumption that this slight increase in *N. pachyderma* indicates arctic water influence. However, *N. incompta,* has a maximum abundance before 1960 AD, and as an indicator of North Atlantic current water it could in fact mean less influence of the current in later periods. As previously discussed*, N. incompta* seems to show 4 separate trends in the period, between 1950- and 1970 AD there are two steps, between 1970- and 1990 AD there is a curved low in abundance and towards present times the species reaches a maximum again. If this is compared to the temperature curve, the increase towards present times is the only clear relation.

Just as *N. pachyderma*, *G. inflata* never exceeds 10% in abundance, with the maximum of this species coinciding with the low of *N. incompta. G. inflata* is found in transitional and

subtropical waters of the Northern and Southern hemispheres and is therefore considered an indicator of Atlantic water influence. In the Southern hemisphere the two different morphotypes of this species have been used to track the subantarctic front (Morard et al., 2016). Since the maximum of these species contradict eachother in terms of indicating Atlantic water influence, there is a change that the signal of *N.incompta* has another more dominant forcing.

According to Ottens, (1991) a sharp faunal boundary can be found at 52°N where the sub-arctic front meets Atlantic Current Water, creating a turnover of subpolar and NAC water. North of this boundary, *G. quinqueloba,* a sub-arctic species known to thrive adjacent to oceanic fronts, and large *G. bulloides* are dominant. South of the boundary, *N. incompta*, *G. inflata* and *G. bulloides* are the most abundant (Ottens, 1991). *G. bulloides* has an abundance around 10% through the whole period, with no major shifts apart from a small decrease around 1980. This species is a strong indicator of Atlantic Water influence (Husum & Hald, 2013; Johannessen et al., 1994). Additionally, increased abundance of *G. quinqueloba* with decreasing *N. incompta* in short-lived faunal oscillations can be interpreted to represent small reductions in inflow of Atlantic Water with current speeds and/or supply of nutrients being a possible factor (Johannessen et al., 1994).

G. quinqueloba would be expected to be in high numbers at the Norwegian coastal front since it is known to be abundant around front areas and in Atlantic Water (Husum & Hald, 2013). An explanation for the low abundance could be that it got lost in the larger fractions since it is a small species. According to Husum & Hald (2012) the species is observed in smaller numbers in fractions larger than 125 μm and 150 μm. According to Hald (2007) the effects of the loss of the smaller size fractions is not apparent for sea-surface temperatures higher than 4°C. *G. quinqueloba* has its lowest abundance before 1960, steadily increasing until it reaches 20% between 1975- and 1985 AD, with an abrupt shift to 5%. It is possible this shift is related to shift in a position of the Norwegian coastal front.

G. uvula dominates coastal waters along with *N. incompta* (Husum & Hald, 2012) and has been found in the inner part of the northern Norwegian shelf (Husum and Hald, 2004). Therefore it is considered to be a strong indicator of coastal water influence. It is a small species and

60

therefore can be lost in larger fractions (Husum & Hald, 2013). The peak in *G. uvula* abundance in 1993 could arguably be an example of dominant coastal water influence over the core site. *G. glutinata* is a strong indicator of North Atlantic Current influence, similar to *G. inflata* (Husum & Hald, 2012). *O. universa* is the most southern-living species, thriving below 40°N on the western coast of Spain (Ottens, 1991). The increase in abundances of *G. inflata*, *G. glutinata* and *O. universa* between 1970-1990 strengthen each other in the argument that the North Atlantic Current influence increases during this period, since all of these species have been brought by the ocean current system from lower latitudes.

If these arguments are compared to the assemblages that were presented for each decade in chapter 4.1.1, the results are as follows: Between 1950-1960 AD there is low polar influence based on the low abundances of *N. pachyderma* and *T. quinqueloba* and low Atlantic Water influence based on low abundances of *G. inflata* and *G. glutinata*. However, *N. incompta* has a maximum abundance during this period. *G. uvula* indicates some dregree of coastal influence. Between 1960-1970 AD there seem to be higher polar influence based on the incresed abundance of *N. pachyderma* and *T. quinqueloba* with another factor arguably affecting the assemblages, due to the slight increase in abundance of several species despite their water mass preferences. Nutrient supply could be a possible factor. An example of this descrepancy is the increase of *G. uvula* which is a strong indicator of higher coastal influence. However, *N. incompta* decreases during the same period. Between 1970-1980 AD there is clearly higher Atlantic Water influence based on the increased abundance of *G. inflata* and *G. glutinata*. *N. incompta* shows an incresing in the first years of the decade, followed by a decrease. Coastal influence seems to decrease according to *G. uvula*. Between 1980-1990 AD there are signs of higher polar influence in the first years of the decade, based on the abundance of *T. quinqueloba*. *N. pachyderma* does not support this. The record lows of both *N. incompta* and *G. bulloides* strongly indicate a weaker inflow of Atlantic Water. Other abundances seem contradicting and if not an unknown hydrographical factor such as mixing, statistical error could be affecting the counts for this decade. Between 1990-2000 AD there is evidentially dominant coastal influence according to *G.uvula*. Lower Atlantic Water influence according to *G. inflata* and *G. glutinata* however contradict the evidence of overall warmer conditions in the area and the increased abundance of *N.incompta*.

Summarizing these results some of the indicators seem contradictory. Espcecially between the abundance of *N. incompta* and of other Atlantic Water indicators. Since *N. incompta* is found in more abundance in core GS13-182-01, the species is assumed to be a stronger local indicator of North Atlantic water inflow and influence. The abundance of more southerly species could be affected by other mechanism and could therefore seem contradictory. Furthermore, the level of correlation between the abundance of *N. incompta* and both the carbonate and foraminifera concentration shown in fig. 5.1. indicates that the species is a reliable proxy for overall changes in productivity in the area.

5.4 Influence of climate variability

The stable oxygen isotope results from core P1-003 indicate a temperature change of 4°C, using the equation by (Shackleton, 1974) with the underlying assumption that temperature is the dominant factor. With a three-point smoothed curve the temperature change is reduced to 2°C (Sejrup et al., 2011). Using the same approach for the stable oxygen isotope data from core GS13-182-01 we get a maximum change of 9°C for the whole period, with a 6°C for the three-point mean. This change is out of range for natural temperature variability. If the period is reduced to the two decades between 1950-1970 AD, the change is on a scale of 2°C which is more in line with previous studies. If the spikes were representing coastal current influence, we would expect lighter spikes because of the freshwater effects, but they have to be attributed to other unknown factors since they are heavier. This can be seen in figure 5.4.
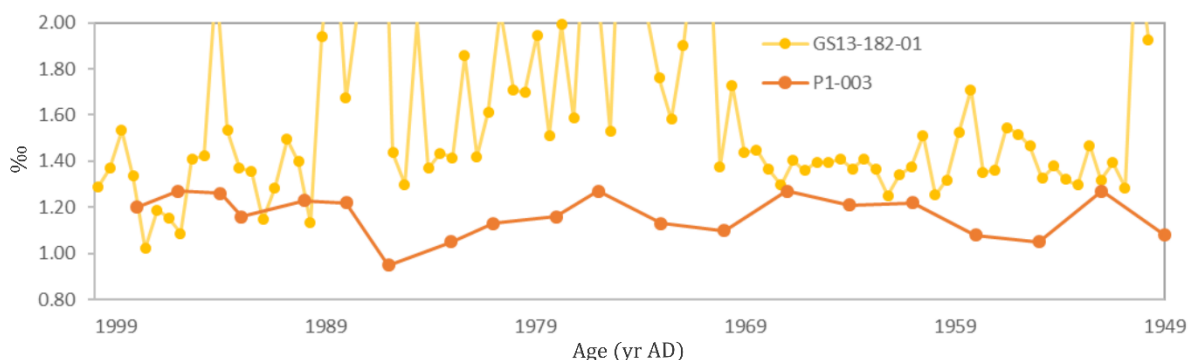
Figure 5.4 Stable oxygen isotope data from core GS13-182-01 and P1-003 (Sejrup et al., 2010; 2011)

In figure 2.16 the results from the stable oxygen isotope analysis from Sejrup et al. (2011) were presented, scaled and compared to temperatures archives from OWSM and Trondheim. As previously established the isotope analysis was performed on *N. incompta* and compared to archives reflecting the presumed time and depth of calcification for that species. In figure 5.5 the stable oxygen isotope data from core GS13-182-01 has been added, focusing on the period between 1950- and 1970 AD. Note that the scale has been reversed to match the graph from Sejrup et al. (2011). It is noteworthy how the high-resolution aids in the comparison to the instumental data. As previously stated, shifts to higher isotopic values indicate lower temperatures. Between 1956- and 1961 AD three lows can clearly be seen, correlating with the surface temperature at OWSM with a short lag. When comparing with the temperatures at Trondheim, this correlation cannot be established. From 1963-1967 AD the isotopes seem to show a regular yearly shift towards lower values which is speculated to represent seasonal changes. As previously stated, the uncertainty of the age model was low, around ±5 years but could influence the correlation.
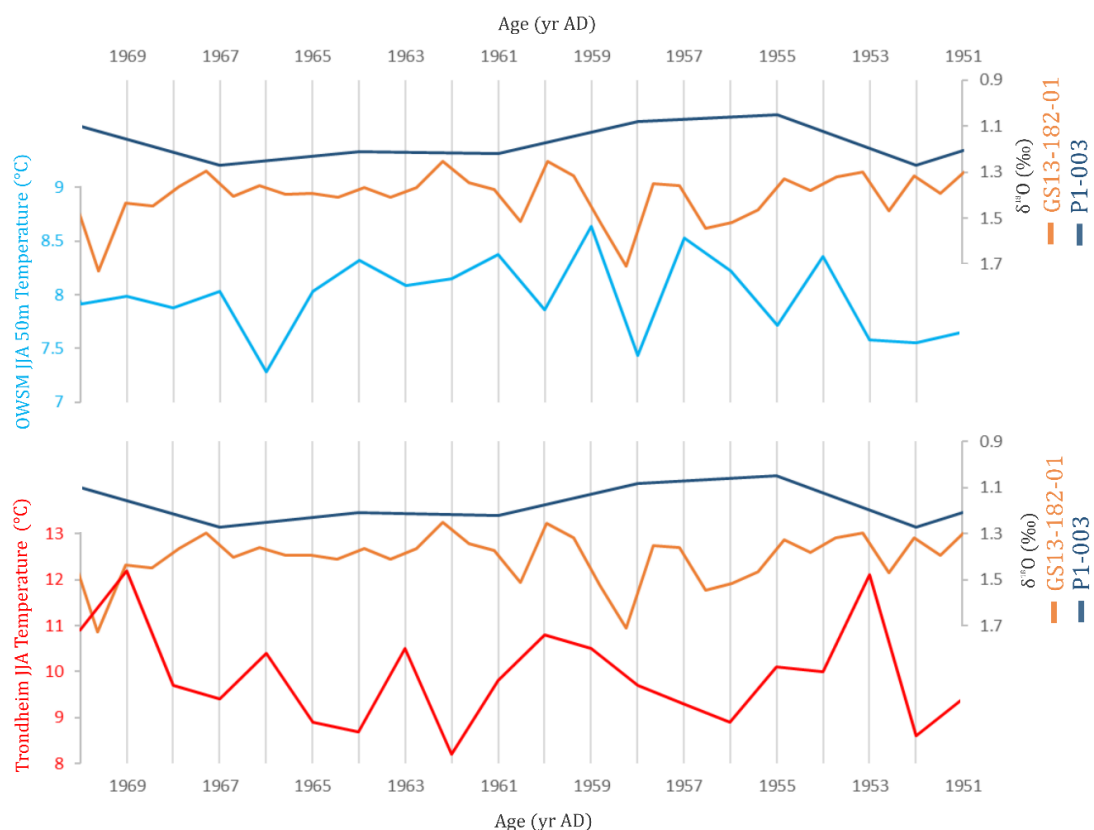
Figure 5.5 Comparison of stable oxygen isotope data from GS13-182-01 and P1-003 (Sejrup et al., 2010; 2011) with SST data from OWSM and JJA temperature from Trondheim (Jensen et al., 2016). This is a follow up comparison to Sejrup et al., (2011).

When compared to known modes of climate variability, the NAO and AMO there seems to be significant correlation between the abundance of *N. incompta* and the NAO index (see fig. 5.6). Periods where the NAO index is predominately positive coincide with periods where *N. incompta* has higher abundance, possibly indicating that the species is more of an Atlantic origin rather than coastal species, since the NAO influences the inflow of Atlantic Water. During a positive phase the inflow of AW should increase and have subsequent positive effects on teh temperature (Berstad et al., 2003). As previously establised, a positive mode of the NAO reflects a period of stronger southerly and westerly winds in the study area, arguably lowering the influence of coastal water and increasing the Atlantic water influence. As previosuly discussed, the decades between 1960-1970 AD and 1980-1990 AD are characterized by higher polar influence. These coincide with periods of a negative NAO index where these stronger winds are not present. This contradicts the results of Risebrobakken et al. (2003) who record a colder subsurface setting in core MD95-2011 coinciding with stronger westerlies during the Holocene (Risebrobakken et al., 2003). However, the offset of the two cores, MD95-2011 and GS13-82-01 could account for this with the latter being situated significantly further south. The decades between 1950-1960, 1970-1980 and 1990-2000 AD are decades of positive NAO index and they all shows signs of lower polar influence, higher Atlantic water influence, and higher coastal influence repsectively. Comparing the results with the AMO index is a bit more difficult since the AMO has a cycle on a scale that exceeds the period we are focusing on. This can clearly be seen in fig. 5.6 where a period of negative AMO index covers almost the whole of the studied period.

Higher frequency variability can be absent due to complications with the age model or because the climate variability has not been recorded by this specific proxy. Since seemingly annual temperature changes are seen in the stable oxygen isotopes results the chronology is believed to be realiable. However, the visualization of variability often varies between archives and localities, in this case of comparison with temperatuer and salinty data, hydrographic variation between the OWSM and coring site can be a factor (Sejrup et al., 2011; Wanner et al., 2008; Bradley & Jones, 1995).
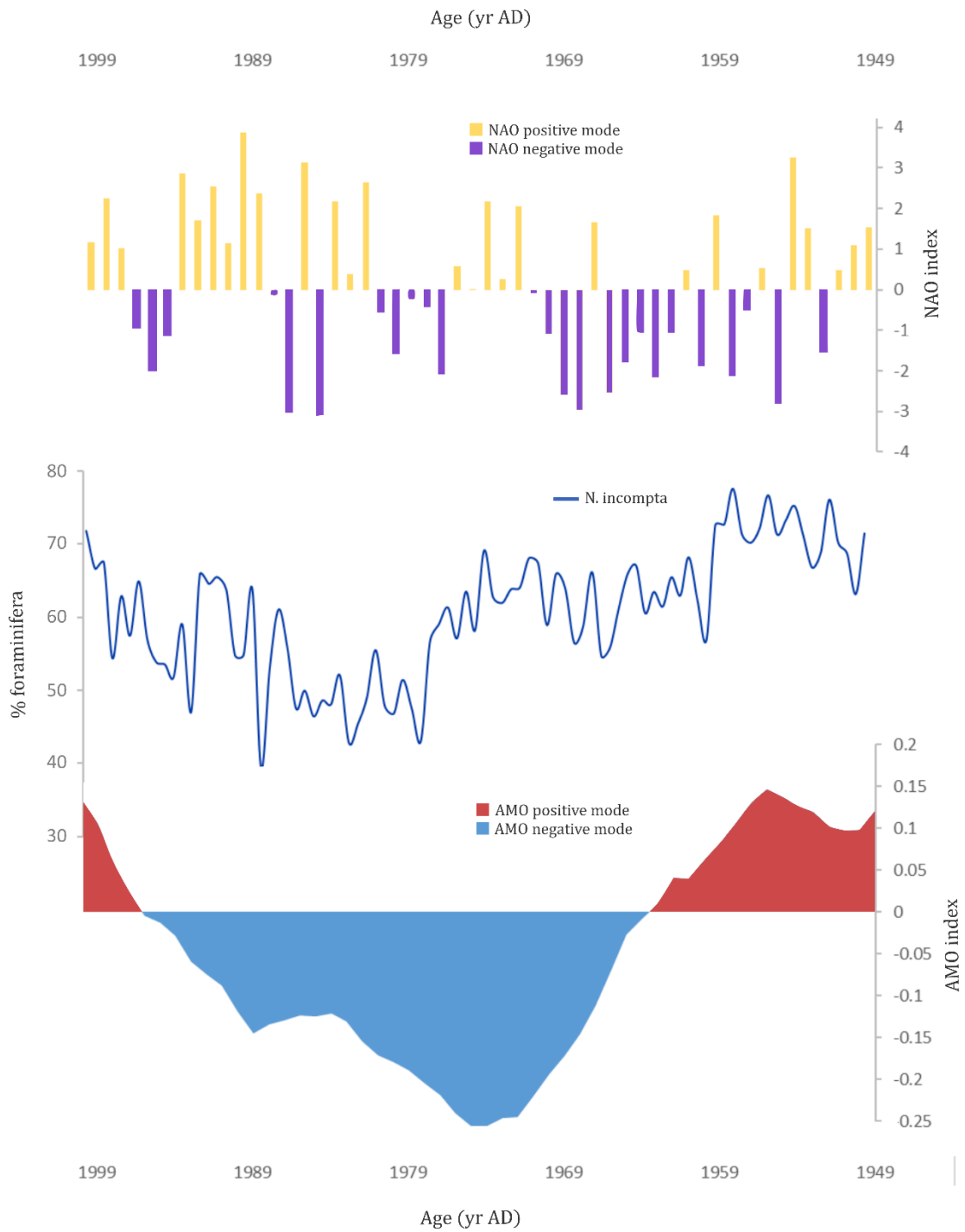
Figure 5.6 Comparison of the NAO index (Hurrell et al., 2016), AMO index (Enfield et al., 2001) and abundance of *N. incompta.*

6 Conclusions

The extremely high resolution data produced from core GS13-182-01 covering the period between 1950- and 2000 AD is unpresented in this area. Conclusions based on this high resolution stable oxygen isotope and assemblage analysis can give valuable insight into the climate variability in the area, most prominently in connection with the NAO and AMO. Any conclusion depends heavily on a reliable chronology since each year is represented by 1-2 samples. The stable oxygen isotopes between 1950-1970 AD show a strong correlation with SST record from OWSM. A comparison with atmospheric summer temperature record from Trondheim does not show the same level of correlation. These results agree with previous studies that conclude that the variability can be attributed to North-Atlantic influence rather than a Scandinavian one (Sejrup et al., 2011; 2010). Furthermore, the isotopic signal reveals seasonal changes.

The planktonic forminifera assemblages are dominated by *N. incompta*, followed by *T. quinqueloba* and *G. bulloides*. This is in good agreement with previous planktonic foraminifera studies performed in the area (Risebrobakken et al., 2003; Andersson et al., 2010; Klitgaard-Kristensen et al., 2001). More southerly species are brought into the area in smaller numbers by the Norwegian branch of the North Atlantic current. *N. incompta* is believed to be a strong local indicator of the inflow of Atlantic Water into the study area. The abundance of *N. incompta* shows a strong correlation with the Ca/Fe data and the concentration of foraminifera curves which might reflect the overall productivity in the area. The NAO evidentially also influences the abundance of *N. incompta* in the area.

The strong correlation between the assemblages and the NAO is compelling. The decades between 1960-1970 AD and 1980-1990 AD are periods where negative NAO index coincides with recorded higher polar influence in the area, most importantly increased abundance of the arctic and front species *N. pachyderma* and *T. quinqueloba.* On the other hand, periods of positive NAO in other decades seems to coincide with recorded lower polar influence and

higher Atlantic Water influence with southerly species like *G. inflata* and *G. glutinata* increasing in abundance. The NAO seems to affect the abundance of the coastal species *G. uvula* with coastal influence being high or average during positive periods. The same level of correlation cannot be established with the AMO which operates on longer timescales than the period covered here.

7 References

Andersen, C., Koc, N., Jennings, A. & Andrews, J.T., 2004. Nonuniform response of the major surface currents in the Nordic Seas to insolation forcing: implications for the Holocene climate variability. *Paleoceanography,* 19.

Andersson, C., Pausata, F. S. R., Jansen, E., Risebrobakken, B. & Telford, R. J., 2010. Holocene trends in the foraminifer record from the Norwegian Sea and the North Atlantic Ocean. *Climate of the Past*, 6, 179-193.

Armstrong, H. A. & Brasier, M. D., 2005. *Microfossils*. Malden/Oxford/Carlton: Blackwell Publishing, 296 pp.

Bauch, D., Darling, K., Simstich, J., Bauch, H. A., Erlenkeuser, H. & Kroon, D., 2003. Palaeoceanographic implications of genetic variation in living North Atlantic Neogloboquadrina pachyderma. *Nature*, 424, 299-302.

Becker et al. in prep. High resolution sea surface condition variability during the last 1000 years in the SE Nordic Seas.

Berstad, I. M., Sejrup, H. P., Klitgaard-Kristensen, D. & Haflidason, H., 2003. Variability in temperature and geometry of the Norwegian Current over the past 600 yr., stable isotope and grain size evidence from the Norwegian margin. *Journal of Quaternary Science*, 18, 591-602.v

Bjerknes, J., 1964: Atlantic air-sea interactions. Advances in Geophysics, 10, 1-82.

Blaauw, M. & Christen, J.A., 2011. Flexible paleoclimate age-depth models using an autoregressive gamma process. *Bayesian Analysis*, 6(3), 457-474.

Blindheim, J. & Østerhus,S., 2005. The Nordic Seas, Main Oceanographic features. In Drange, H., Dokken, T., Furevik, T., Gerdes, R. & Berger, W., (Eds.) *The Nordic Seas: An integrated Perspective*. Washington DC, American Geophysical Union Monograph 158, 11-38 pp.

Blindheim, J. V., Borovkov, B. Hansen, S. A., Malmberg, W. R. Turrell and S. Osterhus, 2000. Upper layer cooling and freshening in the Norwegian Sea in relation to atmospheric forcing. *Deep-Sea Research,* 47, 655-680.

Bond, G., Kromer, B., Beer, J., Muscheler, R., Evans, M.N., Showers, W., Hoffmann, S., Lotti-Bond, R., Hajdas, I. & Bonani, G., 2001. Persistent solar influence on North Atlantic climate during the Holocene. *Science,* 294, 2130-2136.

Bond, G., Showers, W., Cheseby, M., Lotti, R., Almasi, P., deMenoca, P., Priore, P., Cullen, H., Hajdas, I. & Bonani, G., 1997. A pervasive millennial scale cycle in North Atlantic Holocene and glacial climates. *Science*, 278, 1257 – 1266.

BouDagher-Fadel, M. K., 2013. *Biostratigraphic and Geological Significance of Planktonic Foraminifera*. Department of Earth Sciences, University College London, London, UK, 296 pp.

Bradley, R. S., 1999. *Paleoclimatology – Reconstructing climates of the Quaternary* (2nd edition). Academic Press, International geophysics series volume 64.

Bradley, R. S., & Jones, P. D., 1995. *Climate Since A.D*. 1500. Routledge, London.

Cifelli, R., 1961. *Globigerina incompta,* a new species of pelagic foraminifera from North Atlantic. Cushman Found. Foram. Res. Contr., 12, 83-86.

Craig, H. & Gordon, I., 1965. Deuterium and 0-18 variations in the ocean and the marine atmosphere. In: Tongiorgi, E. (Ed.), Coniglio Nazionale Delli Ricerche. *Laboratorio Di Geologica Nucleare*, Pisa, 9-130.

Curry, W. B. & Ostermann, D. R., 1997. Ground-Truthing the Paleoclimate Record: Sediment Trap Observations Aid Paleoceanographers. *Oceanus*, 40(2), 11-14.

d'Orbigny, A. D., 1826. Tableau methodique de la classe des Chephlapodes. *Annales des Sciences Naturelles Paris* Ser. I, 7, 245-314.

Darling, K. F., Kucera, M., Kroon, D. & Wade, C. M., 2006. A resolution for the coiling direction paradox in Neogloboquadrina pachyderma. *Paleoceanography* 21(2), doi:10.1029/2005PA001189

Delworth, T. L., & Mann, M. E., 2000. Observed and simulated multidecadal variability in the Northern Hemisphere. *Climate Dynamics*, 16, 661-676.

d'Orbigny, A. 1839. *Voyage dans l'Amérique Méridionale; Foraminifères,* 5. Levrault, Strasbourg, France.

Drange, H., Dokken, T., Furevik, T., Gerdes, R., Berger, W., Nesje, A., Orvik, K. A., Skagseth, Ø., Skjelvan, I. & Østerhus, S., 2005. The Nordic Seas: An overview. In Drange, H., Dokken, T., Furevik, T., Gerdes, R. & Berger, W., (Eds.) *The Nordic Seas: An integrated Perspective*. Washington DC, American Geophysical Union Monograph 158, 1-10 pp.

Egger, J.G. 1893. Foraminiferen aus Meeresgrunproben, gelohtet von 1874 bis 1876 von S.M. Sch. Gazelle. Königliche Bayerische Akademie der Wissenschaften, Mathematisch-Physikalische Klasse, Abhandlungen, 18(2), 139-458.

Ehrenberg, G.C., 1861. Elemente des tiejen Meeresgrundes in Mexikanischen Golfstrome bei Florida; Über die Tiefgrund-Verhältnisse des Oceans am Eingange der Davisstrasse und bei Island. *Monatsbericht der Koniglichen Preussischen Akademie der Wissenscraften zu Berlin,* 1858:295-311, 324-337.

Eliassen, I. K., Eldevik, T., Berntsen, J., Furnes, G. K., 2000. The Current Condition at Ormen Lange–Storegga. Report for Norsk Hydro and University of Bergen.

Enfield, D.B., Mestas-Nunez, A.M., & Trimble, P.J., 2001. The Atlantic Multidecadal Oscillation and its relationship to rainfall and river flows in the continental U.S., *Geophys. Res. Lett.*, 28, 2077-2080.

Fraile, I., Mulitza, S., & Schulz, M., 2009. Modeling planktonic foraminiferal seasonality: Implications for sea-surface temperature reconstructions. *Marine Micropaleontolology*, 72, 1-9.

Haflidason, H., Sejrup., H. P., Nygård, A., Mienert, J., Bryn, P., Lien, R., Forsberg, C. F., Berg, K. & Masson, D., 2004. The Storegga Slide: architecture, geometry and slide development. *Marine Geology*, 213, 201–234.

Haflidason, H., Eiriksson, J. & Kreveld S. Van, 2000. The tephrochronology of Iceland and the North Atlantic region during the Middle and Late Quaternary. *A review, J. Quat. Sci.*, 15(1), 3–22, doi:10.1002/ (SICI)1099-1417(200001)15:1<3::AID-JQS530>3.0.CO;2-W.

Haflidason, H., King, E. L. & Sejrup, H. P., 1998. Late Weichselian and Holocene sediment fluxes of the northern North Sea Margin. *Marine Geology*, 152, 189–215.

Hald, M., Andersson, C., Ebbesen, H., Jansen, E., Klitgaard-Kristensen, D., Risebrobakken, L., Salomonsen, G.R., Sarnthein, M., Sejrup, H.P. & Telford, R.J., 2007. Variations in temperature and extent of Atlantic Water in the northern North Atlantic during the Holocene. *Quaternary Science Reviews* 26, 3423-3440.

Hansen, B., Østerhus, S., Quadfasel, D. & Turrel, W. R., 2004. Already the Day After Tomorrow? *Science*, 305, 953-954.

Hansen, B. & Østerhus, S., 2000. North atlantic-Nordic seas exchanges. *Progress in Oceanography*, 45, 109-208.

Hjelstuen, B.O., Monsen, S., Sejrup, H.P., Haflidason, H., 2013. Report from calypso-coring at the Møre continental slope (Storegga Slide). Report No. 100-05/13, Department of Earth Science, University of Bergen, Bergen, Norway, 7 pp.

Hjelstuen, B. O., Nygård, A., Sejrup, H. P., Haflidason, H., 2012. Quaternary denudation of southern Fennoscandia - evidence from the marine realm. *Boreas*, 41(3), 379-390.

Hjelstuen, B. O., Sejrup, H. P., Haflidason, H., Berg, K. & Bryn, P., 2004. Neogene and Quaternary depositional environments on the Norwegian continental margin, 62°N-68°N. *Marine Geology*, 213, 257– 276.

Hurrell, J. W., Kushnir, Y., Ottersen, G. & Visbeck, M., 2003. An overview of the North Atlantic Oscillation. In Hurrell, J.W., Kushnir, Y., Ottersen, G., Visbeck, M. (Eds.), *The North Atlantic Oscillation: Climatic Significance and Environmental Impact*. Washington DC, American Geophysical Union Monograph 134, 1-35.

Husum, K. & Hald, M., 2013. Reprint of: Arctic plantic foraminiferal assemblages: Implications for subsurface temperature reconstructions. *Marine Micropaleontology*, 99, 8-17.

Husum, K. & Hald, M., 2012. Arctic Planktic Foraminiferal Assemblages: Implications for Subsurface Temperature Reconstructions. *Marine Micropaleontology,* 96-97, 38-47, doi: 10.1016/j.marmicro.2012.07.001.

Husum, K., Hald, M., 2004. Modern foraminiferal distribution in the subarctic Malangen Fjord and adjoining shelf, Northern Norway. *Journal of Foraminiferal Research* 34, 34–48.

Israelson, C. & Buchardt, B., 1991. The isotopic composition of oxygen and carbon in some fossil and recent bivalve shells from East Greenland. *LUNDQUA Report*, 33, 117-123.

Jansen, E., Andersson, C., Moros, M., Nisancioglu, K. H., Nyland, B. F., and Telford, R. J., 2008. The early to mid-Holocene thermal optimum in the North Atlantic. In: Battarbee, R. W. and Binney, H. A. (Eds.). *Natural Climate Variability and Global Warming – A Holocene Perspective*. Wiley-Blackwell, Chichester, 123–137.

Johannessen, T., Jansen, E., Flatøy, A. & Ravelo, A. C., 1994. The relationship between surface water masses, oceanographic fronts and paleoclimatic proxies in surface sediments of Greenland, Iceland, Norwegian Seas. In: Zahn, R. (ed). Carbon Cycling in the Glacial Ocean: Constraints on the Ocean's Role in Global Change, NATO ASI Ser. I, vol. 17, Springer-Verlag, New York.

Kaufman, D. S., Ager, T. A., Anderson, N. J., Anderson, P. M., Andrews, J. T., Bartlein, P. J., Brubaker, L. B., Coats, L. L., Cwynar, L. C., Duvall, M. L., Dyke, A. S., Edwards, M. E., Eisner, W. R., Gajewski, K., Geirsdottir, A., Hu, F. S., Jennings, A. E., Kaplan, M. R., Kerwin, M. N., Lozhkin, A.V., MacDonald, G. M., Miller, G. H., Mock, C. J., Oswald, W. W., Otto-Bliesner, B. L., Porinchu, D. F., Ruhland, K., Smol, J. P., Steig, E. J., Wolfe, B. B., 2004. Holocene thermal maximum in the western Arctic (0-180 degrees W). *Quaternary Science Reviews,* 23, 529-560.

Kim, J. H., Rimbu, N., Lorenz, S. J., Lohmann, G., Nam, S. I., Schouten, S., Ruhlemann, C. & Schneider, R. R., 2004. North Pacific and North Atlantic sea-surface temperature variability during the Holocene. *Quaternary Science Reviews,* 23, 2141-2154.

Kjennbakken, H., 2013. Holocene high-resolution paleoclimate records from Voldafjorden and the SE Norwegian Sea (Ph.D. dissertation). Department of Earth Science, University of Bergen, Bergen, Norway.

Klitgaard-Kristensen, D., Sejrup H. P. & Haflidason, H., 2001. The last 18 kyr fluctuations in Norwegian Sea surface conditions and implications for the magnitude of climatic change: Evidence from the North Sea. *Paleoceanography*, 16, 455-467.

Kucera, M., and Darling, K. F. (2002), Cryptic species of planktonic foraminifera: their effect on palaeoceanographic reconstructions., *Philos. Trans. A. Math. Phys. Eng. Sci.*, *360*(1793), 695–718, doi:10.1098/rsta.2001.0962.

Mangerud, J., Gyllencreutz, R., Lohne, Ø., Svendsen, J.I., 2011. Glacial history of Norway. In: Ehlers, J., Gibbard, P., Hughes, P. (Eds.), Quaternary Glaciations - Extent and Chronology. Elsevier, Amsterdam.

Marshall, J., Kushnir, Y., Battisti, D., Chang, P., Czaja, A. Dickson, R., Hurrel, J., McCartney, M., Saravanan, R. & Visbeck, M., 2001. North Atlantic climate variability; Phenomena, impacts and mechanisms. *International Journal of Climatology*, 21, 1863-1898.

Morard, R., Reinelt, M., Chiessi, C. M., Groeneveld, J. & Kucera, M., 2016. Tracing shifts of oceanic fronts using the cryptic diversity of the planktonic foraminifera Globorotalia inflata. *Paleoceanography,* doi: 10.1002/2016PA002977.

Mork, K. A., & Ø. Skagseth, 2010. A quantitative description of the Norwegian Atlantic Current by combining altimetry and hydrography. *Ocean Science*, 6(4), 901–911.

Mork, K. A., Skagseth, Ø., 2005. Annual sea surface height variability in the Nordic Seas. In Drange, H., Dokken, T., Furevik, T., Gerdes, R. & Berger, W., (Eds.) *The Nordic Seas: An integrated Perspective*. Washington DC, American Geophysical Union Monograph 158, 51-64 pp.

Muscheler, R., Beer, J. & Kromer, B., 2003. Long-term climate variation and solar effecs. In *Proc. ISCS 2003 Symposium, Solar Variability as an Input to the Earth's Environment*. Tatranska Lomnica, Slovakia, ESA SP-535.

Natland, M. L., 1838. New species of Foraminifera from off the west coast of North America and from the later Tertiary of the Los Angeles Basin. California University, Scripps Institute. Oceanography. Tech. Ser. Bull., 4(5), 137-164.

Norris, R. D. & H. Nishi, 2001. Evolutionary trends in coiling of tropical Paleogene planktic foraminifera. *Paleobiology*, 27, 327–347.

Nyland, B. F., Jansen, E., Elderfield, H. & Andersson, C., 2006. Neogloboquadrina pachyderma (dex. and sin.) Mg/Ca and d18O records from the Norwegian Sea. *Geochem. Geophys. Geosyst.*, 7, Q10P17, doi:10.1029/2005GC001055.

Orvik, K. A., Skagseth, Ø. & Mork, M., 2001. Atlantic inflow to the Nordic Seas: current structure and volume fluxes from moored current meters, VM-ADCP and SeaSoar-CTD observations, 1995-1999. *Deep Sea Research Part I: Oceonographic Research Papers*, 48(4), 937-957.

Osterman, D., Curry, W. B., Honjo, S., Olafsson, J., & Manganini, S. J., 1999. Variability of Foraminiferal Flux and Isotopic Composition at Sites Around Iceland and the Sea of Okhotsk, with a Special Focus on N. pachyderma (sinistral and dextral), G. quinqueloba and G. bulloides. *6th International Conference on Paleoceanography*, August 1999, Lisboa, Portugal.

Ottens, J. J., 1991. Planktic foraminiferaas North Atlantic water mass indicators. *Oceanologica Acta*, 14(2), 123-140.

Ottens, J. J., 1992. Planktic foraminifera in the Northeast Atlantic (Ph.D. dissertation), Planktic foraminifera as indicators of ocean environments in the Northeast Atlantic, *Enschede*, 89 pp.

Ottesen, D., Rise, L., Andersen, E.S., Bugge, T. & Eidvin, T., 2009. Geological evolution of the Norwegian continental shelf between 61°N and 68°N during the last 3 million years. *Norwegian Journal of Geology* Vol. 89, pp. 251-265.

Pearson, G. W. (1986), Precise calendrical dating of known growth-period samples using a curve fitting technique, *Radiocarbon*, 28(2A), 292–299.

Poole, D. A. R., 1994. Neogene and Quaternary paleoenvironments on the North Norwegian shelf (Ph. D. dissertation). University of Tromsø, Tromsø.

Reimer, P.J., 2013. INTCAL13 and MARINE13 Radiocarbon age calibration curves 0-50,000 years CAL BP. *Radiocarbon*, 55(4), 1869–1887.

Risebrobakken, B., Dokken, T., Smedsrud, L., Andersson, C., Jansen, E., Moros, M., & Ivanova, E., 2011. Early Holocene temperature variability in the Nordic Seas: The role of oceanic heat advection versus changes in orbital forcing. *Paleoceanography*, 26, PA4206, doi:10.1029/2011PA002117.

Risebrobakken, B., Moros, M., Ivanova, E. V., Chistyakova, N., & Rosenberg, R., 2010. Climate and oceanographic variability in the SW Barents Sea during the Holocene. *The Holocene*, 20, 609–621, doi:10.1177/0959683609356586.

Risebrobakken, B., Jansen, E., Andersson, C., Mjelde, E. & Hevrøy, K., 2003. A high-resolution study of Holocene paleoclimatic and paleoceanographic changes in the Nordic Seas. Paleoceaonography. 18, doi: 10.1029/2002PA000764.

Ruddiman, W. F., 2013. Earth's Climate Past and Future, New York, W. H. Freeman and Company, 465 pp. 464 pp.

Runarsdottir, R. H., 2014. Breytingar á yfirborðshita sjávar á Nútíma á Drekasvæðinu, Norður Atlantshafi - götungarannsókn á sjávarsetskjarna (B.Sc. dissertation). Department of Earth Science, University of Iceland, Reykjavík, Iceland.

Sejrup, H. P., Haflidason, H. & Andrews J. T., 2011. A Holocene North Atlantic SST record and regional climate variability. *Quaternary Science Reviews,* 30, 3181-3195.

Sejrup, H. P., Lehman, S. J., Haflidason, H., Noone, D., Muscheler, R., Berstad, I. M., & Andrews J. T., 2010. Response of Norwegian Sea temperature to solar forcing since 1000 A.D. *Journal of Geophysical Research*, 115.

Sejrup, H. P., Nygård, A., Hall, A. M., Haflidason, H., 2009. Middle and late Weichselian (Devensian) glaciation history of south-western Norway, North Sea and eastern UK. *Quaternary Science Reviews*, 28 (3-4), 370-380.

Sejrup, H. P., Hjelstuen, B. O., Dahlgren, K. I. T., Haflidason, H., Kuijpers, A., Nygård, A., Praeg, D., Stoker, M. S. & Vorren, T. O., 2005. Pleistocene glacial history of the NW European continental margin. *Marine and Petroleum Geology,* 22 (9-10), 1111-1129

Sejrup, H.P., Aarseth, I., Haflidason, H., Løvlie, R., Bratten, Å ., Tjøstheim, G. & Forsberg, C.F., 1995. Quaternary of the Norwegian Channel: glaciation history and paleoceanography. *Nor. Geol. Tidsskr.*, 75, 65–87.

Sejrup, H. P., Haflidason, H., Aarseth, I., King, E., Forsberg, C.F., Long, D. & Rokoengen, K., 1994. Late Weichselian glaciation history of the northern North Sea. *Boreas,* 23, 1–13.

Sejrup, H. P., Fjæran, T., Hald. M., Beck, L., Hagen, J., Miljeteig, I., Morvik, I. & Norvik, O., 1981. Benthonic foraminifera in surface samples from the norwegian continental margin between 62°N and 65°N. *Journal of Foraminiferal Research*, 11(4), 277-295.

Shackleton, N. J., 1974. Attainment of isotpoic equilibrium between ocean water and the benthic foraminifera genus Uvigerina: Isotopic changes in the ocean during the last glacial. *Les methodes quantitaives d'etude des variations du cimat au cours du pleistocene*. Paris, Colloques Internationaux du Centre National de la Recherche Scientifique, Centre National de la Recherche Scientifique, 219, 203-209.

Shao, Q., & Zhao, J., 2014. On the Deep Water of the Nordic Seas. *Advances in Earth Science*, 29(1), 42-55.

Skagseth, Ø. & Mork, K. A., 2012. Heat Content in the Norwegian Sea, 1995-2010. Ices Journal of Marine Science, 69 (5), 826-832.

Spero, H.J., Lea, D.W., 1996. Experimental determination of stable isotope variability in Globigerina bulloides: implications for paleoceanographic reconstructions. Marine Micropaleontology 28, 231-246.

Sutton, R. T. & Hodson, D. L. R., 2005. Atlantic Ocean Forcing of North Atlantic and European Summer Climate. *Science,* 309, 115-118.

Sætre, R., 2007. *The Norwegian Coastal Current – Oceanography and Climate*. Trondheim, Tapir Academic Press, 159 pp.

Sætre, R., Aure, J., & Ljøen, R., 1988. Wind effects on the lateral extension of the Norwegian Coastal Water. *Continental Shelf Research*, 8, 239–253.

Thornalley, D. J. R., Blaschek, M., Davies, F. J., Praetorius, S., Oppo, D. W., McManus, J. F., Hall, I. R., Kleiven, H., Renssen, H. & McCave, I. N., 2013. Long-term variations in Iceland–Scotland overflow strength during the Holocene. *Climate of the Past*, 9, 2073–2084, doi:10.5194/cp-9-2073-2013

Visbeck, M., Chassignet, E., Curry, R., Delworth, T., Dickson, B., Krahmann, G., 2003. The Ocean's response to North Atlantic oscillation variability. In Hurrell, J.W., Kushnir, Y., Ottersen, G., Visbeck, M. (Eds.), *The North Atlantic Oscillation: Climatic Significance and Environmental Impact*. Washington DC, American Geophysical Union Monograph 134, 113–146.

Wanner, H., Beer, J., Butikofer, J., Crowley, T. J., Cubasch, U., Fluckiger, J., Goosse, H., Grosjean, M., Joos, F., Kaplan, J. O., Kuttel, M., Muller, S. A., Prentice, I. C., Solomina, O., Stocker, T. F., Tarasov, P., Wagner, M. & Widmannm M., 2008. Mid- to Late Holocene climate change: and overview, Quaternary Science Reviews, 27, 1791-1828, doi: 10.1016/j.quascirev.2008.06.013.

Yashayaev, I., Seidov, D. & Demirov, E., 2015. A new collective view of oceanography of the Arctic and North Atlantic basins. *Progress in Oceanography*, 132, 1–21.

Internet references

WORMS (World Register of Marine Species), 2016. *WoRMS.* Retrieved from
http://www.marinespecies.org/. Read 26.09.16.

MSIP (Marine Species Identification Portal), 2016. *Marine Species Identification Portal*.
Retrieved from http://species-identification.org/ Read 26.09.16.

NOAA, 2008. *Ocean Circulations*. Retrieved from
http://oceanservice.noaa.gov/education/yos/resource/JetStream/ocean/circulation
.htm Read 26.09.16.

Climatesnack, 2013. *To index or not to index?* Retrieved from
http://www.scisnack.com/2013/11/26/to-index-or-not-to-index/ Read 26.09.16.

Hurrell, James & National Center for Atmospheric Research Staff (Eds). Last modified 16 Aug
2016."The Climate Data Guide: Hurrell *North Atlantic Oscillation (NAO) Index*
(station-based)." Retrieved from https://climatedataguide.ucar.edu/climate-
data/hurrell-north-atlantic-oscillation-nao-index-station-based Read 26.09.16.

Jensen, I. S., Eriksen, T. G. & Eliassen, A. (Eds). Last modified Aug 2016. *Climate statistics
for Trøndelag*: Long term temperature and precipitation statistics Trøndelag,
with mean average values. Norwegian Meteorological Institute and Norwegian
Broadcasting Corporation. Retrieved from
https://www.yr.no/place/Norway/S%C3%B8r-
Tr%C3%B8ndelag/Trondheim/Trondheim/climate.summer.html Read 26.09.16.

Appendix

Foraminifera counts GS13-182-01 1949-2000 yr AD (%)

index	sample depth (mm)	to (mm)	age (ADBC)	N. incompta	N. pachyderma	T. quinqueloba	G. bulloides	G. glutinata	G. uvula	G. inflata	O. universa	Unknown
2	80	85	1999.83	76.30	2.22	1.48	4.44	1.48	7.41	1.48	0.74	4.44
3	85	90	1999.26	74.29	2.86	10.48	7.62		0.95	0.95		2.86
4	90	95	1998.7	72.73	1.95	4.55	6.49	0.65	3.25		0.65	9.74
5	95	100	1998.15	56.96	2.95	16.46	9.70	3.80	0.84	2.53	0.42	6.33
6	100	105	1997.58	65.88	1.76	8.82	10.00	4.12	1.18	2.35		5.88
7	105	110	1997.02	62.50	1.25	3.75	17.50	1.25	2.50	2.50		8.75
8	110	115	1996.46	67.80	3.95	11.86	9.60	2.26	1.13			3.39
9	115	120	1995.9	58.79	3.03	9.70	10.30	2.42	9.70	1.21		4.85
10	120	125	1995.34	57.84	0.00	5.88	12.75	4.90	0.98	2.94		14.71
11	125	130	1994.77	57.65	2.55	8.67	11.73	6.63	5.10			7.65
12	130	135	1994.22	54.36	2.05	14.36	9.23	9.23	2.05	3.08		5.64
13	135	140	1993.66	62.73	3.64	5.45	10.00	4.55		2.73	0.91	10.00
14	140	145	1993.09	50.00	2.94	5.88	2.94	2.94	23.53	5.88		5.88
15	145	150	1992.53	70.54	2.33	6.98	7.75	7.75		2.33		2.33
16	150	155	1991.96	70.22	0.56	7.30	8.43	3.93		6.18		3.37
17	155	160	1991.4	68.24	4.05	4.05	12.16	5.41	1.35	2.70	0.68	1.35
18	160	165	1990.83	68.36	3.95	1.69	6.21	7.34	1.13	6.21		5.08
19	165	170	1990.27	59.29	0.88	7.96	8.85	7.08	0.88	8.85		6.19
20	170	175	1989.71	62.75	1.96	8.82	3.92	8.82	1.96	2.94	0.98	7.84
21	175	180	1989.15	69.15	2.13	4.26	3.19	5.32	1.06	1.06		13.83
22	180	185	1988.59	46.97	4.55	0.00	9.09	9.09		3.03		27.27
23	185	190	1988.02	57.14	0.00	5.19	5.19	14.29	1.30	2.60		14.29
24	190	195	1987.46	62.70	2.38	4.76	7.14	9.52	3.97	1.59		7.94
25	195	200	1986.9	61.76	4.41	2.94	7.35	5.88	1.47	2.94		13.24
26	200	205	1986.34	56.31	2.91	3.88	11.65	10.68	1.94	2.91		9.71
27	205	210	1985.78	58.67	0.67	8.67	10.00	13.33		3.33		5.33
28	210	215	1985.21	52.63	0.88	18.42	9.65	9.65	1.75	0.88		6.14
29	215	220	1984.65	59.46	3.38	13.51	6.76	8.78		2.70	0.68	4.73
30	220	225	1984.09	53.75	2.50	16.88	5.00	11.88	3.13	2.50	0.63	3.75
31	225	230	1983.52	59.15	2.82	9.86	7.75	10.56	2.82	2.82	1.41	2.82
32	230	235	1982.94	54.62	1.68	18.49	8.40	10.92		5.04		0.84
33	235	240	1982.36	53.98	4.55	14.20	5.11	16.48		3.98		1.70

34	240	245	1981.79	57.14	1.02	10.20	6.12	17.35		4.08		4.08
35	245	250	1981.22	62.39	3.42	9.40	3.42	10.26		5.13	0.85	5.13
36	250	255	1980.64	56.25	2.08	8.33		17.71	3.13	6.25		6.25
37	255	260	1980.05	56.25	1.56	16.67	2.60	10.42	3.13	4.69		4.69
38	260	265	1979.48	55.88	0.74	12.50	2.21	16.18	2.94	5.88		3.68
39	265	270	1978.89	60.17	3.39	10.17	5.08	11.02	0.85	5.93		3.39
40	270	275	1978.31	51.50	2.99	13.77	7.19	11.38	2.99	2.40		7.78
41	275	280	1977.73	60.63	5.51	4.72	5.51	7.09	0.79	4.72		11.02
42	280	285	1977.15	60.91	7.27	5.45	7.27	8.18	1.82	5.45		3.64
43	285	290	1976.57	65.52	6.21	10.34	4.83	4.83	0.69	3.45		4.14
44	290	295	1975.99	59.66	4.20	21.85	3.36	6.72	2.52	0.84		0.84
45	295	300	1975.41	66.10	5.08	5.08	7.63	5.93	2.54			7.63
46	300	305	1974.83	58.23	3.80	0.00	3.80	7.59	2.53	8.86		15.19
47	305	310	1974.25	69.17	5.00	3.33	6.67	5.83	1.67	0.83		7.50
48	310	315	1973.67	65.96	5.32	0.00	14.89	3.19	2.13	1.06		7.45
49	315	320	1973.08	64.67	5.33	6.67	5.33	4.67	2.00	2.67		8.67
50	320	325	1972.51	70.32	1.29	7.10	8.39	4.52	5.81	0.65		1.94
51	325	330	1971.94	65.29	7.65	12.35	1.76	4.71	4.12	1.76		2.35
52	330	335	1971.36	71.01	2.90	4.83	5.80	3.86	4.35	2.42		4.83
53	335	340	1970.77	68.15	3.70	5.19	5.93	4.44	3.70	1.48		7.41
54	340	345	1970.2	60.26	4.37	14.85	8.73	5.24	5.68	0.87		
55	345	350	1969.62	66.39	5.46	10.50	8.82	4.62	2.94	0.42		0.84
56	350	355	1969.03	64.02	5.82	11.11	8.47	4.23	3.70	1.59	0.53	0.53
57	355	360	1968.45	58.33	7.74	8.33	12.50	5.95	1.79	2.38		2.98
58	360	365	1967.88	60.63	5.63	16.25	6.88	3.75	4.38	1.88		0.63
59	365	370	1967.29	66.19	5.04	7.19	12.23	3.60	3.60	1.44		0.72
60	370	375	1966.71	56.55	4.17	11.31	11.90	7.14	4.76	2.98		1.19
61	375	380	1966.15	57.06	8.24	11.18	11.18	5.88	3.53	1.76		1.18
62	380	385	1965.58	62.31	6.53	10.05	11.56	3.02	2.51	3.52		0.50
63	385	390	1965.01	67.21	5.74	5.33	11.07	2.46	3.69	2.46		2.05
64	390	395	1964.46	67.66	3.59	5.99	11.98	2.40	2.40	3.59		2.40
65	395	400	1963.89	61.62	6.06	9.60	9.60	4.04	3.54	5.05		0.51
66	400	405	1963.33	65.50	4.00	10.00	8.00	5.50	3.50	2.00		1.50
67	405	410	1962.76	61.97	7.04	7.04	12.21	4.23	3.29	1.88		2.35
68	410	415	1962.2	66.81	3.45	12.07	9.48	2.59	1.72	1.72	0.43	1.72
69	415	420	1961.63	63.54	3.65	8.33	10.42	3.65	4.17	3.65		2.60
70	420	425	1961.09	70.90	1.59	5.29	10.05	4.76	2.65	2.65		2.12
71	425	430	1960.52	63.68	5.83	4.04	11.66	5.83	3.59	3.59		1.79
72	430	435	1959.95	58.42	3.96	10.89	12.38	3.96	5.94	2.97		1.49
73	435	440	1959.38	74.06	2.36	3.77	9.91	4.25	2.36	1.42		1.89
74	440	445	1958.8	73.64	3.18	4.09	5.45	4.55	1.82	4.09	0.45	2.73
75	445	450	1958.24	77.62	0.95	4.29	7.14	1.90	2.86	4.29		0.95
76	450	455	1957.66	74.37	4.02	6.03	6.53	1.01	1.51	2.51		4.02
77	455	460	1957.1	71.91	2.68	3.68	7.69	3.68	2.68	4.68	0.33	2.68
78	460	465	1956.53	73.44	3.44	4.69	11.56	2.50		1.88	0.63	1.88

index	sample depth (mm)	to (mm)	age (yr BP)	N. incompta	N. pachyderma	T. quinqueloba	G. bulloides	G. glutinata	G. uvula	G. inflata	O. universa	Unknown
79	465	470	1955.97	78.45	1.72	3.88	6.03	3.02	2.16	3.45		1.29
80	470	475	1955.41	73.40	4.71	5.39	7.74	3.70	0.67	1.68		2.69
81	475	480	1954.84	75.24	1.61	6.11	8.68	3.22	1.29	2.25		1.61
82	480	485	1954.28	76.68	2.83	3.18	7.77	4.24	1.41	2.83		1.06
83	485	490	1953.72	71.21	2.65	7.20	6.06	3.03	2.27	4.17		3.41
84	490	495	1953.15	67.89	5.26	4.21	10.53	4.74	6.32			1.05
85	495	500	1952.59	70.17	2.52	7.14	10.92	5.88	1.68	0.84		0.84
86	500	505	1952.04	76.52	3.41	4.92	4.92	5.68	2.27	0.76		1.52
87	505	510	1951.47	70.63	2.78	7.54	5.95	4.76	3.17	1.98		3.17
88	510	515	1950.9	69.17	5.00	5.42	10.42	2.92	2.50	1.25	0.42	2.92
89	515	520	1950.34	65.09	2.36	8.02	11.32	2.36	3.30	1.42		6.13
90	520	525	1949.78	71.85	2.98	4.64	10.26	4.97	1.66	1.66		1.99

Foraminifera count GS13-182-01

index	sample depth (mm)	to (mm)	age (yr BP)	N. incompta	N. pachyderma	T. quinqueloba	G. bulloides	G. glutinata	G. uvula	G. inflata	O. universa	Unknown
394	2445	2450	437.5099	54.29	6.43	17.86	11.43	0.71	0.25			9.29
413	3395	3400	688.7016	58.89	5.00	10.56	15.00	2.78	0.48	0.56		4.44
431	4295	4300	939.1053	45.83	10.98	12.88	18.94	0.76	0.70			7.20
450	5245	5250	1195.598	56.10	4.88	10.98	8.54	3.66	0.89			8.54
466	6045	6050	1440.992	58.47	5.46	13.66	7.10	4.37	1.07	1.09	0.55	7.10
481	6795	6800	1687.519	54.70	3.31	11.05	16.57	2.21	1.25	7.73		3.31
498	7495	7500	1936.198	41.73	5.51	4.33	27.17	4.72	1.41	3.54		7.87
512	8195	8200	2198.494	42.20	1.42	14.54	28.37	5.32	1.56	2.48		2.84
524	8795	8800	2442.811	72.00	4.00	8.80	14.00		1.72			1.20
536	9395	9400	2699.561	63.52	2.46	14.75	10.66	1.64	1.87	0.41		1.23
546	9895	9900	2928.214	46.95	4.27	15.24	16.46	6.71	2.01	1.83		4.88
557	10445	10450	3192.724	68.38	1.98	7.11	14.62	1.19	2.15	0.79	1.19	3.56
567	10945	10950	3441.061	64.32	2.90	3.73	7.88	2.49	2.29	1.66		5.39
576	11395	11400	3677.281	53.91	0.78	12.50	23.44	3.91	2.43	1.56		3.13
586	11895	11900	3949.898	49.82	3.61	10.11	15.88	3.25	2.56		0.72	6.50
594	12295	12300	4175.451	60.86	2.96	7.24	21.05	3.95	2.69	1.97		1.32
606	12745	12750	4432.442	56.71	6.49	8.66	6.49	6.06	2.81	1.73		5.19
615	13195	13200	4701.607	67.79	1.12	7.49	16.10	3.37	2.93	0.37	0.37	1.87
623	13595	13600	4947.34	54.67	3.11	14.67	10.22	4.44	3.05	3.56		4.89
631	13995	14000	5196.885	62.94	7.11	10.15	12.69	2.03	3.17	1.02		3.05
639	14395	14400	5454.702	44.09	9.14	13.98	16.13	4.30	3.29			4.84
646	14745	14750	5685.437	67.63	3.60	3.60	15.11	2.16	3.41	4.32	0.72	0.72

index	from	to	age									
654	15145	15150	5955.327	44.21	6.32	11.58	10.53	9.47	3.52	2.11	1.05	6.32
661	15495	15500	6160.643	46.53	5.94	22.28	13.86	3.96	3.63	1.98	0.50	1.98
668	15845	15850	6443.461	60.00	2.35	11.76	21.18	1.18	3.74			3.53
675	16195	16200	6698.009	52.92	3.75	15.00	20.00	5.00	3.85	1.25		0.00
681	16495	16500	6922.133	45.36	7.22	10.31	10.31	4.12	3.96			9.28
688	16845	16850	7187.176	36.17	14.89	14.89	14.89	4.26	4.07	6.38		2.13
694	17145	17150	7425.577	38.46	2.56	7.69	20.51	7.69	4.18			5.13
700	17445	17450	7672.045	41.67	8.33		8.33		4.29		8.33	8.33
706	17745	17750	7927.693	44.12	8.82	5.88	11.76	11.76	4.39			11.76

Isotope analysis

index	sample depth (mm)	to (mm)	age (ADBC)	d 13C/12C Mean	d 18O/16O Mean
2	80	85	2000	0.13	1.29
3	85	90	1999	0.17	1.37
4	90	95	1999	0.19	1.53
5	95	100	1998	0.21	1.34
6	100	105	1998	0.00	1.02
7	105	110	1997	0.02	1.19
8	110	115	1996	-0.03	1.15
9	115	120	1996	0.04	1.09
10	120	125	1995	0.09	1.41
11	125	130	1995	0.18	1.42
12	130	135	1994	-0.44	2.04
13	135	140	1994	0.20	1.53
14	140	145	1993	-0.07	1.37
15	145	150	1993	0.07	1.36
16	150	155	1992	0.12	1.15
17	155	160	1991	0.10	1.28
18	160	165	1991	0.09	1.50
19	165	170	1990	0.07	1.40
20	170	175	1990	0.21	1.13
21	175	180	1989	0.29	1.94
22	180	185	1989	0.24	2.33
23	185	190	1988	0.29	1.67
24	190	195	1987	0.18	2.04
25	195	200	1987	0.11	2.71
26	200	205	1986	0.19	3.09
27	205	210	1986	0.24	1.44
28	210	215	1985	0.35	1.30
29	215	220	1985	0.16	1.83
30	220	225	1984	0.25	1.37
31	225	230	1984	0.16	1.44
32	230	235	1983	0.25	1.42
33	235	240	1982	0.32	1.86
34	240	245	1982	0.25	1.42
35	245	250	1981	0.27	1.61
36	250	255	1981	0.17	2.05
37	255	260	1980	0.32	1.71
38	260	265	1979	0.27	1.70
39	265	270	1979	0.32	1.95
40	270	275	1978	0.43	1.51
41	275	280	1978	0.33	1.99
42	280	285	1977	0.08	1.59
43	285	290	1977	0.38	2.45
44	290	295	1976	0.29	2.13
45	295	300	1975	0.31	1.53
46	300	305	1975	0.51	2.73
47	305	310	1974	0.32	2.11
48	310	315	1974	0.48	2.03
49	315	320	1973	0.23	1.76
50	320	325	1973	0.16	1.58
51	325	330	1972	0.35	1.90
52	330	335	1971	0.26	2.36
53	335	340	1971	0.42	2.48
54	340	345	1970	0.28	1.38
55	345	350	1970	0.26	1.73
56	350	355	1969	0.44	1.44
57	355	360	1968	0.47	1.45
58	360	365	1968	0.23	1.36

59	365	370	1967	0.38	1.30
60	370	375	1967	0.31	1.40
61	375	380	1966	0.25	1.36
62	380	385	1966	0.38	1.40
63	385	390	1965	0.19	1.39
64	390	395	1964	0.37	1.41
65	395	400	1964	0.14	1.37
66	400	405	1963	0.42	1.41
67	405	410	1963	0.41	1.37
68	410	415	1962	0.36	1.25
69	415	420	1962	0.31	1.34
70	420	425	1961	0.35	1.37
71	425	430	1961	0.49	1.51
72	430	435	1960	0.36	1.25
73	435	440	1959	0.34	1.32
74	440	445	1959	0.45	1.52
75	445	450	1958	0.35	1.71
76	450	455	1958	0.29	1.35
77	455	460	1957	0.46	1.36
78	460	465	1957	0.47	1.55
79	465	470	1956	0.31	1.52
80	470	475	1955	0.40	1.47
81	475	480	1955	0.41	1.33
82	480	485	1954	0.34	1.38
83	485	490	1954	0.37	1.32
84	490	495	1953	0.43	1.30
85	495	500	1953	0.47	1.47
86	500	505	1952	0.34	1.32
87	505	510	1951	0.37	1.39
88	510	515	1951	0.41	1.29
89	515	520	1950	0.37	2.35
90	520	525	1950	0.43	1.93